Electronic Supplementary Material (ESI) for ChemComm.

ON/OFF metal-triggered molecular tweezers for fullerene recognition

Adriana Sacristán-Martín,[a †] Héctor Barbero,[a †] Sergio Ferrero,[a] Daniel Miguel,[a] Raúl García-Rodríguez [a *] and Celedonio M. Álvarez [a *]

[a] GIR MIOMeT, IU CINQUIMA/Química Inorgánica, Facultad de Ciencias, Universidad de Valladolid, E47011, Valladolid, Spain. Email: raul.garcia.rodriguez@uva.es; celedonio.alvarez@uva.es
[†] These authors equally contributed to this work.

Table of Contents

Experimental Procedures

General methods

Reagents were purchased from regular suppliers and used without further purification. 1-Bromocorannulene was acquired from Synoi Chemicals (http://synoichemicals.uva.es/). Solvents were of analytical grade or spectrophotometric grade. They were either used as purchased or dried according to procedures described elsewhere.[1,2] Microwave reactions were carried out with an Anton Paar Monowave 300 Reactor using tightly capped flasks G10 and G4 (for volumes up to 10 mL and 4 mL, respectively) especially designed for the apparatus. All reactions under inert atmosphere (when needed) were performed with standard Schlenk techniques. They were also used as a preliminary step for degassing microwave flasks when inert atmosphere was necessary in microwave reactions. Column chromatography separations were carried out by using Silica gel 60 (particle size 0.040-0.063 mm; 230-400 mesh; Merck, Germany) as the stationary phase and TLCs were performed on precoated silica gel plates (0.25 mm thick, 60 F254, Merck, Germany) and observed under UV light. Purifications by centrifugation were performed in a Nahita 2600. NMR spectra were recorded on Agilent DD2 500 and Agilent MR 400 instruments. ^{1}H and ^{13}C NMR chemical shifts are reported in parts per million (ppm) and are referenced to TMS, using solvents as an internal reference. Coupling constants (*J*) are reported in hertz (Hz). Standard abbreviations used to indicate multiplicity: s = singlet, d = doublet, t = triplet, m = multiplet, dd = doublet of doublets. ^{1}H and ^{13}C assignments were performed by utilizing 2D NMR methods (COSY, DQCOSY, band selective ROESY, band selective HSQC, band selective HMBC, and gradient crisis HMBC). Some quaternary carbon atoms were not directly detected by 1D $^{13}C\{^{1}H\}$ NMR experiment, but they were located thanks to HMBC correlations. Additionally, in the case of compound **L1b**, direct carbon detection was not possible due to the poor solubility of the sample. High resolution mass spectra were recorded at mass spectrometry service of the Laboratory of Instrumental Techniques of the University of Valladolid (L.T.I., www.laboratoriotecnicasinstrumentales.es). A MALDI-TOF system (MALDI-TOF) Bruker Autoflex Speed (N_2 laser (337 nm, pulse energy 100 μJ, 1 ns), acceleration voltage 19 kV, reflector positive mode) was used. Trans-2-[3-(4-tert-butylphenyl)-2-methyl-2-propenylidene]malonitrile (DCTB) and 1,8-dihydroxy-9(10H)-anthracenone (dithranol) were used as matrixes. A UPLC-MS system (UPLC: Waters ACQUITY H-class UPLC; MS: Bruker Maxis Impact) by electrospray ionization (ESI positive and negative) was utilized as well. HRMS spectra were analyzed using Bruker DataAnalysis 4.1© (www.bruker.com). Steady state UV/Vis absorption spectroscopy was carried out on a Perkin Elmer Lambda 265 spectrophotometer, whereas emission spectroscopy was performed on a Perkin Elmer LS-55 fluorescence spectrophotometer, using quartz cuvettes with a path length of 1 cm in dichloromethane as the solvent. Cyclic voltammetry was carried out using a PalmSens4 potentiostat, with a 0.1 M solution of tetrabutylammonium hexafluorophosphate (NBu_4PF_6) as the supporting electrolyte in dry dichloromethane as the solvent. Solutions were deaerated with a nitrogen stream prior to each measurement. Experiments were performed in a one-compartment cell equipped with a glassy carbon electrode, a silver wire counter electrode, and an Ag/AgCl wire as pseudo-reference electrode. All potentials were referenced against the ferrocene/ferrocenium couple (Fc/Fc^{+}) after each experiment.

Synthesis overview

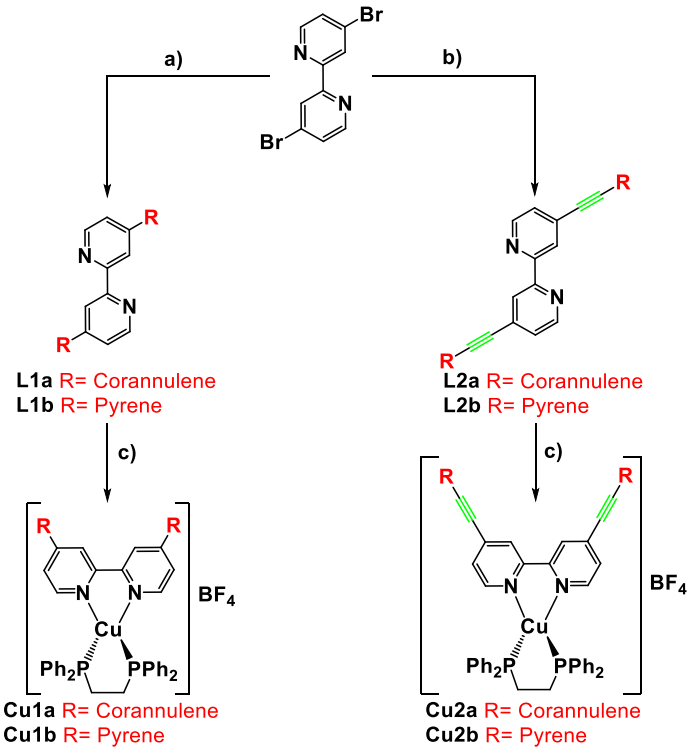

Scheme S 1. Synthesis routes to achieve ligands **L1a,b** and **L2a,b** as well as Copper complexes **Cu1a,b** and **Cu2a,b** functionalized with polycyclic aromatic hydrocarbons (PAH). Reagents and conditions: (a) Bpin-PAH, $[PdCl_2(dppf)]$, ^tBuONa, toluene, MW, 130 °C; (b) PAH-acetylene-TMS, $[PdCl_2(dppf)]$, TBAF in THF (1M); (c) $[Cu(NCMe)_4]BF_4$, dppe, DCM.

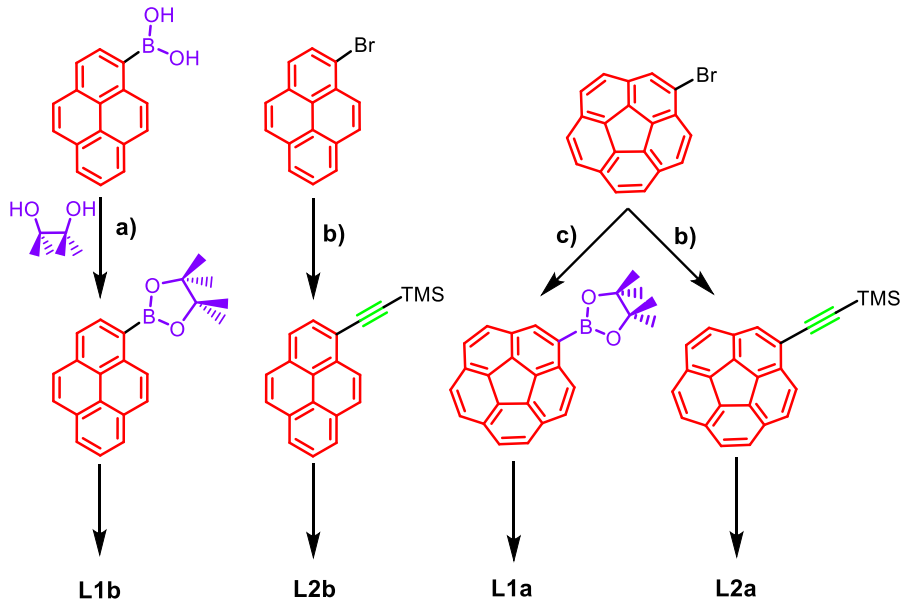

Scheme S 2. Synthesis of PAH intermediates prior to **L1a,b** and **L2a,b** preparation. Reagents and Conditions: a) Pinacol, MW, 150 °C; b) ethynyltrimethylsilane, [$PdCl_2$(dppf)], CuCl, NEt_3, MW, 85 °C; c) $B_2(pin)_2$, [$PdCl_2$(dppf)], KOAc, dioxane, MW, 130 °C.

Synthetic procedures

Preparation of pyrene-1-boronic acid pinacol ester

Pyrene-1-boronic acid (0.1 g, 0.38 mmol) and pinacol (70 mg, 0.58 mmol) were mixed in a microwave flask. The mixture was irradiated in the absence of solvent in a microwave reactor at 150 °C for 15 min without stirring allowing pinacol to melt and, then, stirred at 600 rpm (pressure never increased throughout the whole process). Formed water droplets at the top of the vial were gently removed. Resulting light brown crude was collected and used in the next step without further purification. (0.11 g, 87% yield) The spectral data were in agreement with those reported in the literature.[3]

Preparation of corannulene-1-boronic acid pinacol ester

1-Bromocorannulene (50 mg, 0.15mmol), bis(pinacolato)diboron (58 mg, 0.23 mmol), [PdCl2(dppf)] (5.2 mg, 7 µmol) and potassium carbonate (46 mg, 0.46 mmol) were mixed in a microwave flask under inert atmosphere. Dry dioxane (2.0 mL) was added and the mixture was degassed. It was then irradiated in a microwave reactor at 130 °C for 75 min with stirring at 600 rpm (maximum pressure reached was 6.0 bar). Solvent was removed under vacuum before a purification by column chromatography on silica gel (9:1 to 7:3 hexane/CH_2Cl_2) to give the expected compound as a light brown solid (40 mg, 70% yield). The spectral data were in agreement with those reported in the literature.[4]

General method for trimethylsilylacetylene arene preparation

Bromoarene (0.30 mmol), ethynyltrimethylsilane (0.21 mL, 1.5 mmol), [$PdCl_2$(dppf)] (22 mg, 0.030 mmol) CuCl (3.0 mg, 0.030 mmol) and NEt_3 (3.0 mL, 21.5 mmol) were mixed in a microwave flask. Then, the mixture was irradiated in a microwave reactor at 85 °C for 60 min with stirring at 600 rpm (maximum pressure reached was 2.0 bar). After finishing, solvent was removed under vacuum and the resulting crude was subjected to purification by column chromatography on silica gel (hexane) to give the expected compound as a yellowish solid (76 mg, 85% yield and 73 mg, 70% yield for pyrene and corannulene derivatives, respectively). The spectral data were in agreement with those reported in the literature.[5]

General method for Suzuki coupling (compounds **L1a** and **L1b**)

4,4'-dibromo-2,2'bipyridine (20 mg, 64 µmol), arene boronate ester (0.14 mmol) [$PdCl_2$(dppf)] (19 mg, 25 µmol), and ^{t}BuONa (37 mg, 0.38 mmol) were mixed in a microwave flask under inert atmosphere. Dry and degassed toluene (3.0 mL) was then added. The solution was irradiated in a microwave reactor at 130 °C for 90 minutes with stirring at 700 rpm (maximum pressure reached was 4.8 bar). The solvent was removed under vacuum before

subjecting the remaining material to purification by carrying out washes with ethanol (3 x 10 mL) followed by centrifugations at 3500 rpm. Undesired liquid was decanted, and the solid was collected and dried in an oven at 80 °C to furnish the expected compounds as grey solids (35 mg, quantitative yield and 41 mg, quantitative yield for **L1a** and **L1b**, respectively).

General method for Sonogashira coupling (compounds **L2a** and **L2b**)

4,4'-dibromo-2,2'-bipyridine (20 mg, 64 µmol), trimethysilylethynylarene (0.14 mmol), [$PdCl_2$(dppf)] (2.8 mg, 3.8 µmol), and TBAF 1M in THF 0.38 mL, 0.38 mmol) were mixed in a Schlenk flask under inert atmosphere. The mixture was heated at 70°C for 1 hour. Then the solvent was removed in vacuo and the crude was purified by washes with ethanol (2 x 10 mL) followed by centrifugations at 3500 rpm. Undesired liquid was decanted, and the solid was collected and dried in an oven at 80 °C, giving rise to expected compounds as brown solids (35 mg, 90% yield and 40.5 mg, 90% yield for **L2a** and **L2b**, respectively).

General method for complexes preparation

Cu1a/Cu1b

To a colorless solution of [$Cu(NCMe)_4$]BF_4 (10 mg, 32 µmol) in dry DCM (10 mL) kept in a Schlenk under inert atmosphere, bipyridine **L1a/L1b** (32 µmol) was added. The solution was stirred at room temperature for 10 minutes before adding dppe (13 mg, 32 µmol). The mixture immediately became yellow and was further stirred at room temperature for 10 min. It was then filtered under nitrogen atmosphere, concentrated and precipitated with hexane. A yellow solid crushed out and was isolated by solvent removal under vacuum. (23 mg, 65% yield and 23 mg, 60% yield for **Cu1a** and **Cu1b**, respectively).

Cu2a/Cu2b

To a colorless solution of [$Cu(NCMe)_4$]BF_4 (10 mg, 32 µmol) in dry DCM (10 mL) kept in a Schlenk under inert atmosphere, bipyridine **L2a/L2b** (32 µmol) was added. The solution was stirred at room temperature for 10 minutes before adding dppe (13 mg, 32 µmol). The mixture immediately became green and turned to a dark red color after further stirring at room temperature for 15 min. It was then filtered under nitrogen atmosphere, concentrated and precipitated with hexane. A dark orange solid crushed out and was isolated by solvent removal under vacuum. (24 mg, 65% yield and 24 mg, 60% yield for **Cu2a** and **Cu2b**, respectively).

Characterization details

L1a

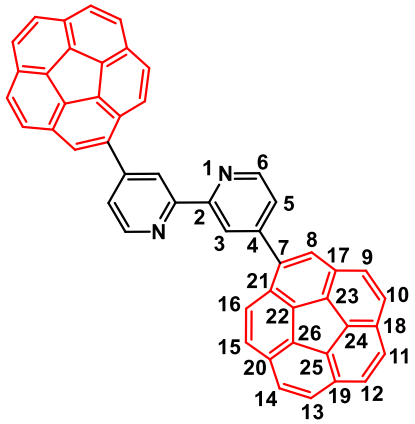

^{1}H NMR (500 MHz, $CDCl_3$) δ 8.96 (d, *J* = 1.7 Hz, 2H, H_3), 8.88 (d, *J* = 4.9 Hz, 2H, H_6), 8.12 (s, 2H, H_8), 7.94 - 7.88 (m, 6H, H_9, H_{11} and H_{13}), 7.88 - 7.85 (m, 6H, H_{15}, H_{12} and H_{14}), 7.83 - 7.81 (m, 4H, H_{10} and H_{16}), 7.80 (d, *J* = 4.9, 1.7 Hz, 2H, H_5). ^{13}C NMR (126 MHz, $CDCl_3$) δ 149.6 (C_6), 148.4 (C_4), 139.5 (C_7), 131.2 - 130.8 ($C_{q\ CORA}$), 130.5 ($C_{q\ CORA}$), 128.9–128.4 ($C_{q\ CORA}$), 127.9 (C_{16}), 127.6 – 127.0 (CH_{CORA} and $C_{q\ CORA}$), 127.0 (C_8 and C_{10}), 126.4 (C_9), 124.9 (C_5), 122.1 (C_3). HRMS (MALDI): *m/z* = 653.1989 $[M+H]^+$ calculated 653.2012 for $C_{50}H_{25}N_2$).

L2a

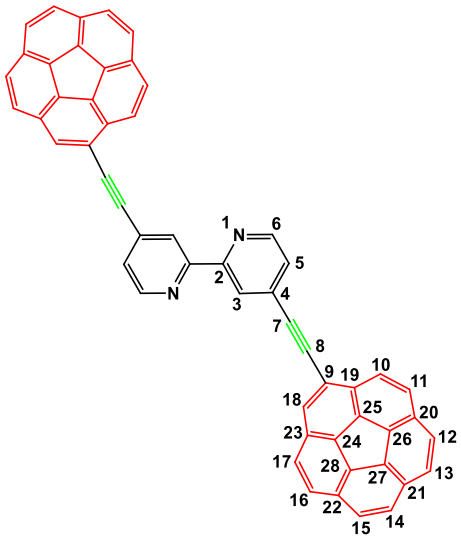

^{1}H NMR (500 MHz, methylene chloride-d_2) δ 8.79 (dd, J = 5.0, 0.7 Hz, 2H, H_6), 8.76 (dd, J = 1.5, 0.7 Hz, 2H, H_3), 8.22 (d, J = 8.9 Hz, 2H, H_{10}), 8.21 (s, 2H, H_{18}), 7.98 (d, J = 8.9 Hz, 2H, H_{11}), 7.92 – 7.84 (m, 12H, H_{12}, H_{13}, H_{14}, H_{15}, H_{16} and H_{17}), 7.63 (dd, J = 5.0, 1.5 Hz, 2H, H_5) ^{13}C NMR (126 MHz, methylene chloride-d_2) δ 155.8 (C_2), 149.4 (C_6), 136.0 (C_q), 135.7 (C_q), 135.1 (C_9), 132.3 (C_{18} and C_4), 131.6 (C_q), 131.4 (C_q), 130.8 (C_q) 130.2 (C_q), 127.9 (C_{11}), 127.7 (C_{17}), 127.6 (CH_{CORA}), 127.5 (CH_{CORA}), 127.2 (CH_{CORA}), 126.7 (CH_{CORA}), 125.8 (C_{10}), 125.7 (C_5), 123.0 (C_3), 92.0 (C_8), 90.6 (C_7) (HRMS (MALDI): m/z = 701.1963 $[M+H]^+$ (calculated 701.2012 for $C_{54}H_{25}N_2$).

L1b

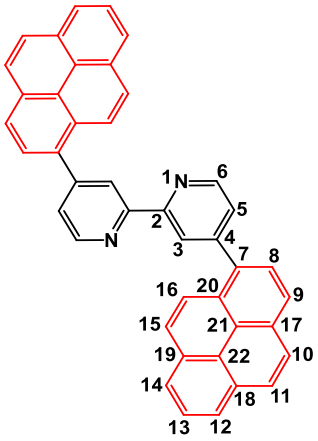

^{1}H NMR (500 MHz, $CDCl_3$) δ 8.86 (d, J = 6.4 Hz, 2H, H_6), 8.85 (d, J = 1.8 Hz, 2H, H_3), 8.30 (d, J = 7.8 Hz, 2H, H_9), 8.26 (d, J = 7.6 Hz, 2H, H_{12}), 8.23 (d, J = 9.3 Hz, 2H, H_{16}), 8.22 (d, J = 7.6 Hz, 2H, H_{14}), 8.17 (d, J = 10.8 Hz, 2H, H_{11}), 8.15 (d, J = 10.8 Hz, 2H, H_{10}), 8.12 (d, J = 9.3 Hz, 2H, H_{15}), 8.10 (d, J = 7.8 Hz, 2H, H_8), 8.06 (t, J = 7.6 Hz, 2H, H_{13}), 7.64 (dd, J = 6.4, 1.8 Hz, 2H, H_5). ^{13}C NMR (Indirect detection by HMBC) δ 156.4 (C_2), 150.2 (C_4), 149.3 (C_6), 134.8 (C_7), 131.4 (C_{22}), 130.9 (C_{18}), 130.8 (C_{19}), 128.3 (C_{21} and C_{17}), 128.2 (C_{15},), 128.0 (C_{11}), 127.4 (C_{10}), 127.2 (C_8), 126.2 (C_{13}), 125.7 (C_5), 125.6 (C_{12}), 125.2 (C_{14}), 124.8 (C_9 and C_{20}), 124.5 (C_{16}), 123.1 (C_3). HRMS (MALDI): m/z = 557.2033 $[M+H]^+$ (calculated 557.2012 for $C_{42}H_{25}N_2$).

L2b

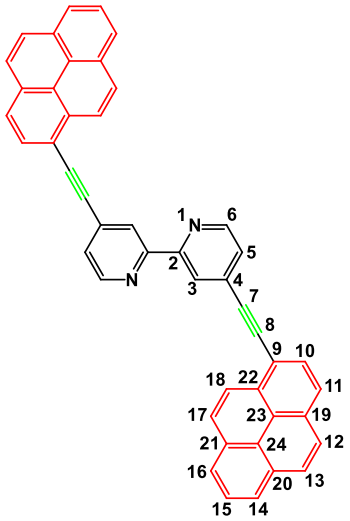

^{1}H NMR (500 MHz, $CDCl_3$) δ 8.82 (dd, *J* = 4.9, 0.8 Hz, 2H, H_6), 8.77 (dd, *J* = 1.6, 0.8 Hz, 2H, H_3), 8.71 (d, *J* = 9.1 Hz, 2H, H_{18}), 8.29 (d, *J* = 7.6 Hz, 2H, H_{16}), 8.27 (m, 4H, H_{10} and H_{17}), 8.25 (d, *J* = 7.6 Hz, 2H, H_{14}), 8.19 (d, *J* = 8.0 Hz, 2H, H_{11}), 8.16 (d, *J* = 9.0 Hz, 2H, H_{13}), 8.10 (d, *J* = 9.0 Hz, 2H, H_{12}) 8.07 (t, *J* = 7.6 Hz, 2H, H_{15}) 7.64 (dd, *J* = 4.9, 1.6 Hz, 2H, H_5). ^{13}C NMR (126 MHz, $CDCl_3$) δ 155.9 (C_2), 149.4 (C_6), 132.8 (C_4), 132.3 (C_{22}), 132.0 (C_{19}), 131.2 (C_{20}), 131.0 (C_{21}), 130.0 (C_{10}), 128.8 (C_{17}), 128.7 (C_{13}), 127.2 (C_{12}), 126.4 (C_{15}), 123.0 (C_{16}), 125.9 (C_{14}), 125.7 (C_5), 125.4 (C_{18}), 124.6 (C_{11}), 124.5 (C_{23}), 124.3 (C_{24}), 123.2 (C_3), 116.5 (C_9), 93.5 (C_8), 92.6 (C_7). HRMS (MALDI): *m/z* = 605.2020 $[M+H]^+$ (calculated 605.2012 for $C_{46}H_{25}N_2$).

Cu1a

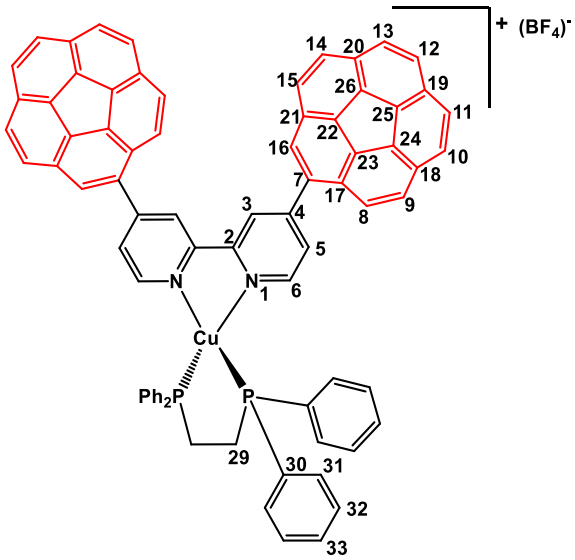

^{1}H NMR (500 MHz, methylene chloride-d_2) δ 8.89 (s, 2H, H_3), 8.61 (d, *J* = 5.4 Hz, 2H, H_6), 8.18 (s, 2H, H_{16}), 7.99 (dd, *J* = 5.4, 2H, H_5), 7.96 (d, *J* = 9.0 Hz, 2H, H_{15}), 7.94 (d, *J* = 9.0 Hz, 2H, H_{14}), 7.93 – 7.89 (m, 6H, $H_{10,}$ H_{13} and H_{11} or H_{12}), 7.88 (d, *J* = 8.9 Hz, 2H, H_9), 7.85 (d, *J* = 8.7 Hz, 2H, H_{11} or H_{12}), 7.81 (d, *J* = 8.9 Hz, 2H, H_8), 7.56 – 7.42 (m, 10H, H_{31}, H_{32} and H_{33}), 2.77 (t, *J* = 6.0 Hz, 4H, H_{29}). ^{13}C NMR (126 MHz, methylene chloride-d_2) δ 152.6 (C_2), 150.5 (C_4), 150.2 (C_6), 136.7 (C_7), 136.2 (C_q), 136.2 (C_q), 135.7 (C_q), 132.3 (C_{Ph}), 132.1 (C_{Ph}),131.6 (C_q), 131.1 (C_q), 130.8 (C_{Ph}), 130.2 (C_q)129.4 (C_{Ph}), 128.4 (C_9), 128.0 (C_{14}), 127.9 ($C_{16,}$ C_{11} or C_{12}), 127.8 (C_{10} or C_{13}),127.7 (C_q) 127.5 (C_{10} or C_{13}), 127.0 (C_{11} or C_{12}), 126.93 (C_5), 126.9 (C_{15}), 125.2 (C_8), 123.1 (C_3), 25.8 (C_{29}). HRMS (MALDI): *m/z* =1113.2556 $[M]^+$ (calculated 1113.2583 for $C_{76}H_{48}CuN_2P_2$).

Cu2a

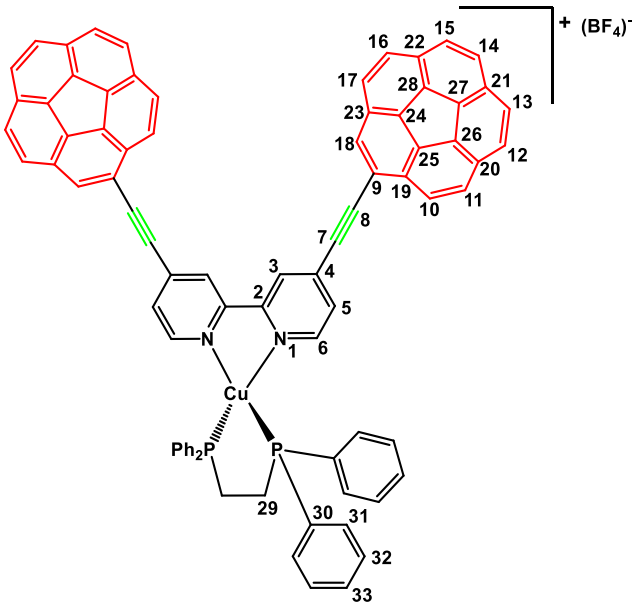

^{1}H NMR (500 MHz, methylene chloride-d_2) δ 8.71 (d, J = 1.3 Hz, 2H, H_3), 8.44 (d, J = 5.4 Hz, 2H, H_6), 8.31 (s, 2H, H_{18}), 8.22 (d, J = 8.8 Hz, 2H, H_{10}), 8.03 (d, J = 8.8 Hz, 2H, H_{11}), 7.96 – 7.87 (m, 20H, H_{12}, H_{13}, H_{14}, H_{15}, H_{16} and H_{17}), 7.78 (dd, J = 5.4, 1.3 Hz, 2H, H_5), 7.51 – 7.38 (m, 20H, H_{31}, H_{32} and H_{33}), 2.74 (t, J = 5.8 Hz, 4H, H_{29}). ^{13}C NMR (126 MHz, methylene chloride-d_2) δ 153.7 (C_2), 151.8 (C_6), 138.0 (C_q), 137.7 (C_q), 137.0 (C_q), 136.3 (C_q), 135.2 (C_9), 134.4 (C_4), 134.1 (C_q), 133.8 (C_q), 133.4 (C_{18}), 133.2 (C_q), 132.7 (C_{Ph}), 131.4 (C_q), 132.0 (C_q), 132.0 (C_q), 131.3 (C_{31}), 130.1 (C_{11}), 130.0 (CH_{cora}), 129.9 ($CH_{cora,}$ C_5), 129.8 ($CH_{cora,}$ C_4), 129.3 (CH_{cora}), 129.2 ($CH_{cora,}$ C_{12}), 128.6 (C_{17}), 127.2 (C_{10}), 126.3 (C_3), 98.3 (C_8), 91.0 (C_7). HRMS (MALDI): *m/z* = 1161.2554 $[M]^+$ (calculated 1161.2583 for $C_{80}H_{48}CuN_2P_2$).

Cu1b

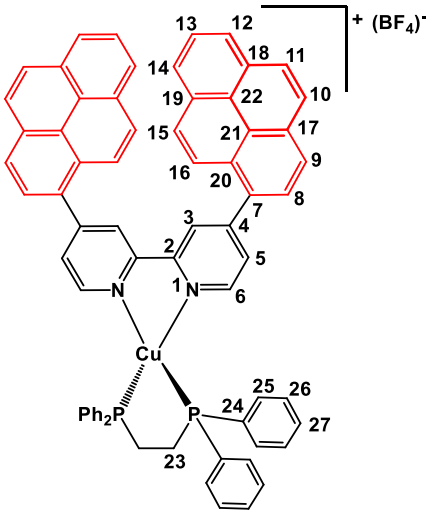

^{1}H NMR (500 MHz, methylene chloride-d_2) δ 8.73 (d, J = 1.5 Hz, 2H, H_3), 8.63 (d, J = 5.3 Hz, 2H, H_6), 8.34 (d, J = 8.0 Hz, 2H, H_9), 8.31 (d, J = 7.7 Hz, 2H, H_{12}), 8.26 (d, J = 7.7 Hz, 2H, H_{14}), 8.22 (d, J = 9.0 Hz, 2H, H_{11}), 8.19 – 8.15, (m, 6H, H_{10}, H_{15} and H_{16}), 8.13 – 8.07 (m, 4H, H_8 and H_{13}), 7.87 (dd, J = 5.3, 1.5 Hz, 2H, H_5), 7.59 – 7.46 (m, 20H, H_{25}, H_{26} and H_{27}), 2.78 (t, J = 6.0 Hz, 4H, H_{23}). ^{13}C NMR (126 MHz, methylene chloride-d_2) δ 152.4 (C_2), 152.3 (C_4), 149.9 (C_6), 132.3 (C_{25}), 132.2 (C_7), 132.17 (C_{24}), 131.4 (C_q), 130.8 (C_{27}), 130.6 (C_{19} or C_{20}), 130.5 (C_q), 129.4 (C_{26}) 129.0 (C_{15}), 128.8 (C_{11}), 128.1 (C_{19} or C_{20}), 127.9 (C_5), 127.2 (C_{10}) , 126.9 (C_8), 126.7 (C_{13}), 126.3 (C_{12}), 125.7 (C_{14}), 125.0 (C_9), 124.9 (C_{21}), 124.4 (C_{22} and C_{18}), 124.2 (C_3), 123.2 (C_{16}), 25.5 (C_{23}). HRMS (MALDI): *m/z* = 1017.2566 $[M]^+$ (calculated 1017.2583 for $C_{68}H_{48}CuN_2P_2$).

Cu2b

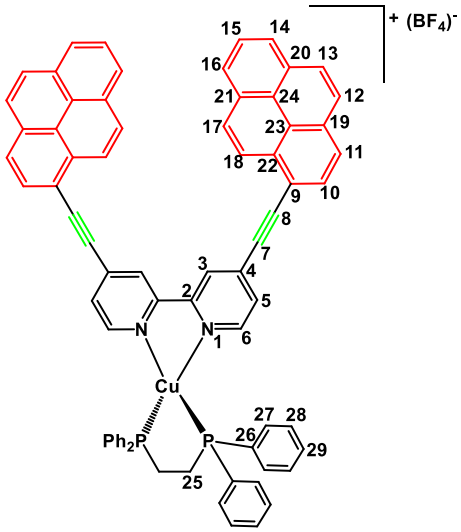

^{1}H NMR (500 MHz, methylene chloride-d_2) δ 8.78 (s, 1H, H_3), 8.76 (s, 1H, H_{18}), 8.46 (d, J = 5.3 Hz, 2H, H_6), 8.39 – 8.32 (m, 8H, H_{10}, H_{17}, H_{16} and H_{14}), 8.28 (d, J = 8.0 Hz, 2H, H_{11}), 8.25 (d, J = 8.9 Hz, 2H, H_{13}), 8.17 (d, J = 8.9 Hz, 2H, H_{12}), 8.14 (t, J = 7.6 Hz, 2H, H_{15}), 7.82 (d, J = 5.3 Hz, 2H, H_5), 7.53 – 7.37 (m, 20H, H_{27}, H_{28} and H_{29}), 2.74 (t, J = 5.8 Hz, 4H, H_{25}). ^{13}C NMR (101 MHz, methylene chloride-d_2) δ 151.8 (C_2), 149.9 (C_6), 134.6 (C_4), 132.6 (C_{24}), 132.1 (C_{27}), 131.8 (C_{26}), 131.2 (C_{20}), ,130.8 (C_{21}), 130.77 (C_{29}), 130.2 (C_{10}), 129.4 (C_{13}), 129.35 (C_{28}), 129.3 (C_{17}), 127.7 (C_3), 127.2 (C_{12}), 126.7 (C_{15}), 126.5(C_{14}), 126.4 (C_{16}), 124.8 (C_{11}), 124.4 (C_{18}), 124.3 (C_{23}), 124.2 (C_5), 124.0 (C_{19} and C_{22}), 115.2 (C_9), 97.5 (C_8), 91.3 (C_7), 25.4 (C_{25}). HRMS (MALDI): m/z = 1065.2574 $[M]^+$ (calculated 1065.2583 for $C_{72}H_{48}CuN_2P_2$).

NMR and HR-MS spectra

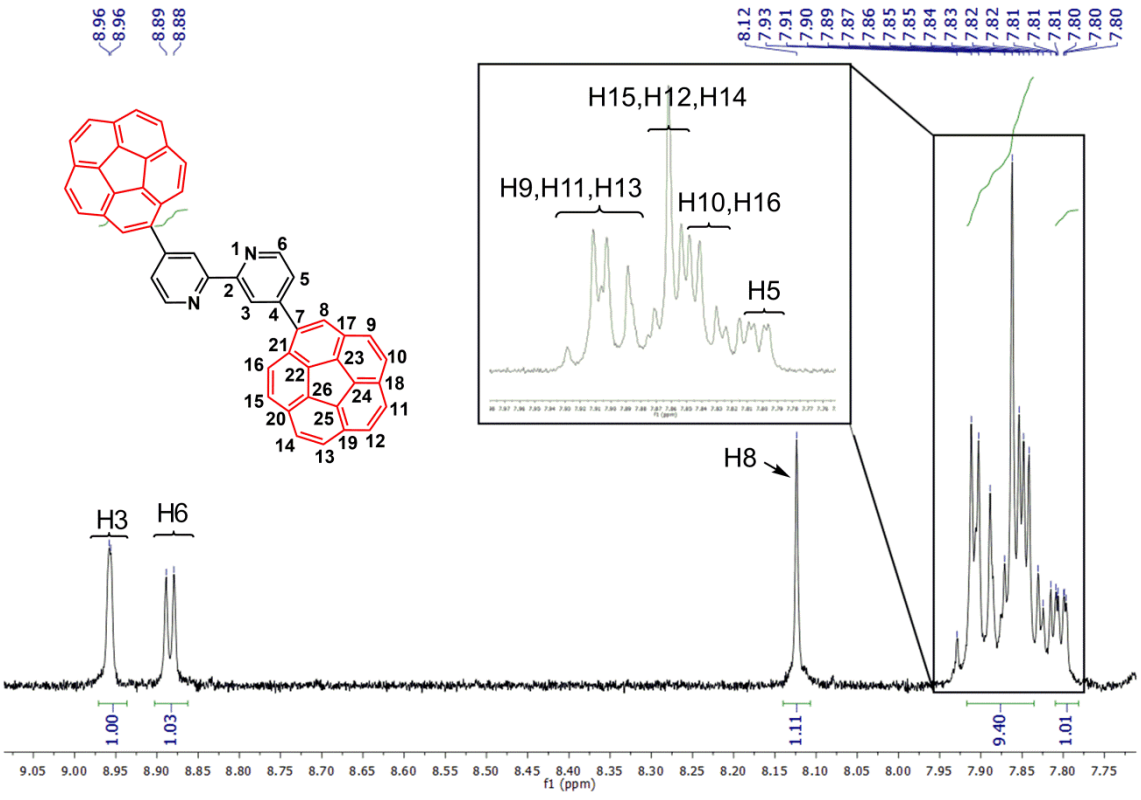

Figure S 1. ^{1}H-NMR (500 MHz, $CDCl_3$) spectrum of compound **L1a**.

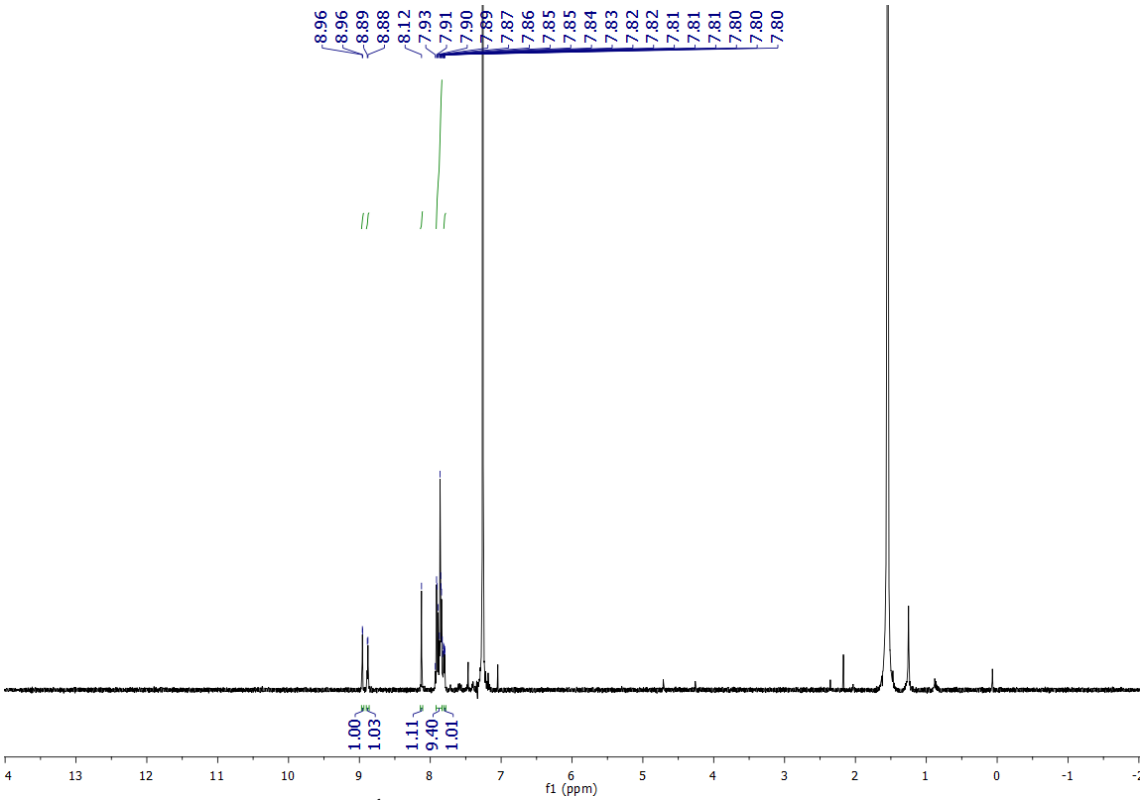

Figure S 2. Full ^{1}H-NMR (500 MHz, $CDCl_3$) spectrum of compound **L1a**.

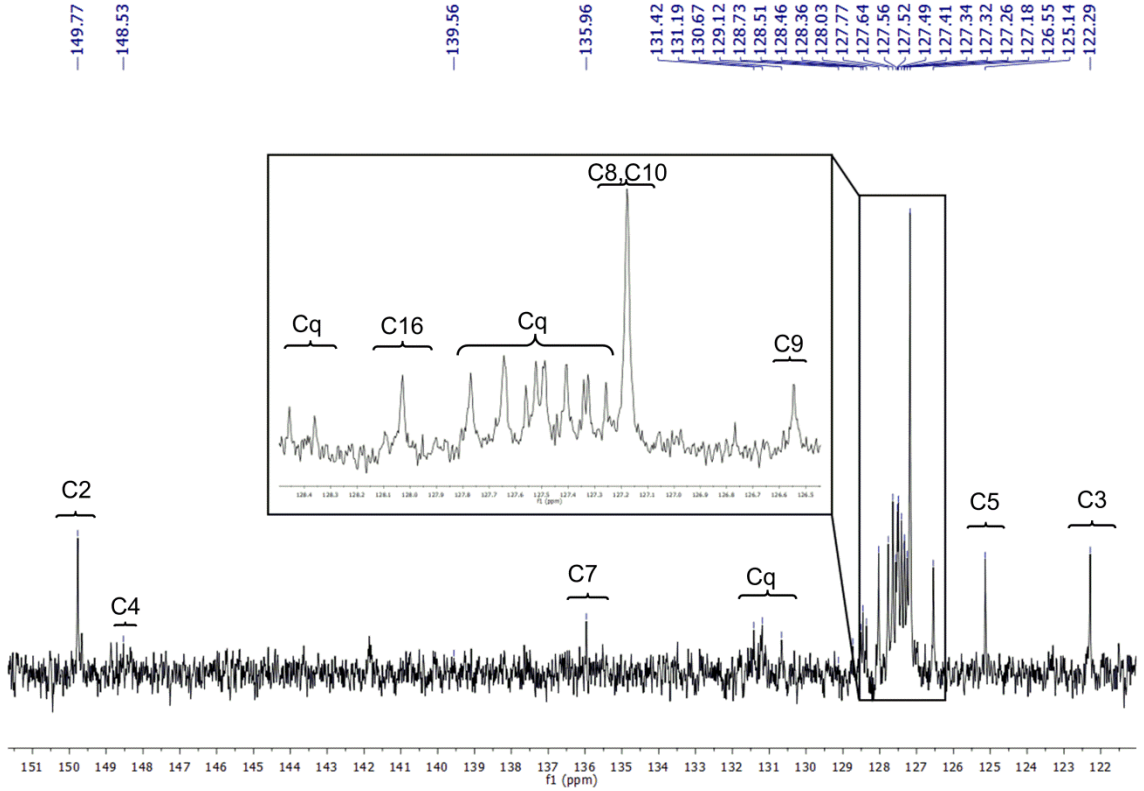

Figure S 3. $^{13}C\{^{1}H\}$-NMR (126 MHz, $CDCl_3$) spectrum of compound **L1a**.

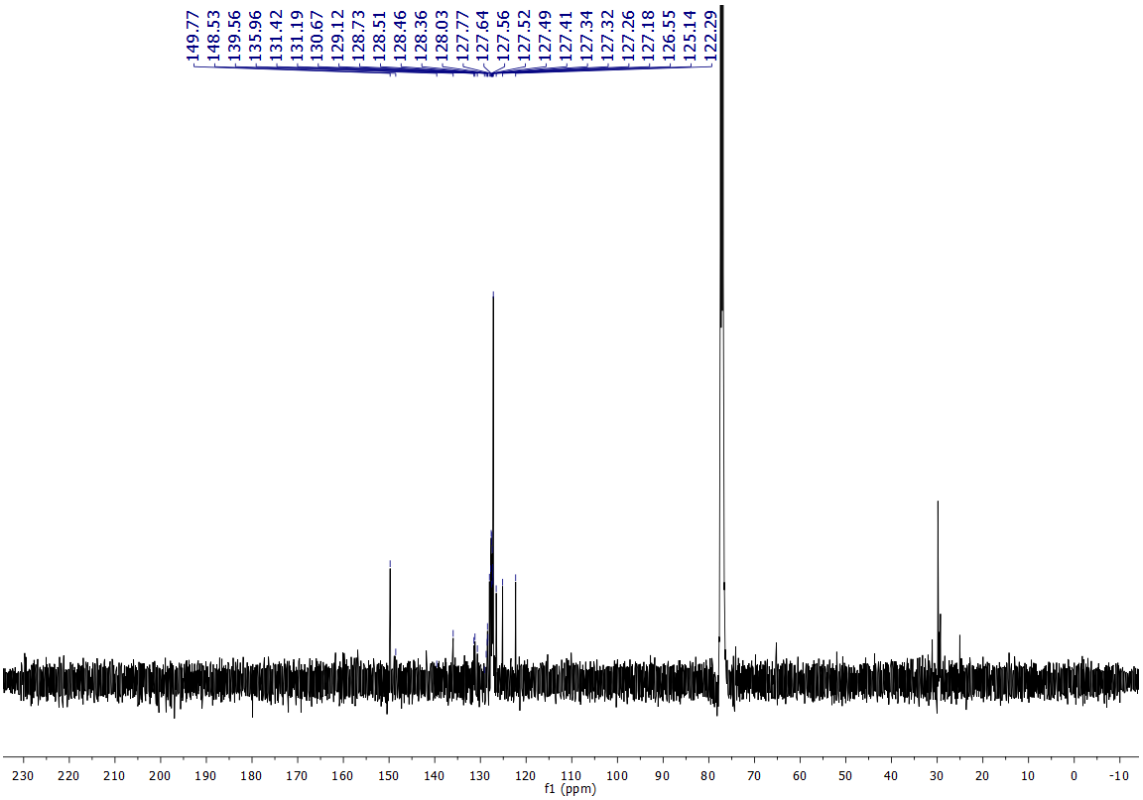

Figure S 4. Full $^{13}C\{^{1}H\}$-NMR (126 MHz, $CDCl_3$) spectrum of compound **L1a**.

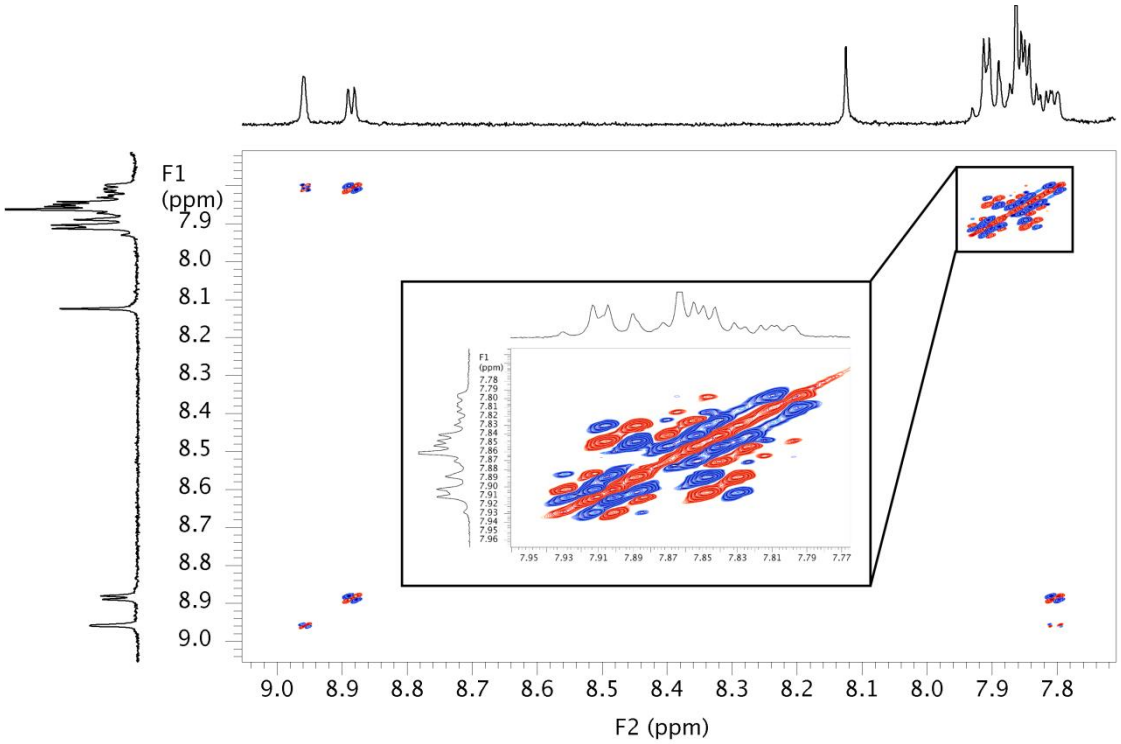

Figure S 5. ^{1}H-^{1}H gDQFCOSY (500 MHz, $CDCl_3$) spectrum of compound **L1a.**

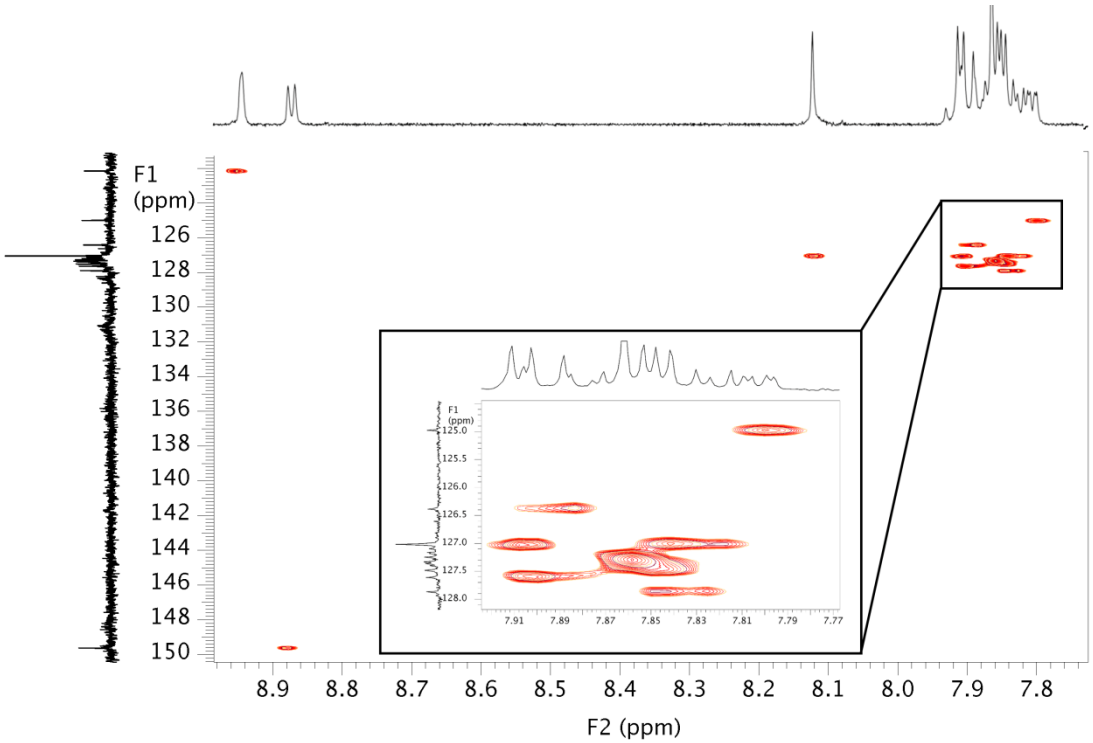

Figure S 6. ^{1}H-^{13}C bsgHSQCAD (500 MHz, $CDCl_3$) spectrum of compound **L1a**.

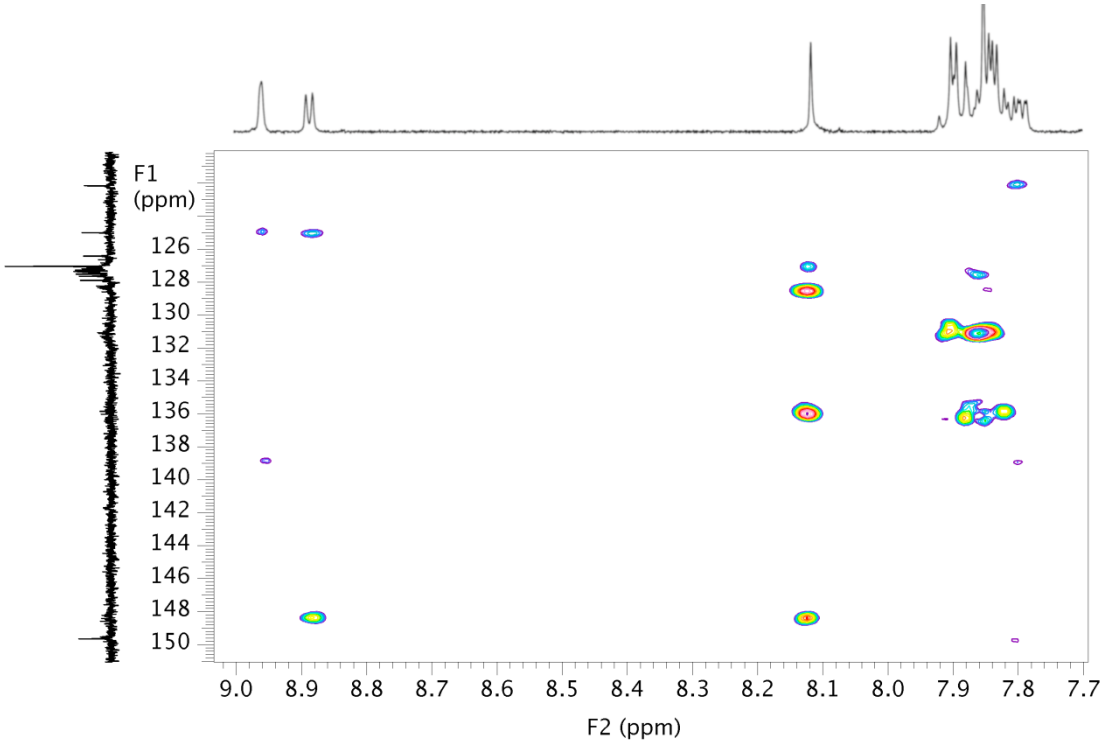

Figure S 7. ^{1}H-^{13}C bsgHMBC (500 MHz, $CDCl_3$) spectrum of compound **L1a**.

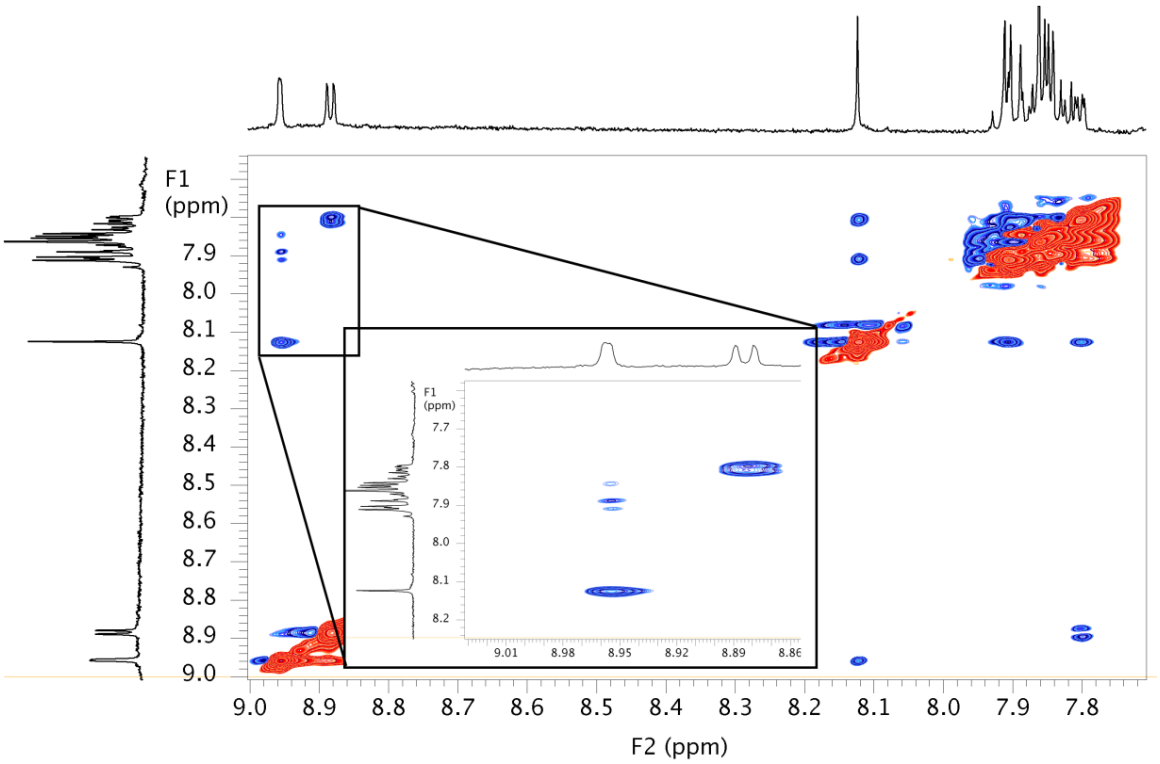

Figure S 8. ^{1}H-^{1}H bashdNOESY (500 MHz, $CDCl_3$) spectrum of compound **L1a**. Some correlations are shown between pyridine and corannulene protons (H_3 and H_8) which permit the determination of those nuclei.

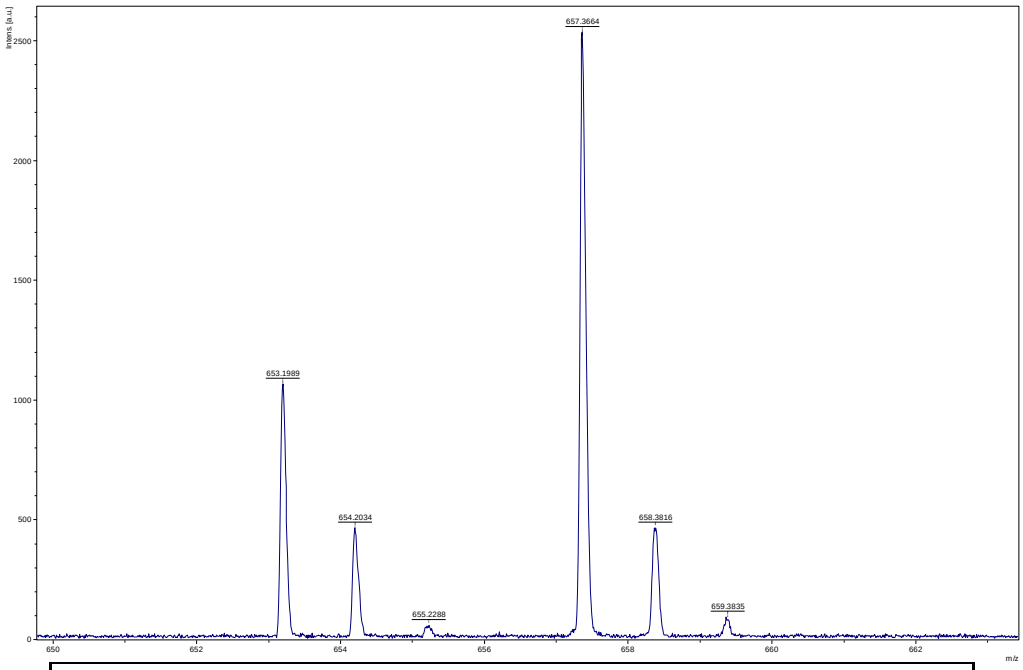

Meas. m/z	m/z	err [ppm]	Ion Formula
653.1989	653.2012	-2.3	$C_{50}H_{25}N_2$

Figure S 9. HRMS (MALDI) of compound **L1a** $[M+H]^+$.

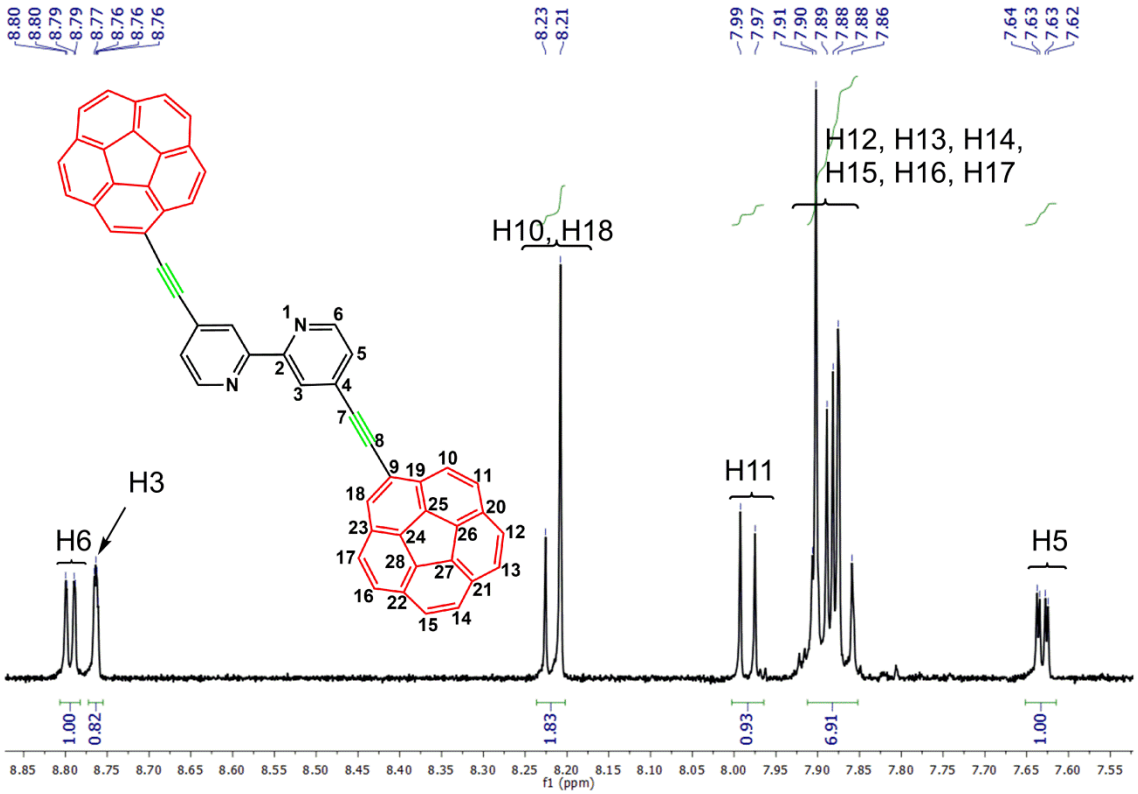

Figure S 10. ^{1}H-NMR (500 MHz, CD_2Cl_2) spectrum of compound **L2a**.

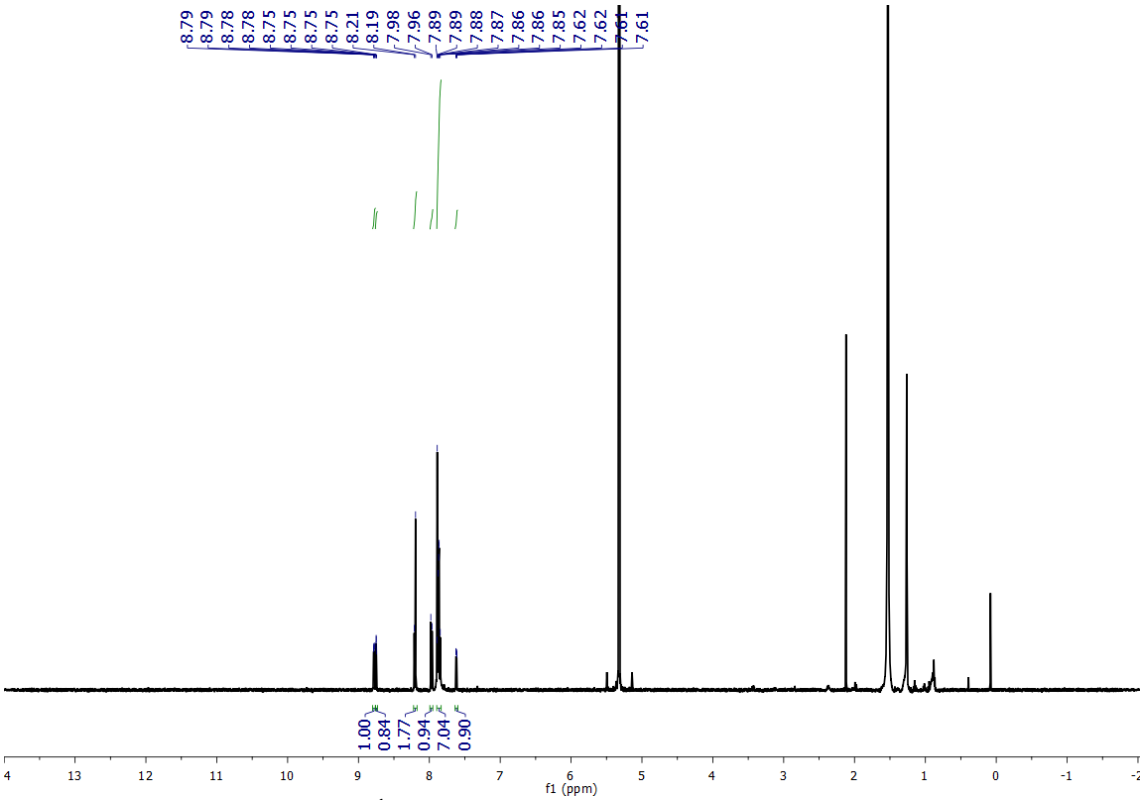

Figure S 11. Full ^{1}H-NMR (500 MHz, CD_2Cl_2) spectrum of compound **L2a**.

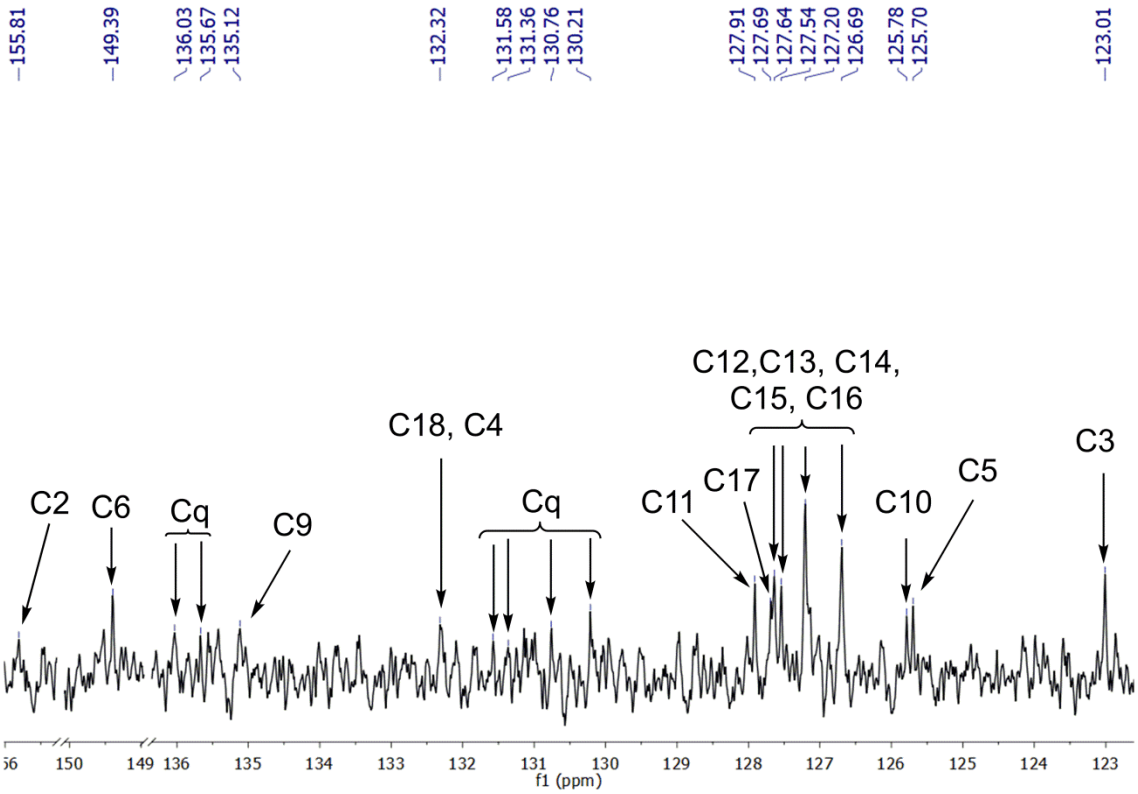

Figure S 12. $^{13}C\{^{1}H\}$-NMR (126 MHz, CD_2Cl_2) spectrum of compound **L2a**.

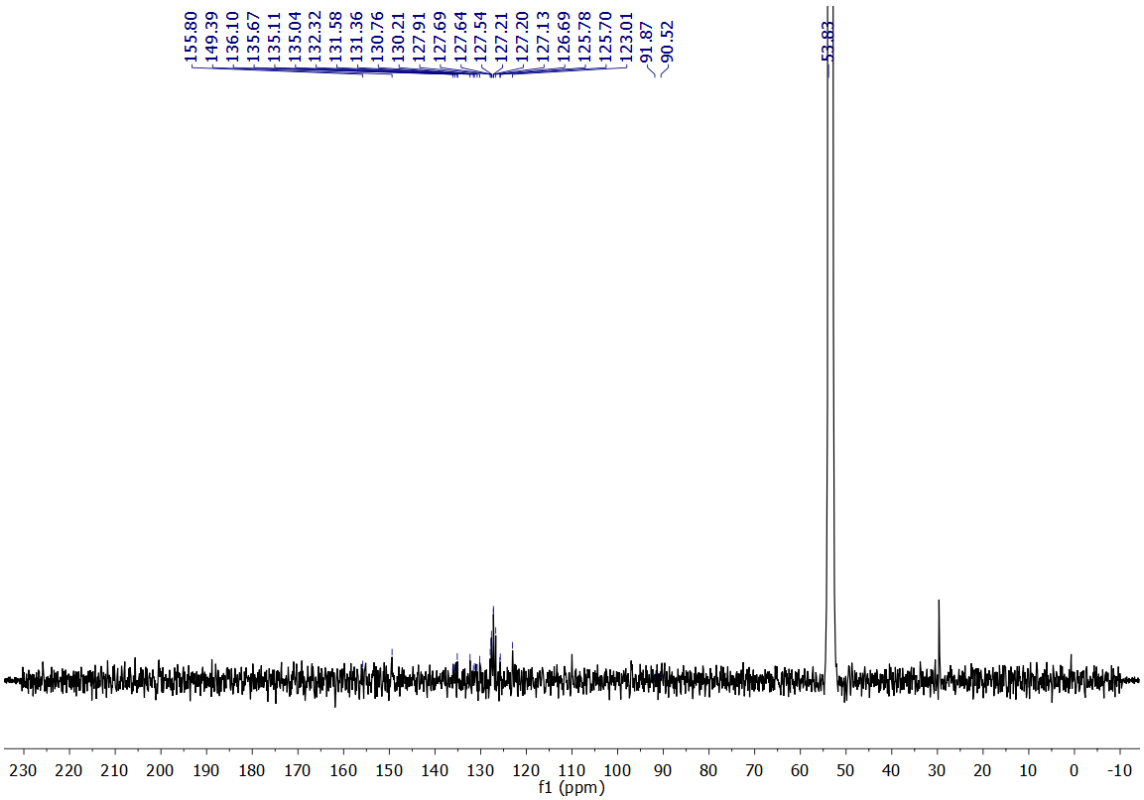

Figure S 13. Full $^{13}C\{^{1}H\}$-NMR (126 MHz, CD_2Cl_2) spectrum of compound **L2a**.

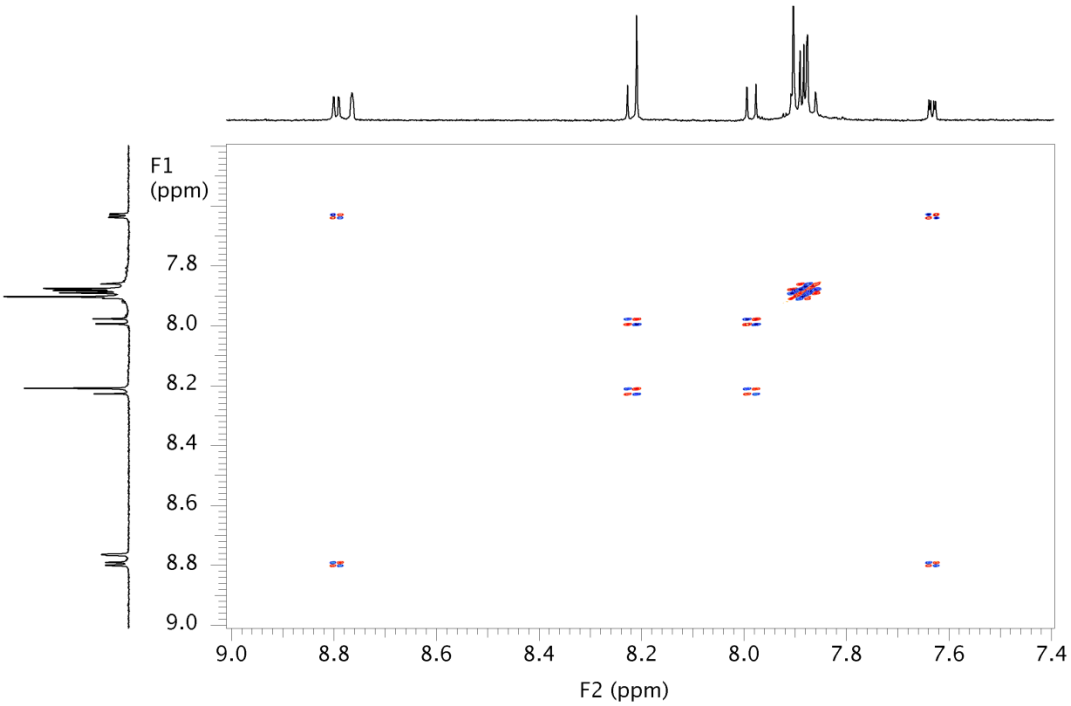

Figure S 14. ^{1}H-^{1}H gDQFCOSY (500 MHz, CD_2Cl_2) spectrum of compound **L2a**.

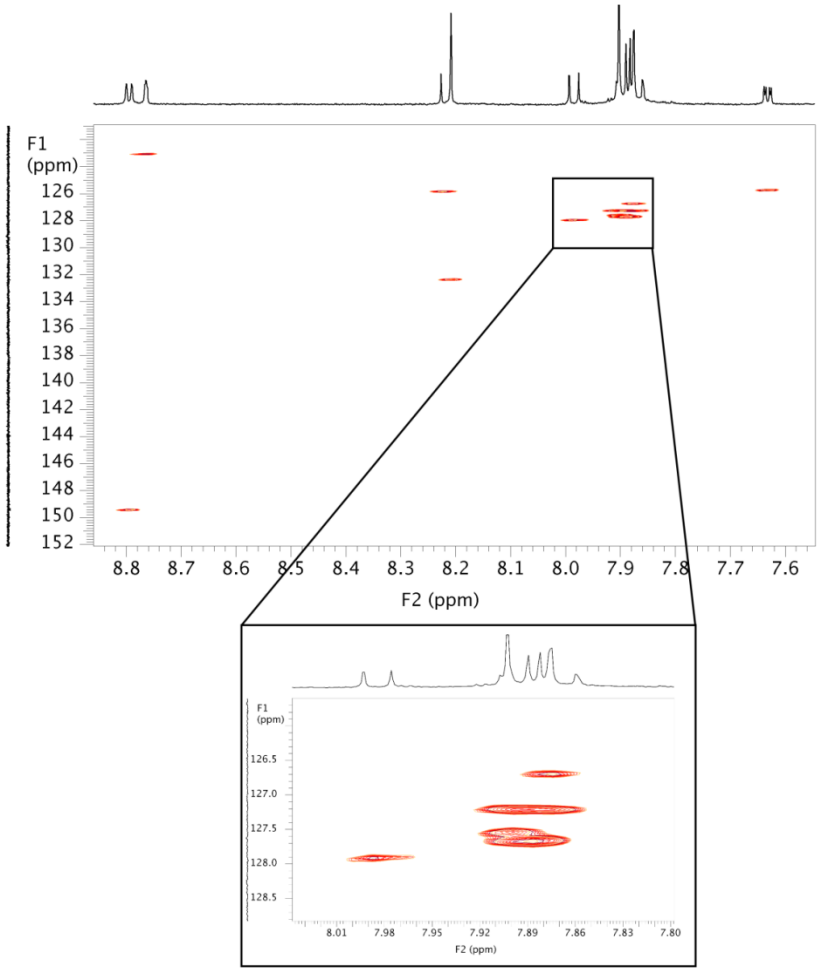

Figure S 15. ^{1}H-^{13}C bsgHSQCAD (500 MHz, CD_2Cl_2) spectrum of compound **L2a**.

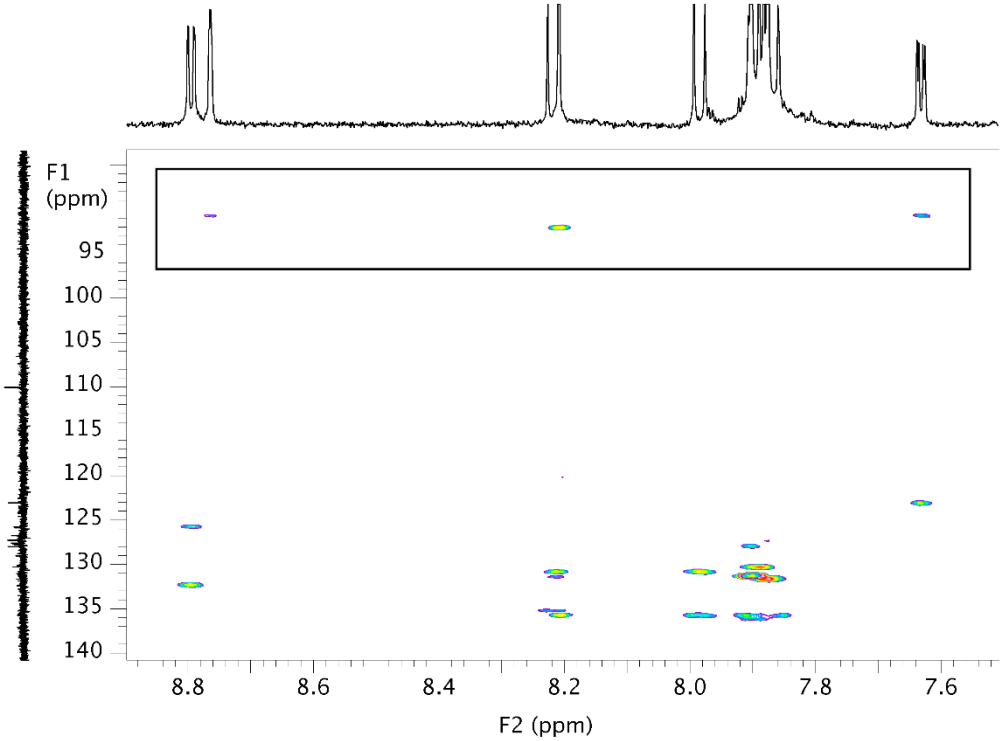

Figure S 16. ^{1}H-^{13}C g2cHMBC (500 MHz, CD_2Cl_2) spectrum of compound **L2a**. In this experiment, carbons C_7 and C_8 have been determined by cross peaks with protons from bipyridine (H_3 and H_5) and corannulene (H_{18}) moieties.

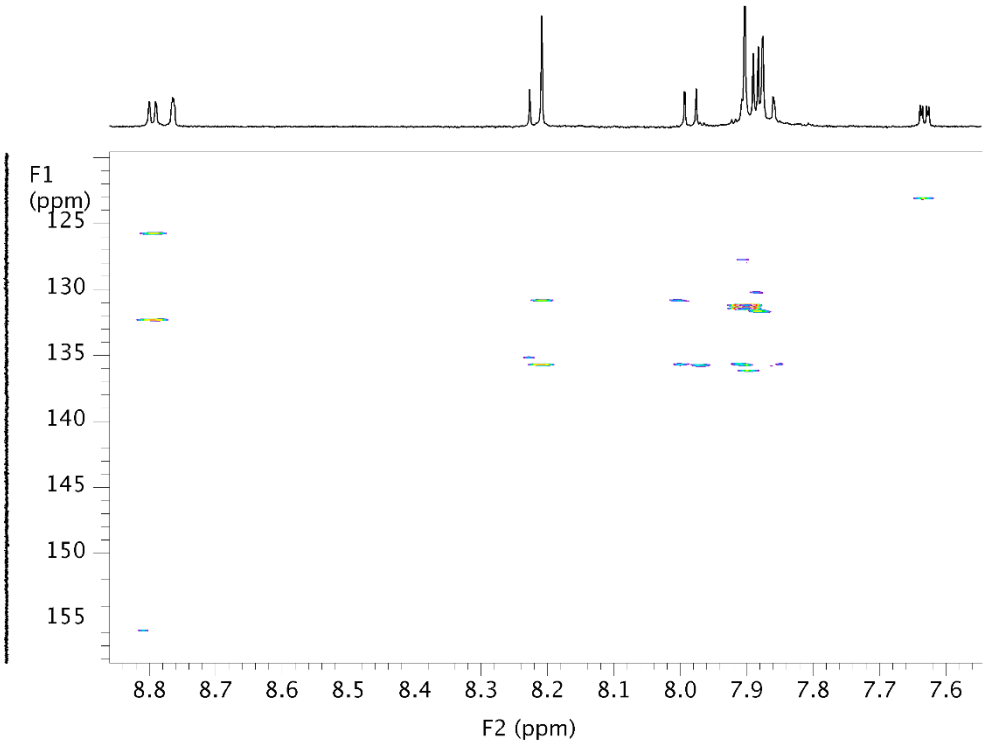

Figure S 17. ^{1}H-^{13}C bsgHMBC (500 MHz, CD_2Cl_2) spectrum of compound **L2a**.

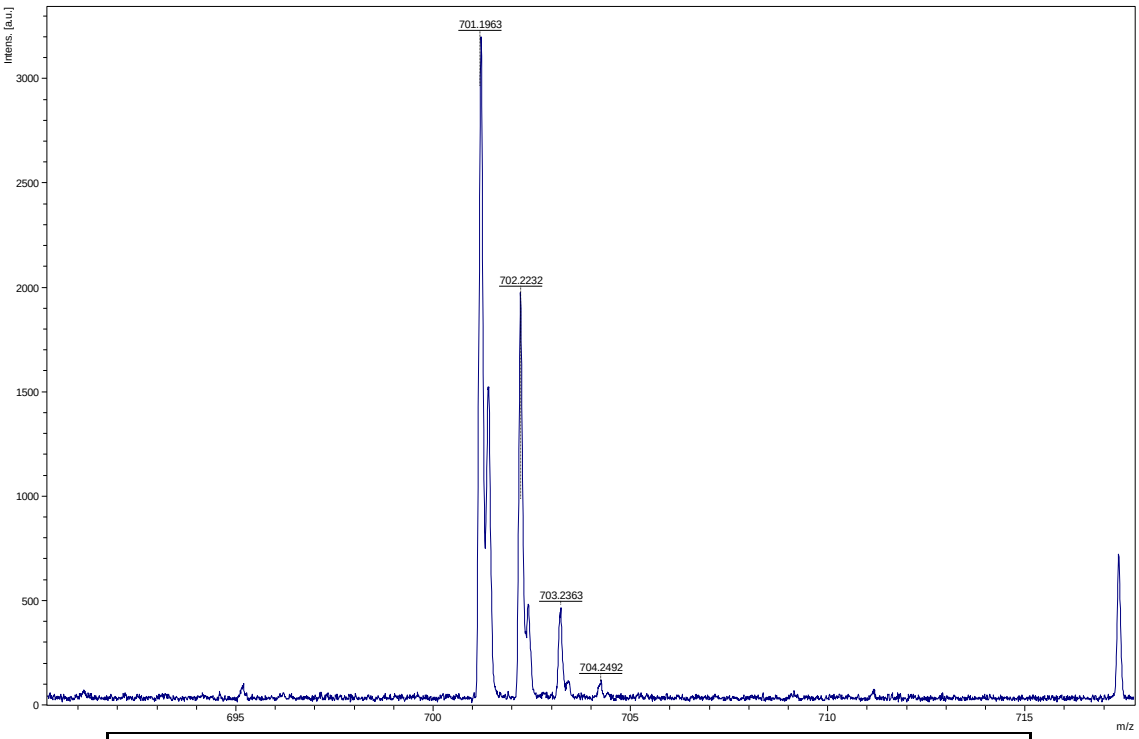

Meas. m/z	m/z	err [ppm]	Ion Formula
701.1963	701.2012	-4.9	$C_{54}H_{25}N_2$

Figure S 18. HRMS (MALDI) of compound **L2a** $[M+H]^+$.

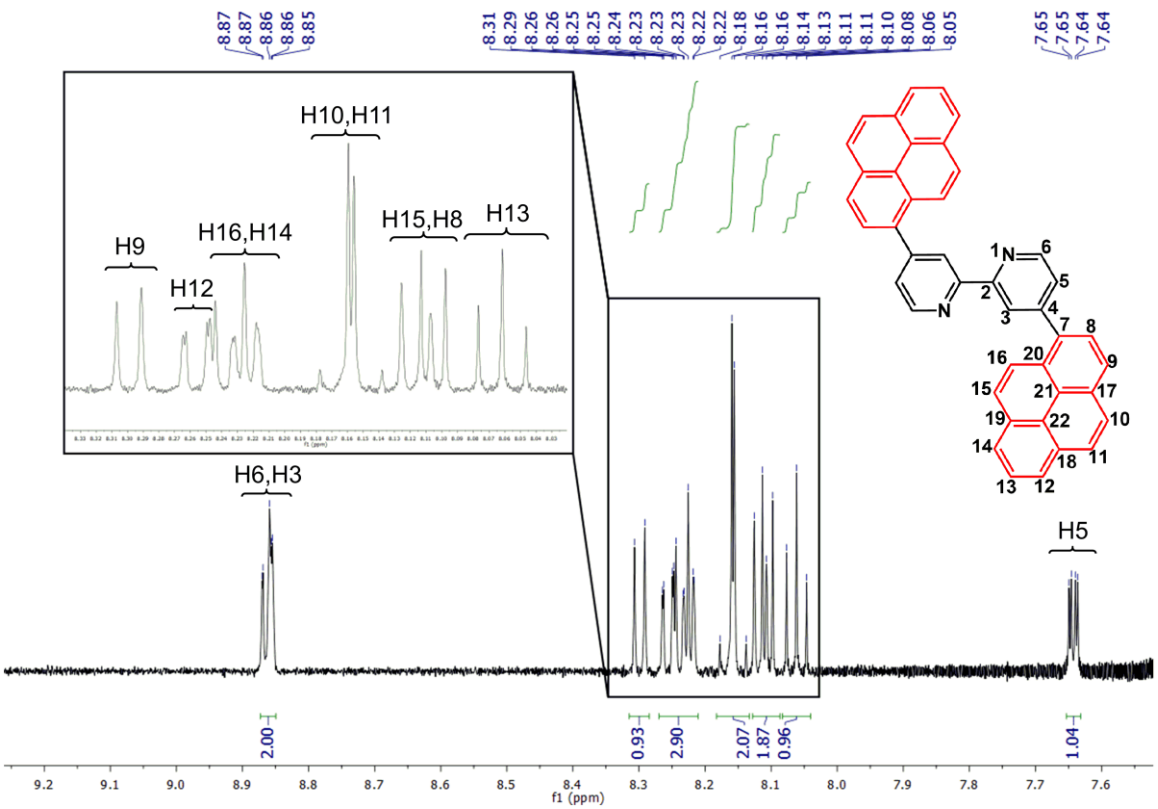

Figure S 19. ^{1}H-NMR (500 MHz, $CDCl_3$) spectrum of compound **L1b**.

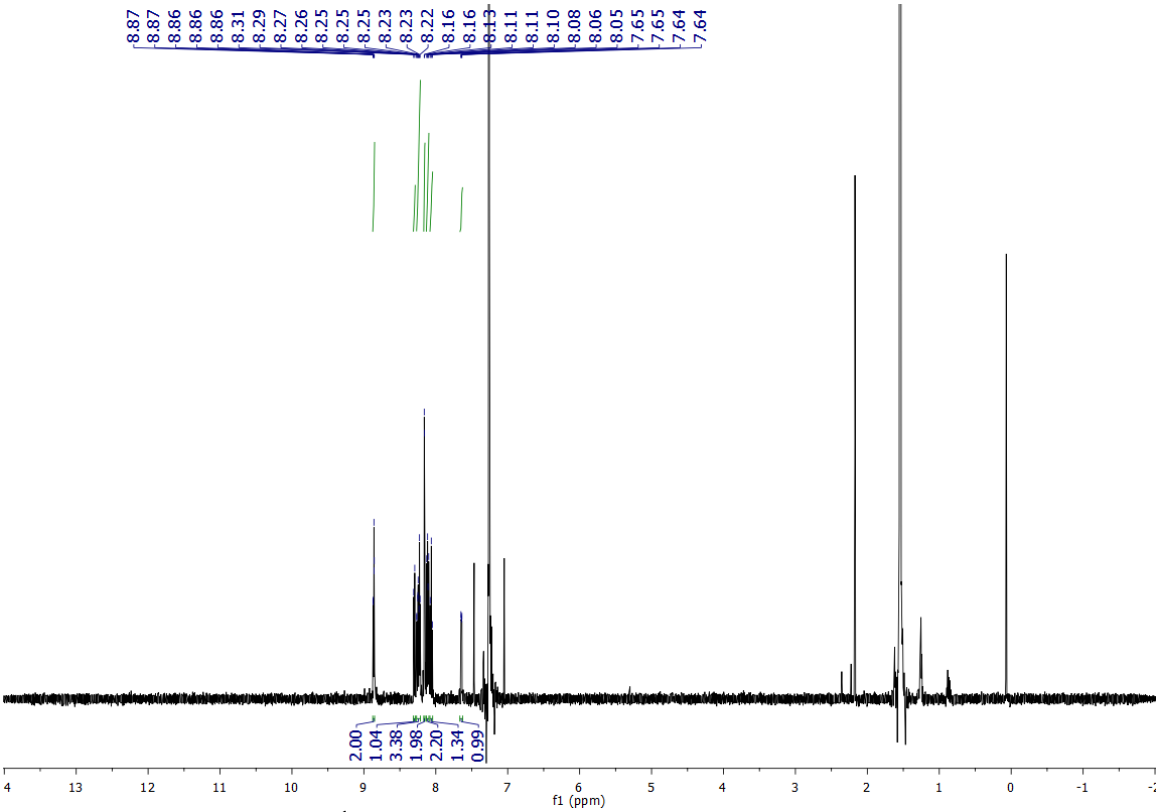

Figure S 20. Full ^{1}H-NMR (500 MHz, $CDCl_3$) spectrum of compound **L1b**.

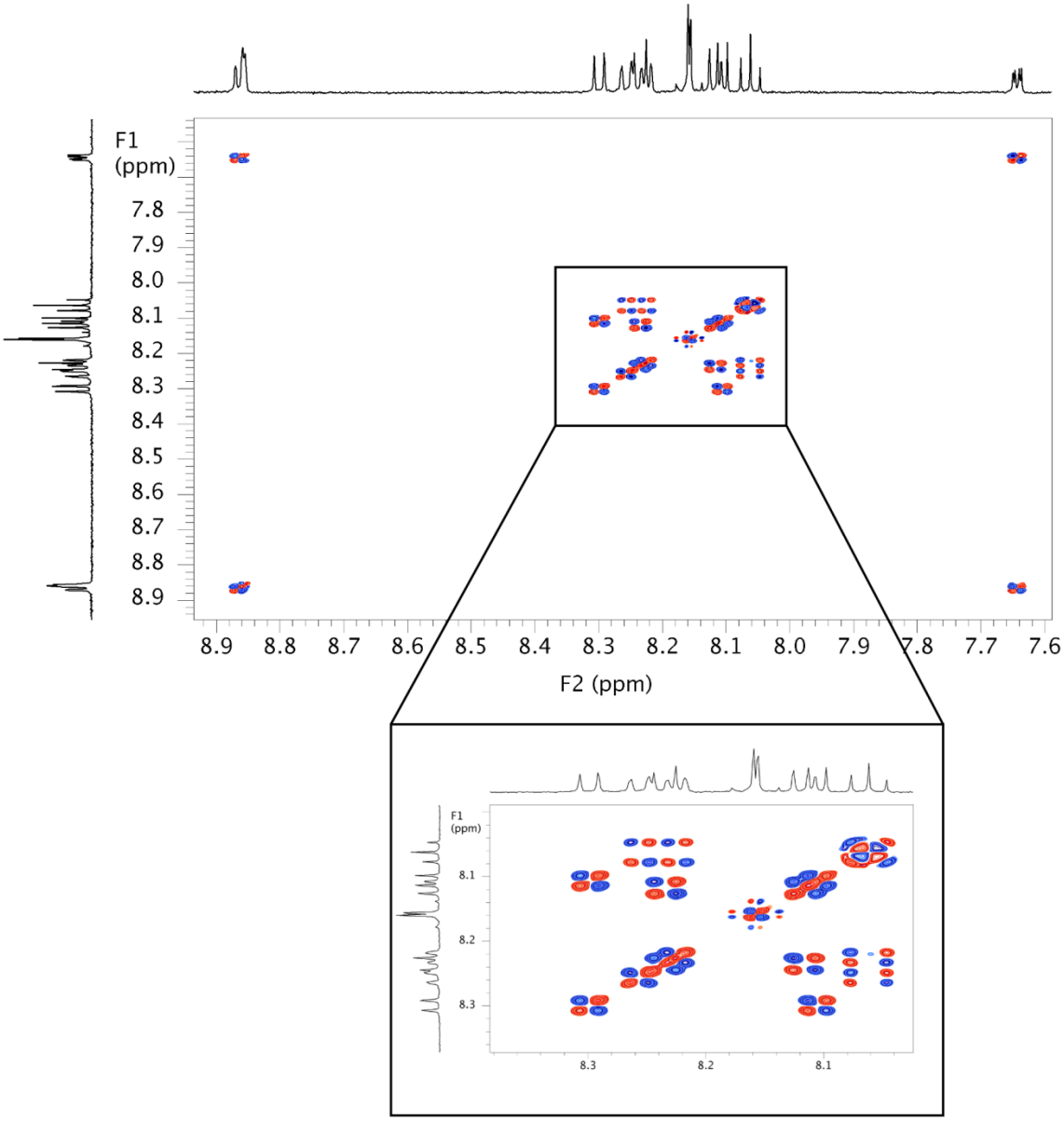

Figure S 21. ^{1}H-^{1}H gDQFCOSY (500 MHz, CDCl3) spectrum of compound **L1b.**

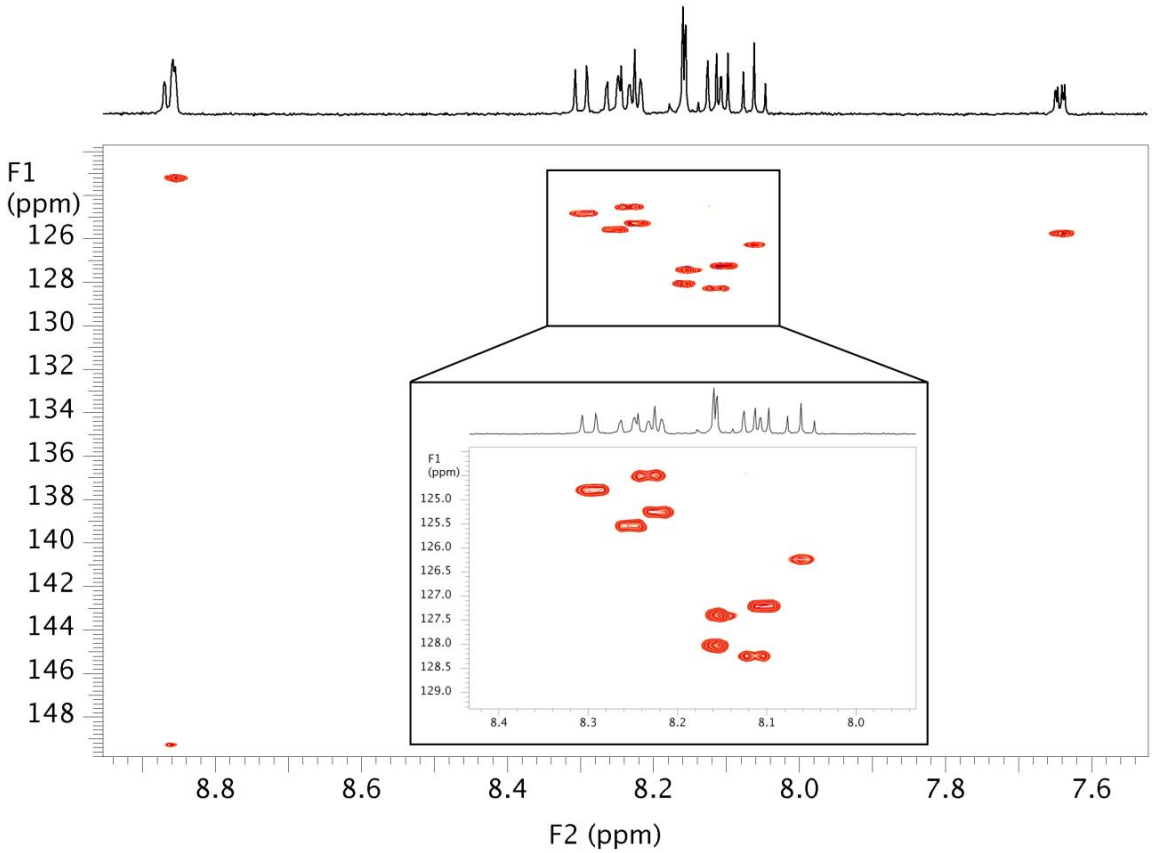

Figure S 22. ^{1}H-^{13}C bsgHSQCAD (500 MHz, $CDCl_3$) spectrum of compound **L1b**.

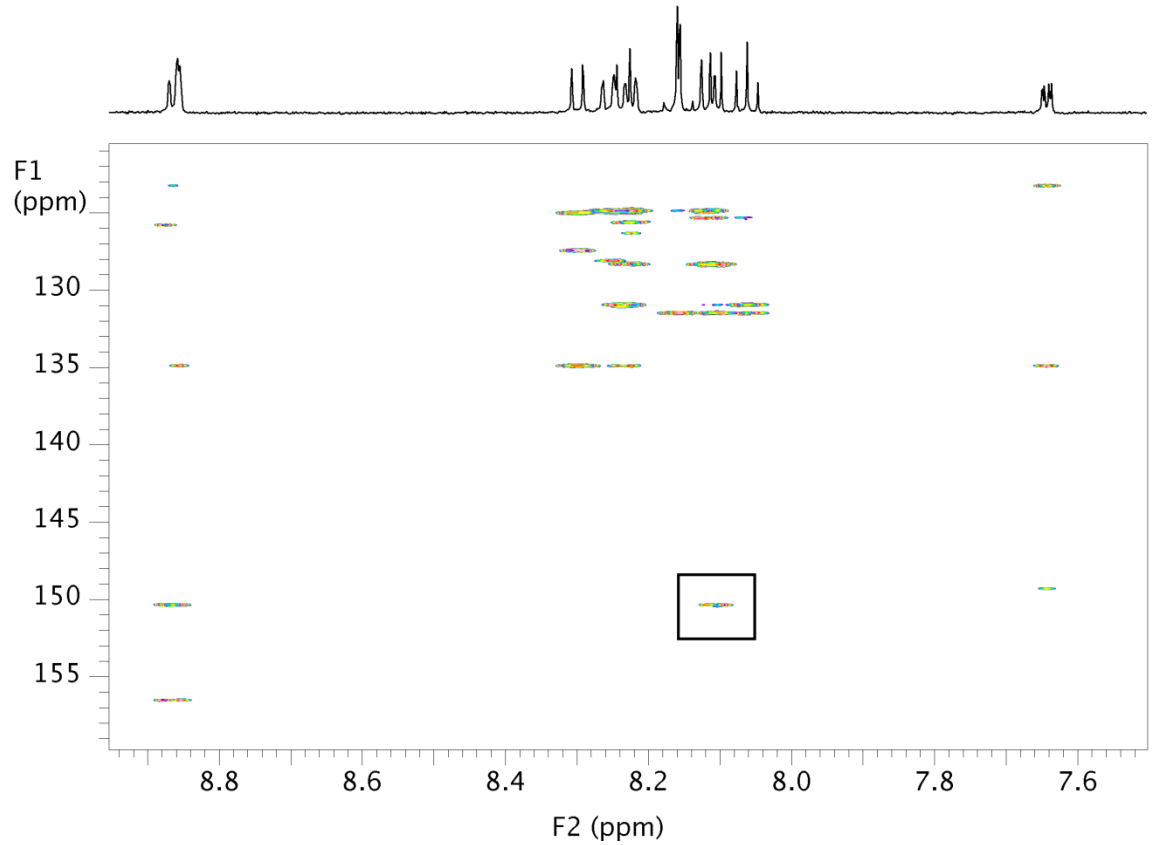

Figure S 23. ^{1}H-^{13}C bsgHMBC (500 MHz, $CDCl_3$) spectrum of compound **L1b**. The cross peak between C_4 and H_8 is essential to distinguish between H_8 and H_{16} in the pyrene scaffold.

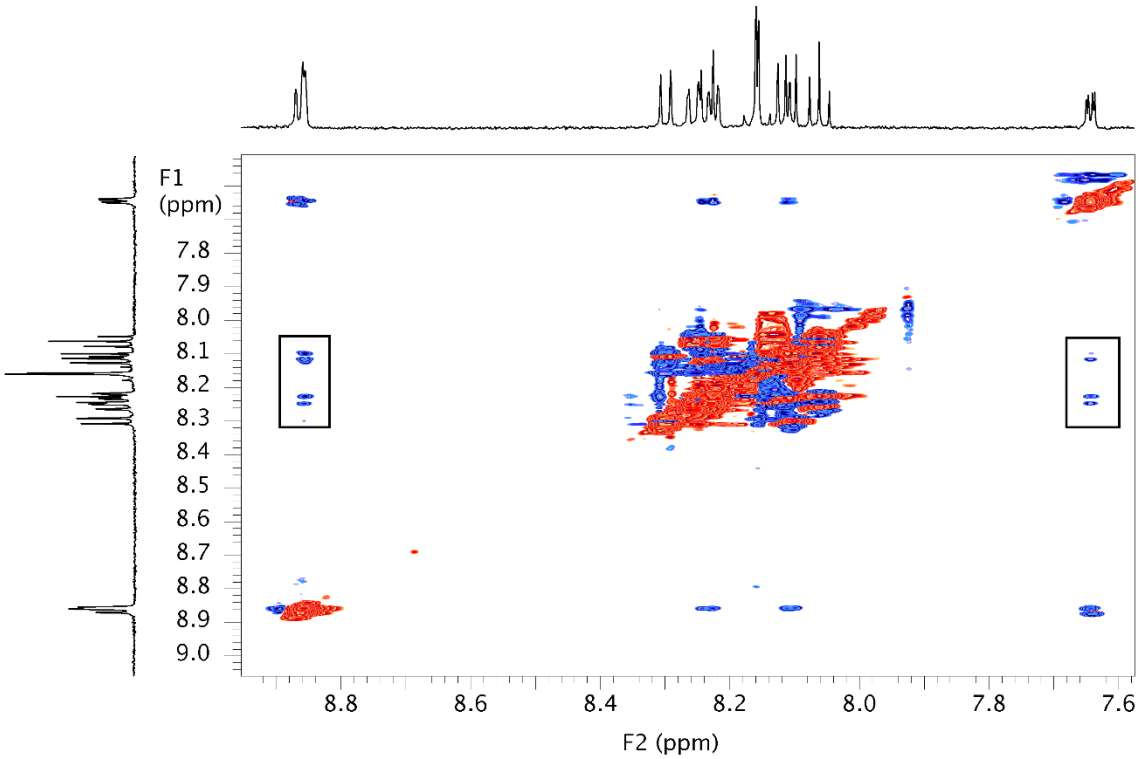

Figure S 24. ^{1}H-^{1}H bashdROESY (500 MHz, $CDCl_3$) spectrum of compound **L1b**. There are some correlations between pyridine and pyrene protons allowing the differentiation between H_8 and H_{16} in pyrene moiety. This experiment along with previously shown ^{1}H-$^{-13}$C bsghHMBC spectrum were crucial for such a task.

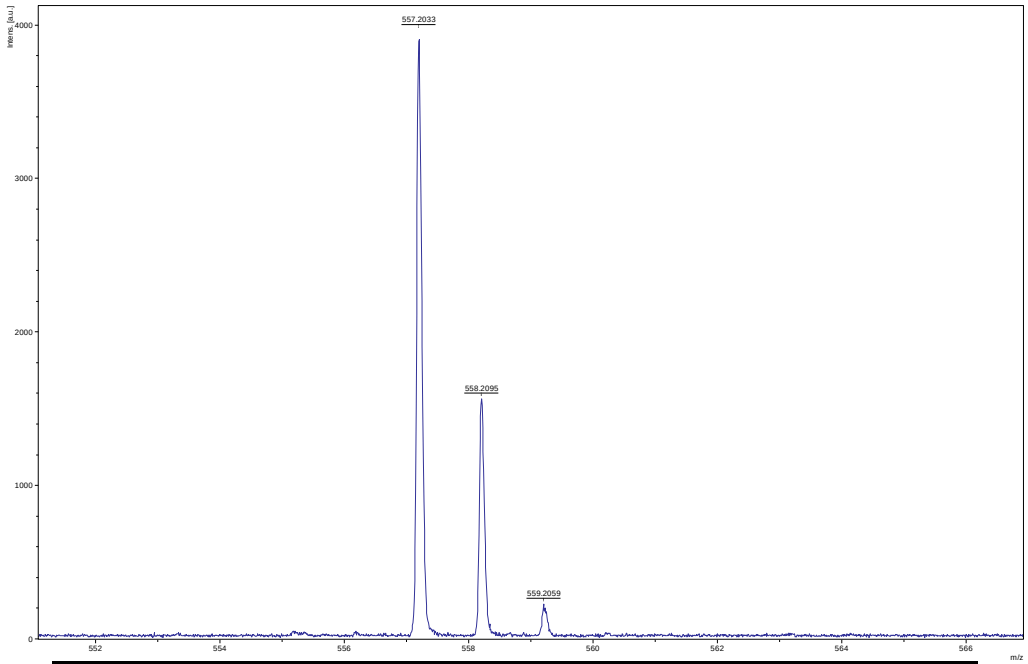

Meas. m/z	m/z	err [ppm]	Ion Formula
557.2033	557.2012	2.1	$C_{42}H_{25}N_2$

Figure S 25. HRMS (MALDI) of compound **L1b** $[M+H]^+$.

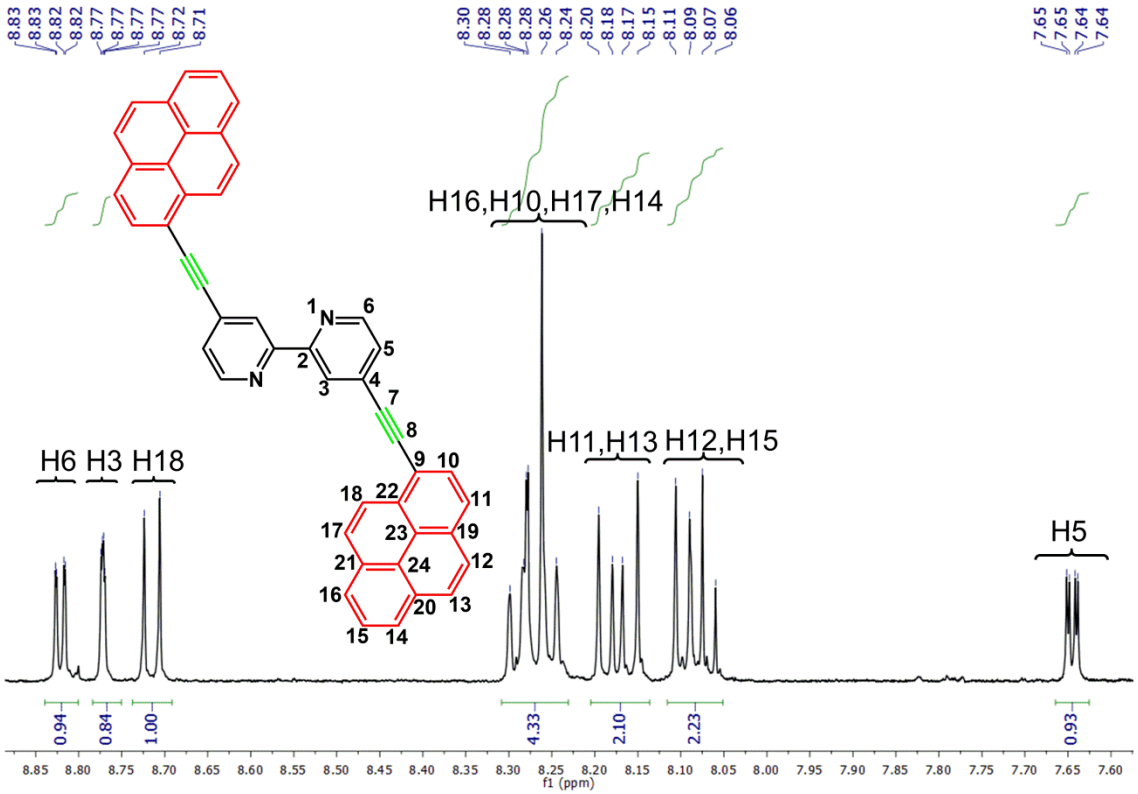

Figure S 26. ^{1}H-NMR (500 MHz, $CDCl_3$) spectrum of compound **L2b**.

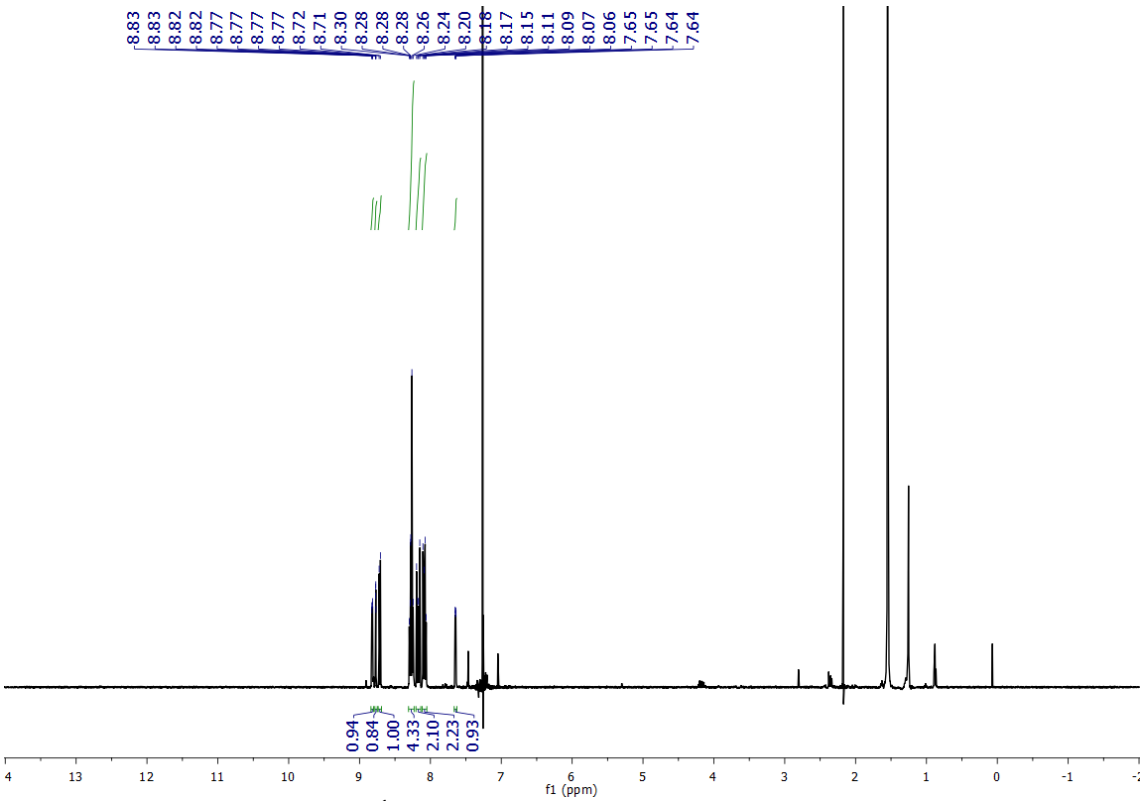

Figure S 27. Full ^{1}H-NMR (500 MHz, $CDCl_3$) spectrum of compound **L2b**.

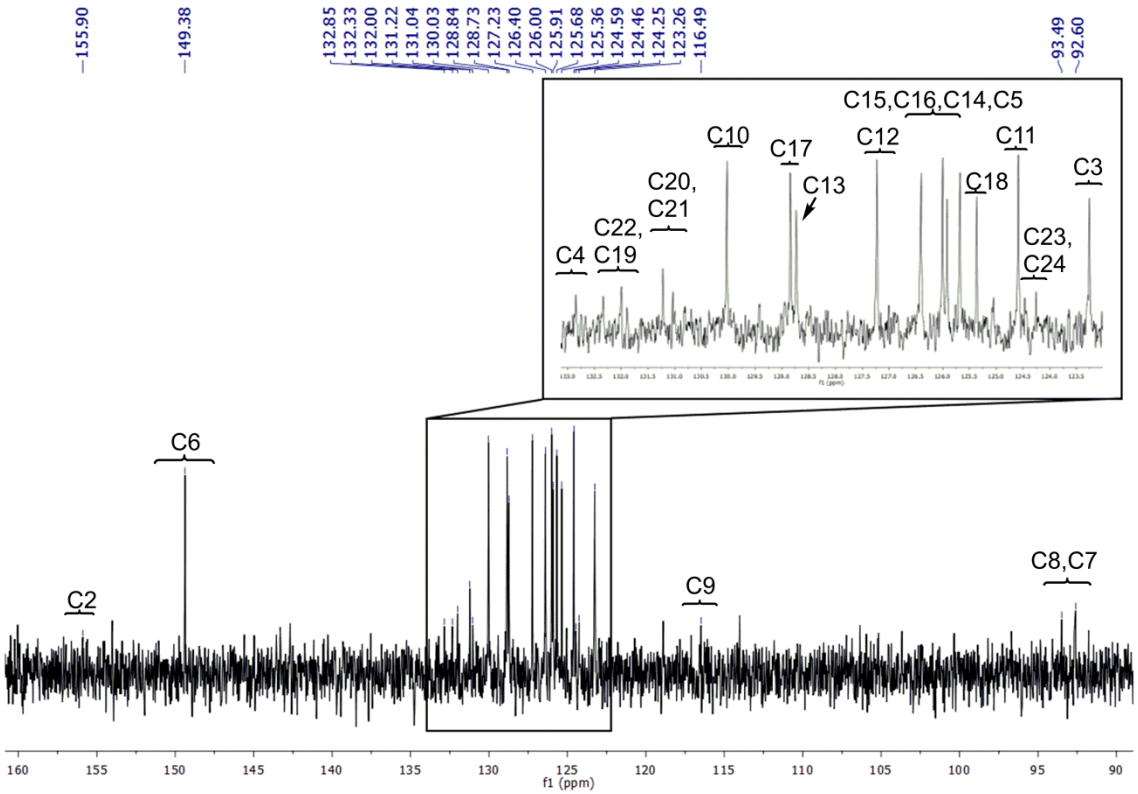

Figure S 28. $^{13}C\{^{1}H\}$-NMR (126 MHz, $CDCl_3$) spectrum of compound **L2b**.

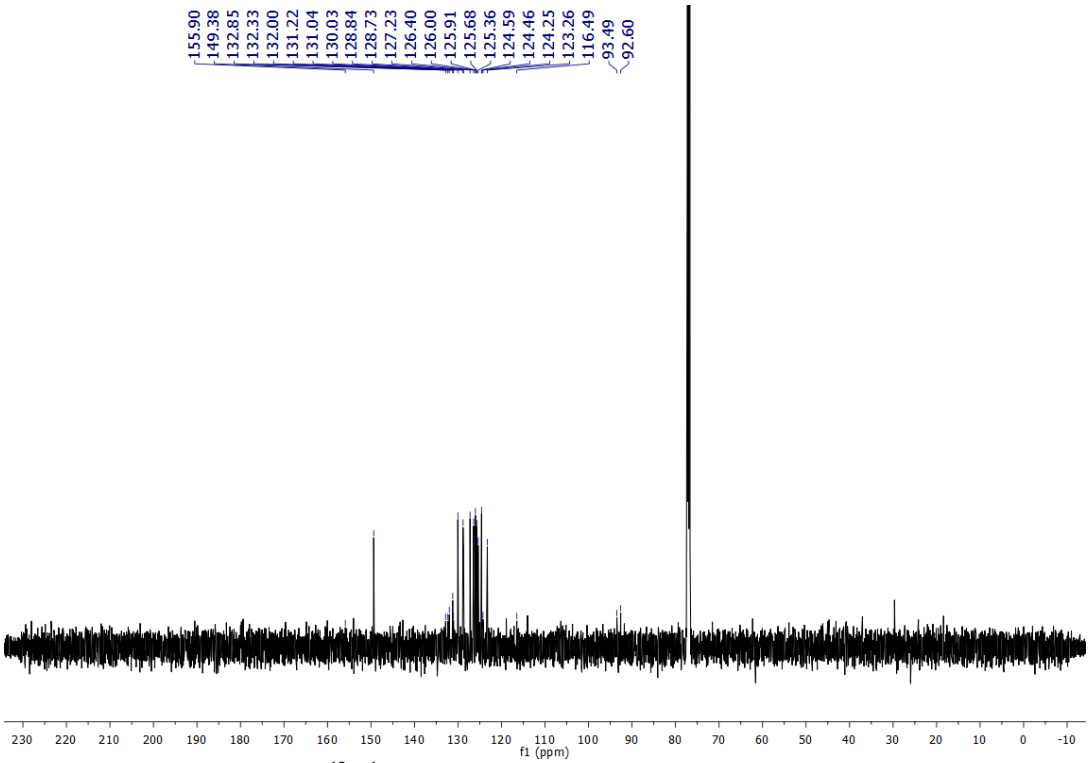

Figure S 29. Full $^{13}C\{^{1}H\}$-NMR (126 MHz, $CDCl_3$) spectrum of compound **L2b**.

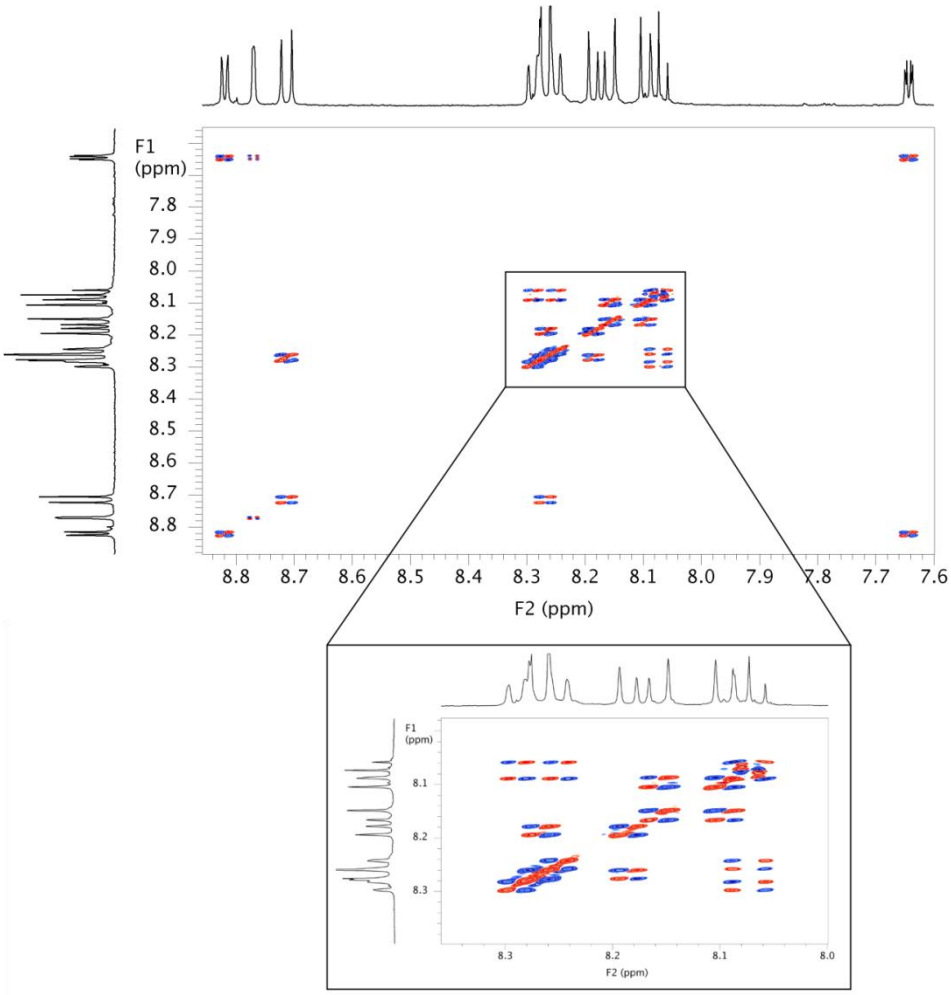

Figure S 30. ^{1}H-^{1}H gDQFCOSY (500 MHz, $CDCl_3$) spectrum of compound **L2b**.

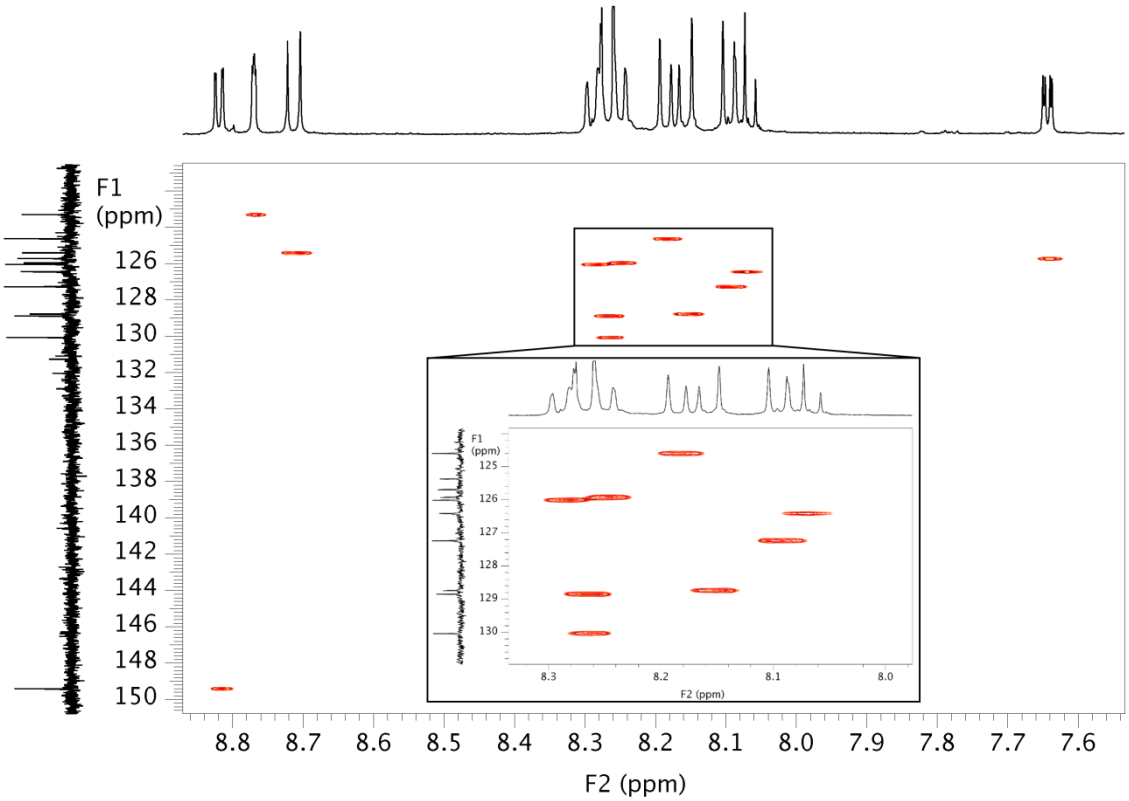

Figure S 31. ^{1}H-^{13}C bsgHSQCAD (500 MHz, $CDCl_3$) spectrum of compound **L2b**.

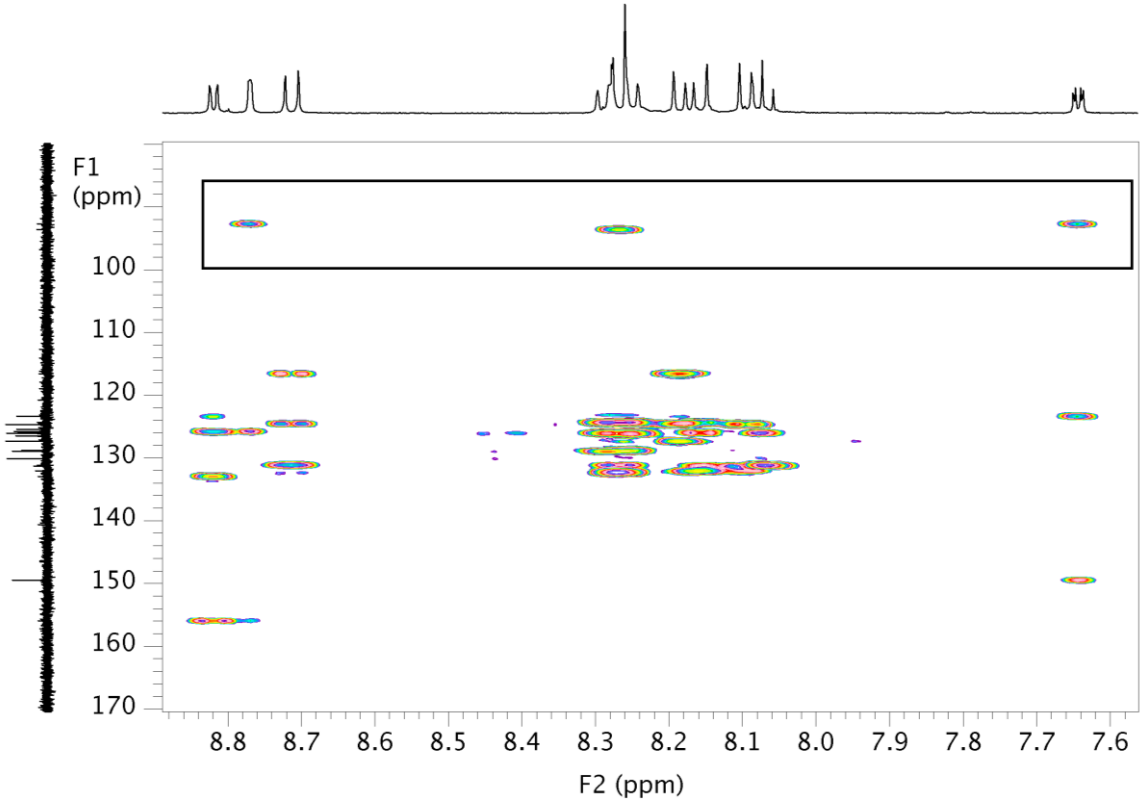

Figure S 32. ^{1}H-^{13}C g2cHMBC (500 MHz, $CDCl_3$) spectrum of compound **L2b**. In this experiment, carbons C_7 and C_8 have been determined by cross peaks with protons from bipyridine (H_3 and H_5) and pyrene (H_{10}) moieties.

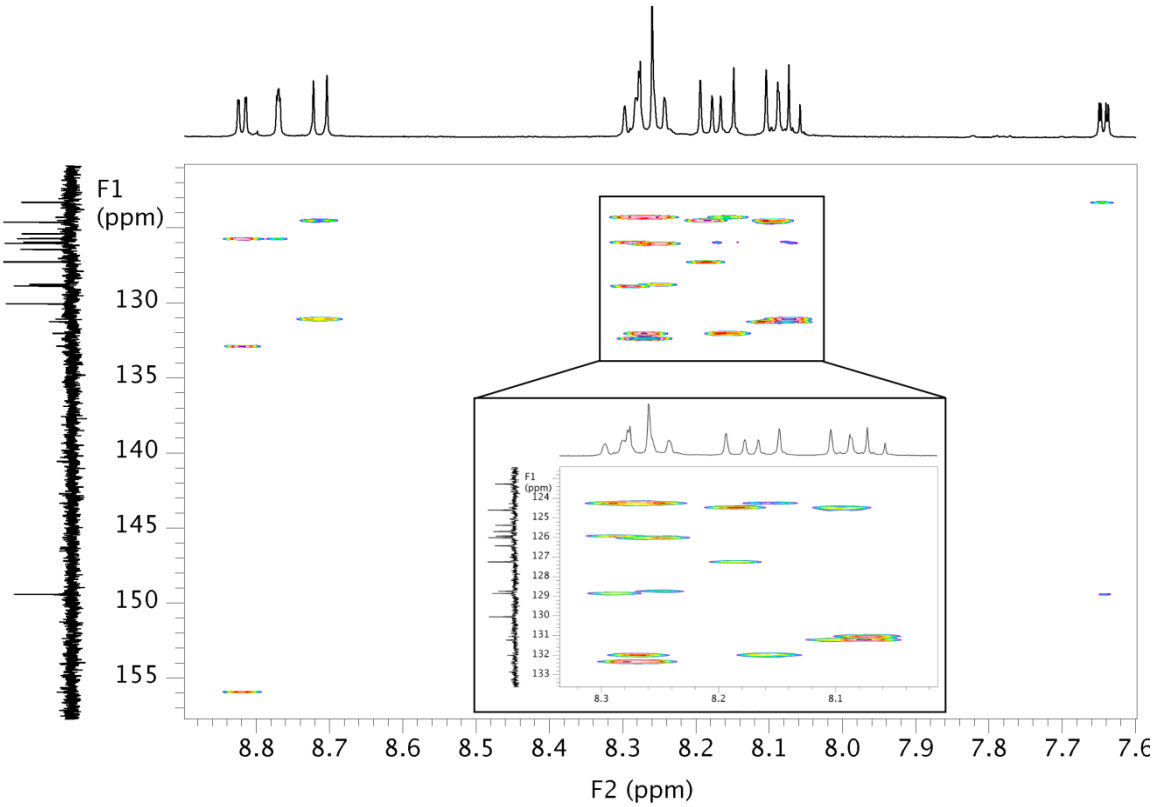

Figure S 33. ^{1}H-^{13}C bsgHMBC (500 MHz, $CDCl_3$) spectrum of compound **L2b**.

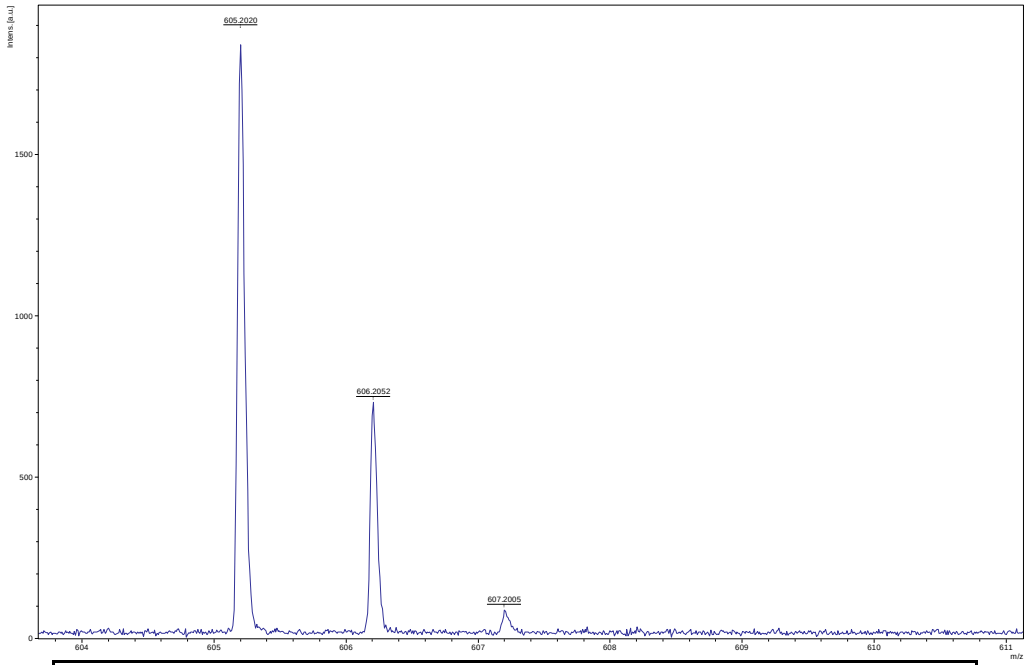

Meas. m/z	m/z	err [ppm]	Ion Formula
605.2020	605.2012	0.8	$C_{46}H_{25}N_2$

Figure S 34. HRMS (MALDI) of compound **L2b** $[M+H]^+$.

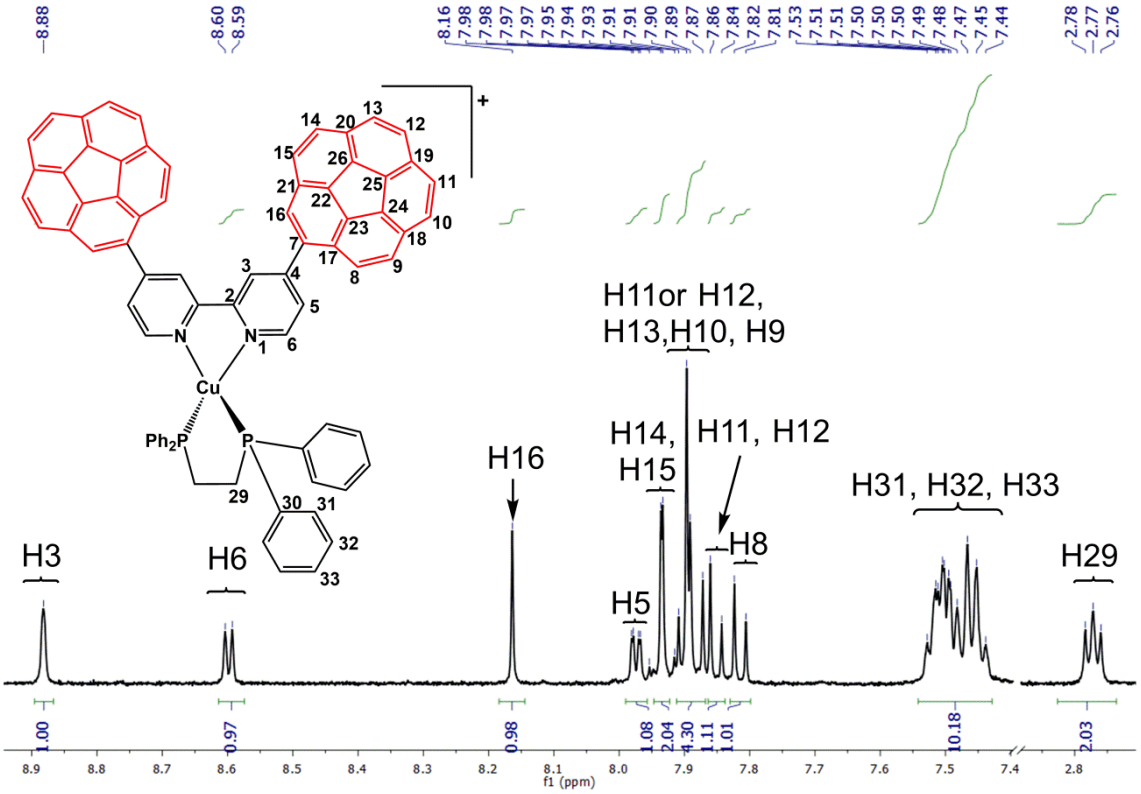

Figure S 35. ^{1}H-NMR (500 MHz, CD_2Cl_2) spectrum of complex **Cu1a**.

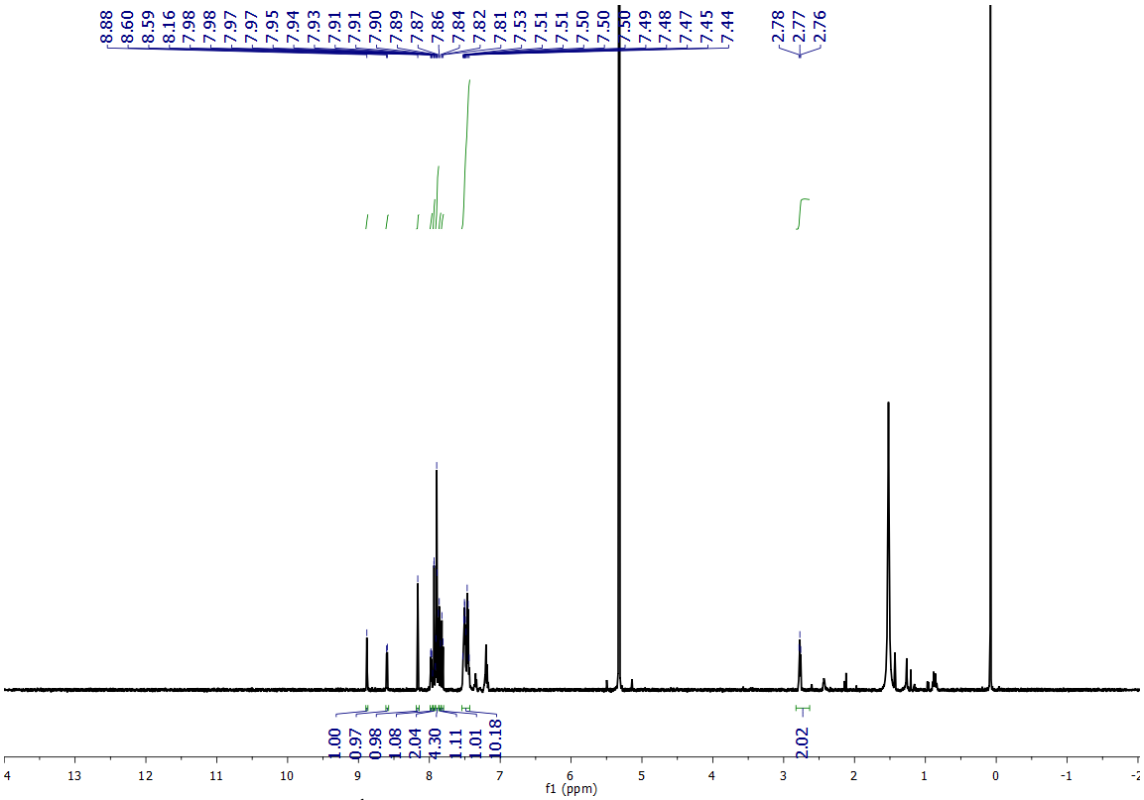

Figure S 36. ^{1}H-NMR (500 MHz, CD_2Cl_2) spectrum of complex **Cu1a**.

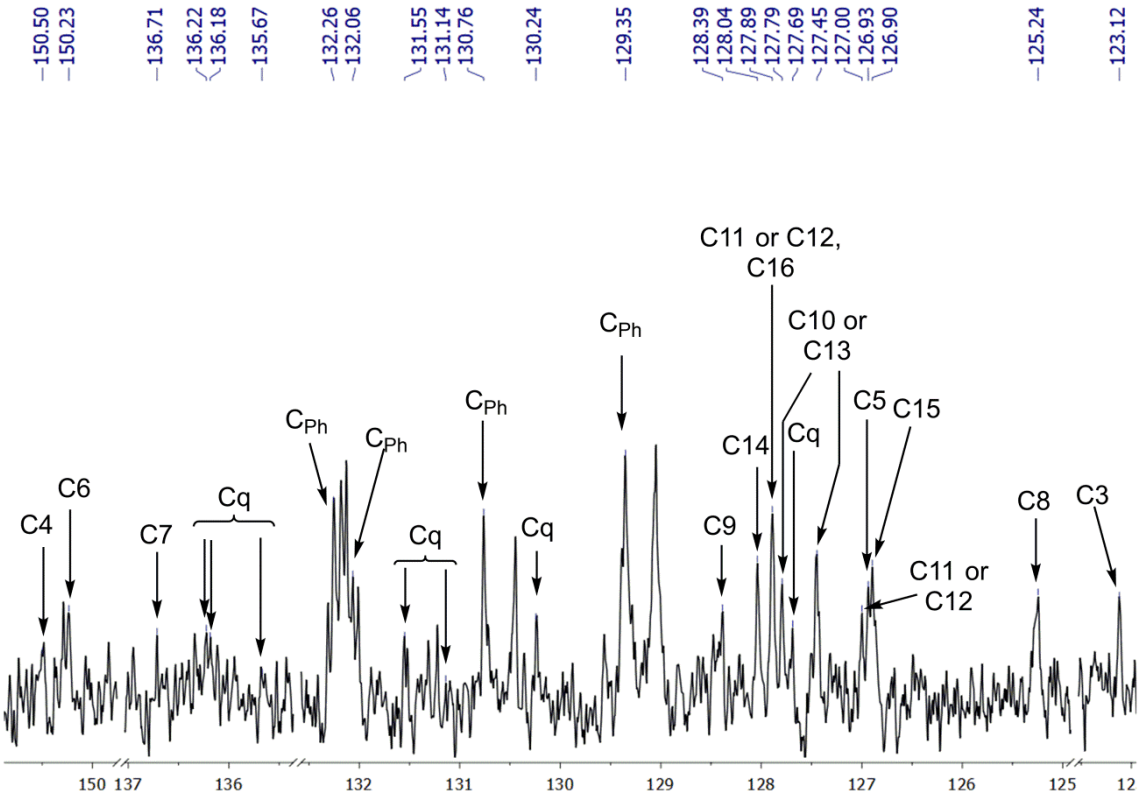

Figure S 37. $^{13}C\{^{1}H\}$-NMR (126 MHz, CD_2Cl_2) spectrum of **Cu1a**.

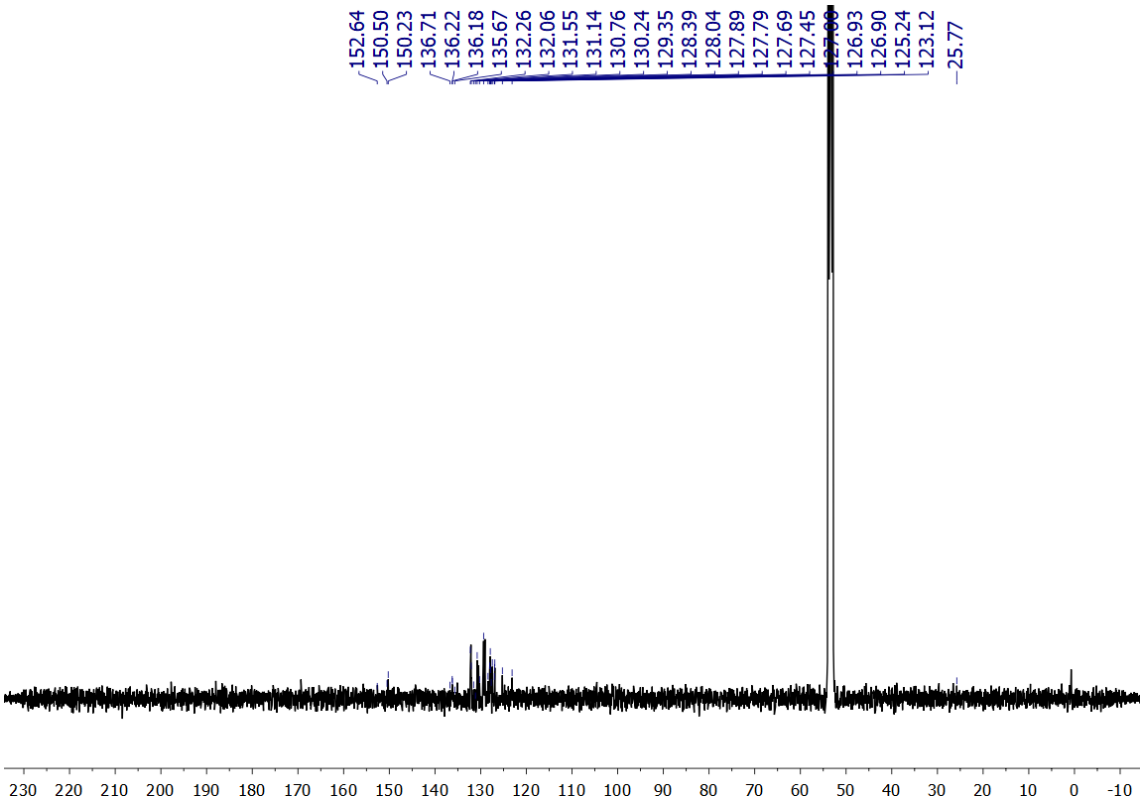

Figure S 38. Full $^{13}C\{^{1}H\}$-NMR (126 MHz, CD_2Cl_2) spectrum of complex **Cu1a**.

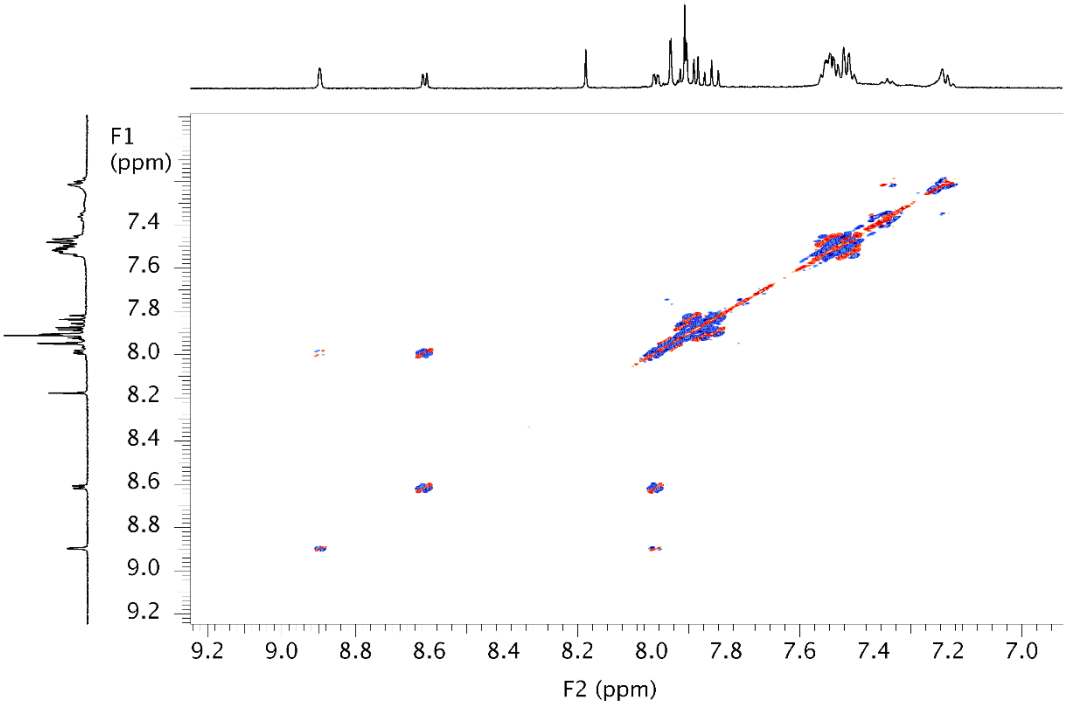

Figure S 39. ^{1}H-^{1}H gDQFCOSY (500 MHz, CD_2Cl_2) spectrum of complex **Cu1a**.

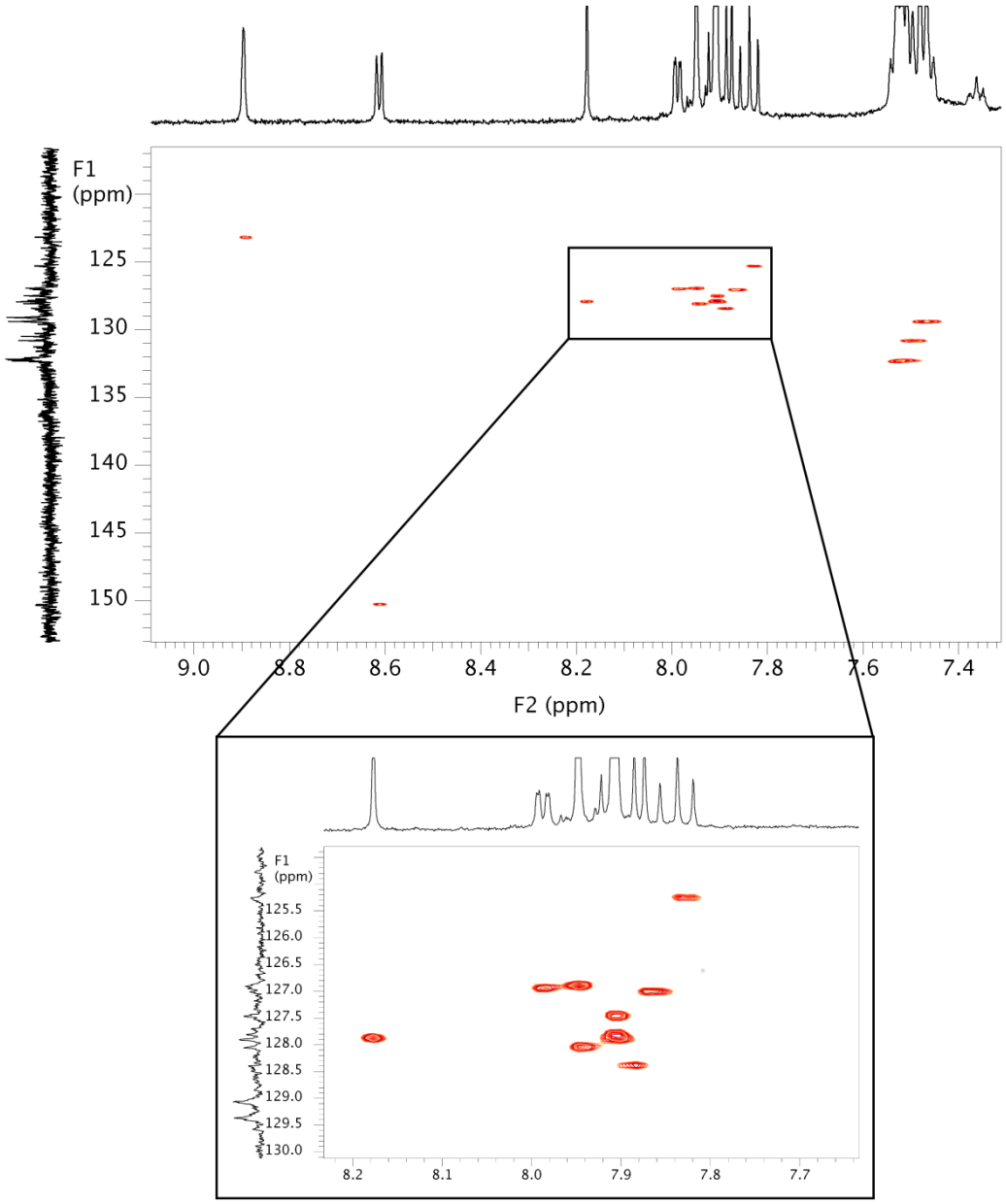

Figure S 40. ^{1}H-^{13}C bsgHSQCAD (500 MHz, CD_2Cl_2) spectrum of complex **Cu1a**.

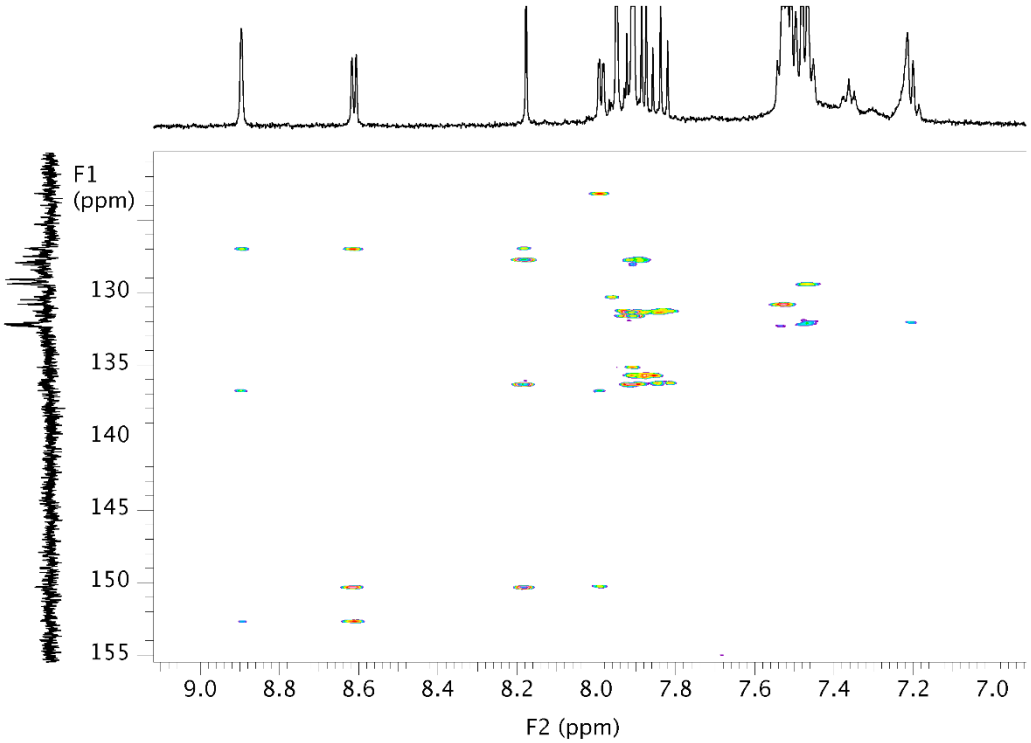

Figure S 41. ^{1}H-^{13}C bsgHMBC (500 MHz, CD_2Cl_2) spectrum of complex **Cu1a**.

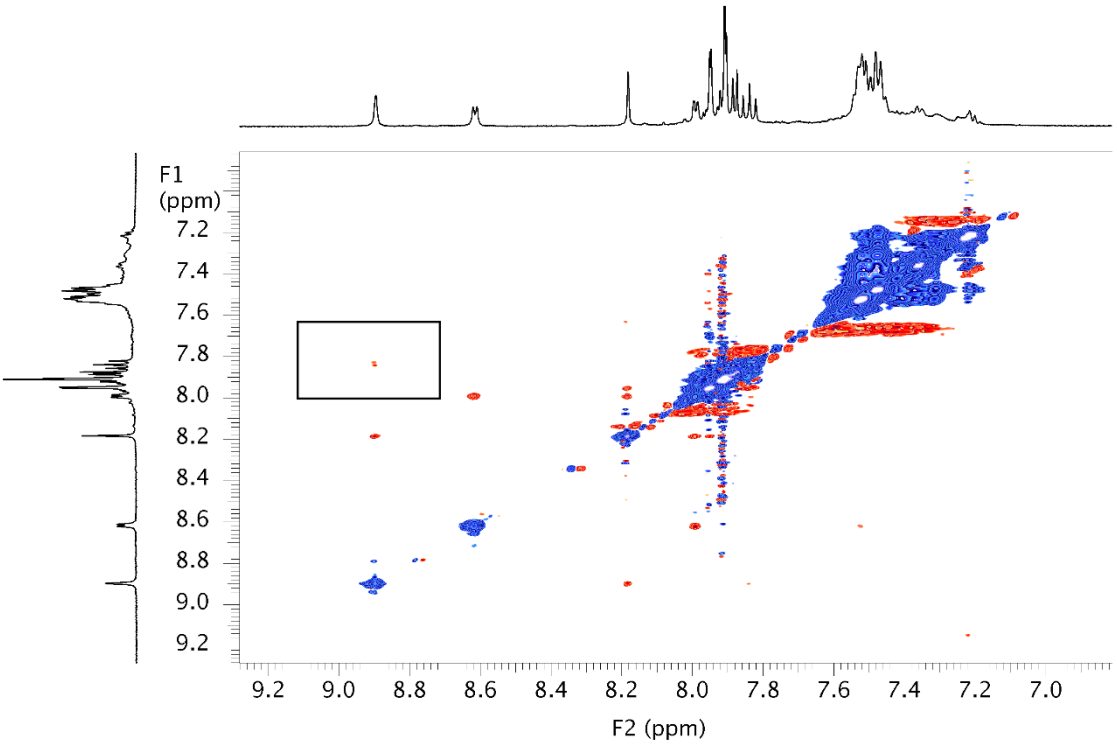

Figure S 42. ^{1}H-^{1}H ROESYAD (500 MHz, CD_2Cl_2) spectrum of complex **Cu1a**. An interesting correlation is showed between pyridine and corannulene protons (H_3 and H_8, respectively) which allows us to determine the structure of the molecule.

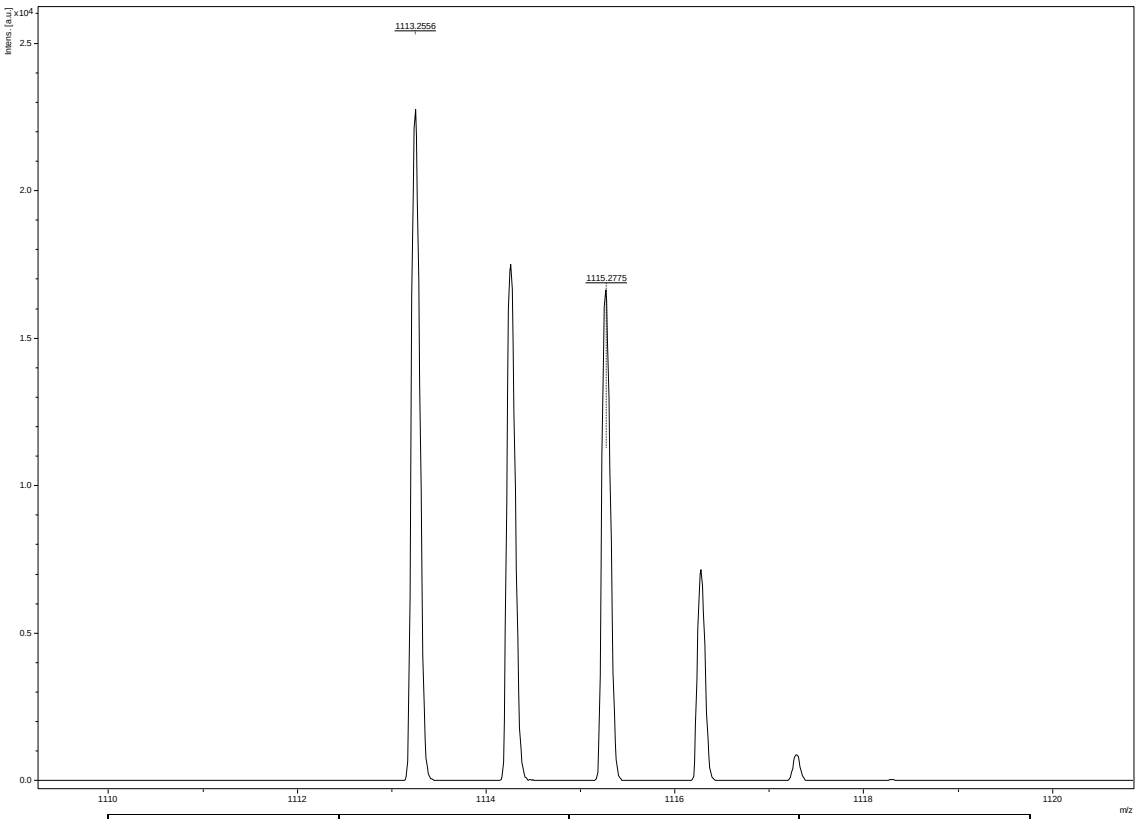

Meas. m/z	m/z	err [ppm]	Ion Formula
1113.2556	1113.2583	-2.7	$C_{76}H_{48}CuN_2P_2$

Figure S 43. HRMS (MALDI) of complex **Cu1a** $[M]^+$

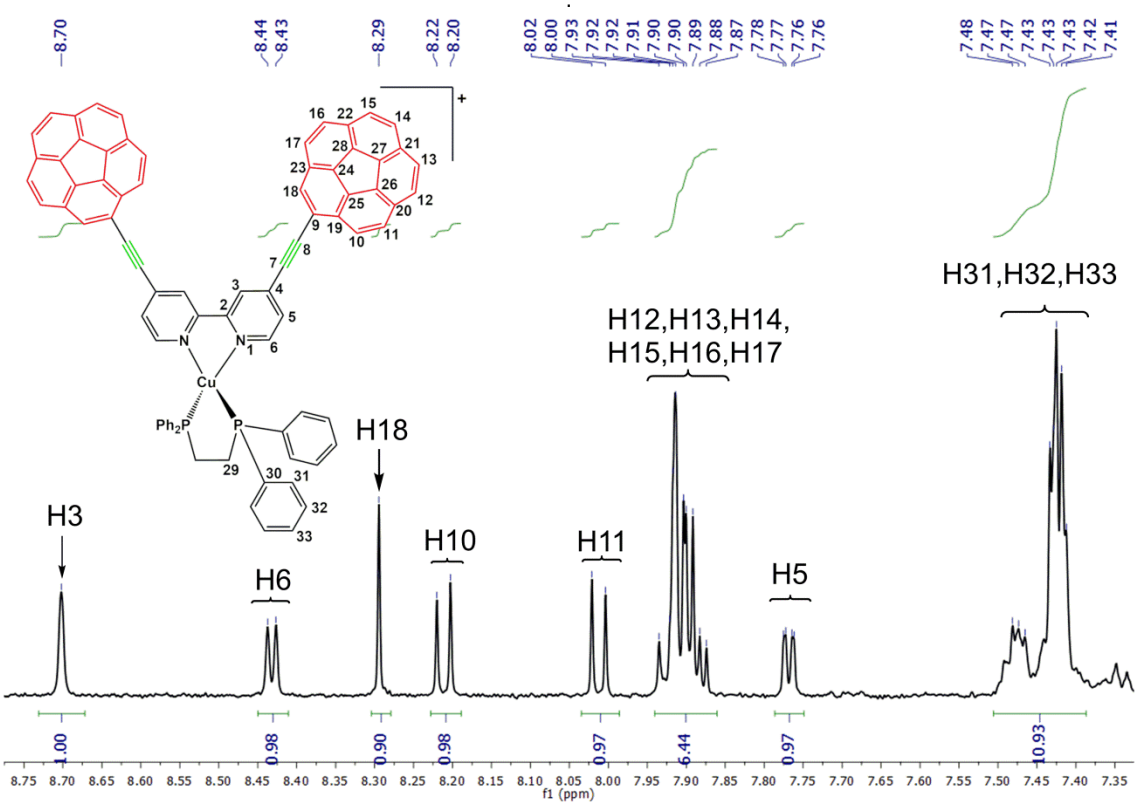

Figure S 44. ^{1}H-NMR (500 MHz, CD_2Cl_2) spectrum of complex **Cu2a**.

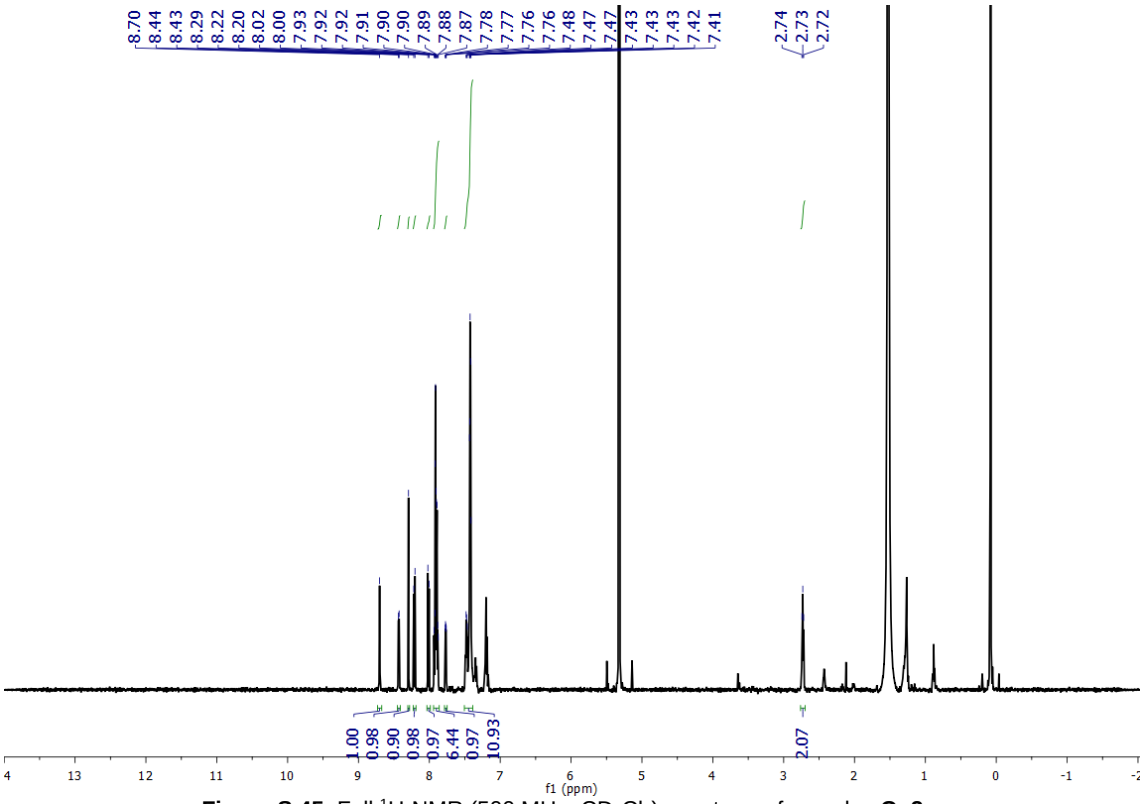

Figure S 45. Full ^{1}H-NMR (500 MHz, CD_2Cl_2) spectrum of complex **Cu2a**.

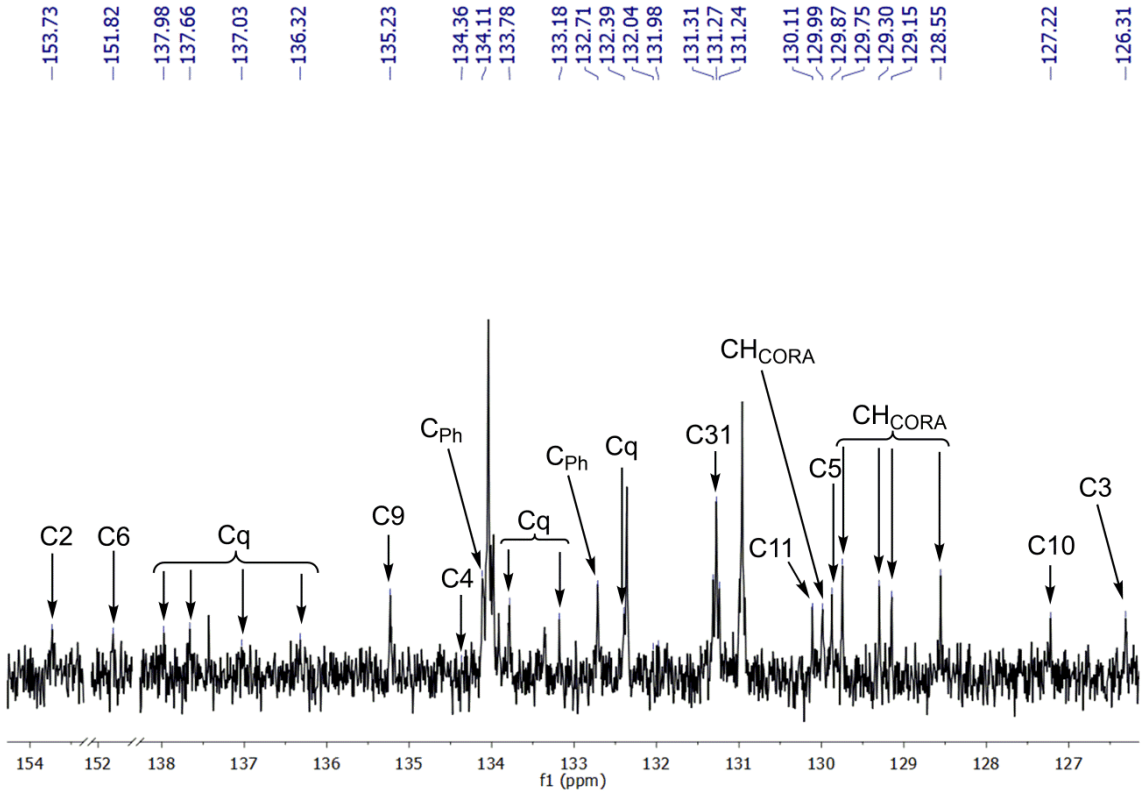

Figure S 46. ^{13}C{^{1}H}-NMR (126 MHz, CD_2Cl_2) spectrum of complex **Cu2a**.

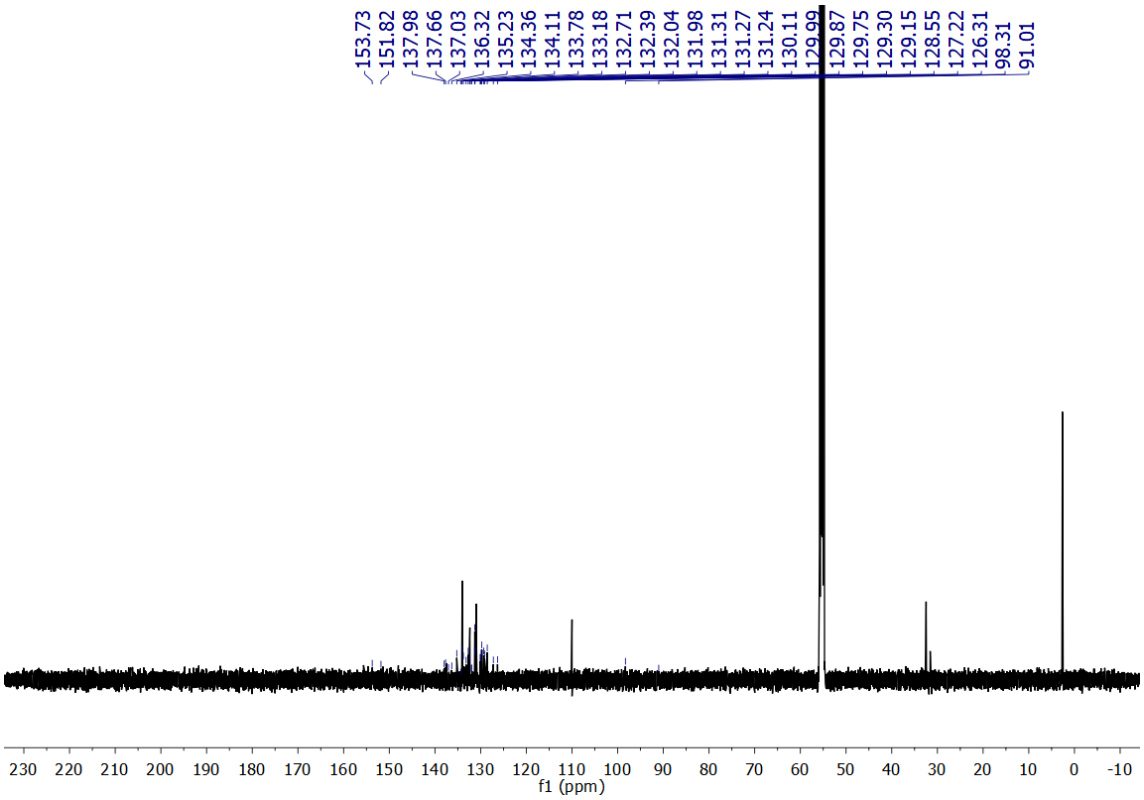

Figure S 47. Full $^{13}C\{^{1}H\}$-NMR (126 MHz, CD_2Cl_2) spectrum of complex **Cu2a**.

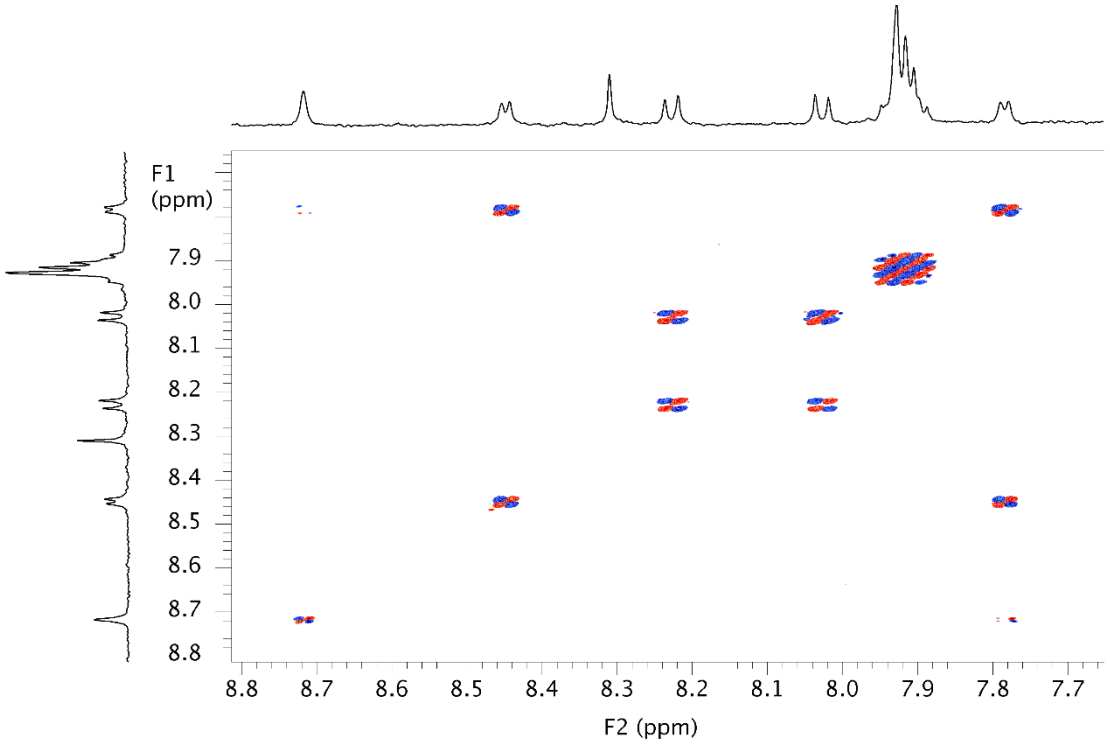

Figure S 48. ^{1}H-^{1}H gDQFCOSY (500 MHz, CD_2Cl_2) spectrum of complex **Cu2a**.

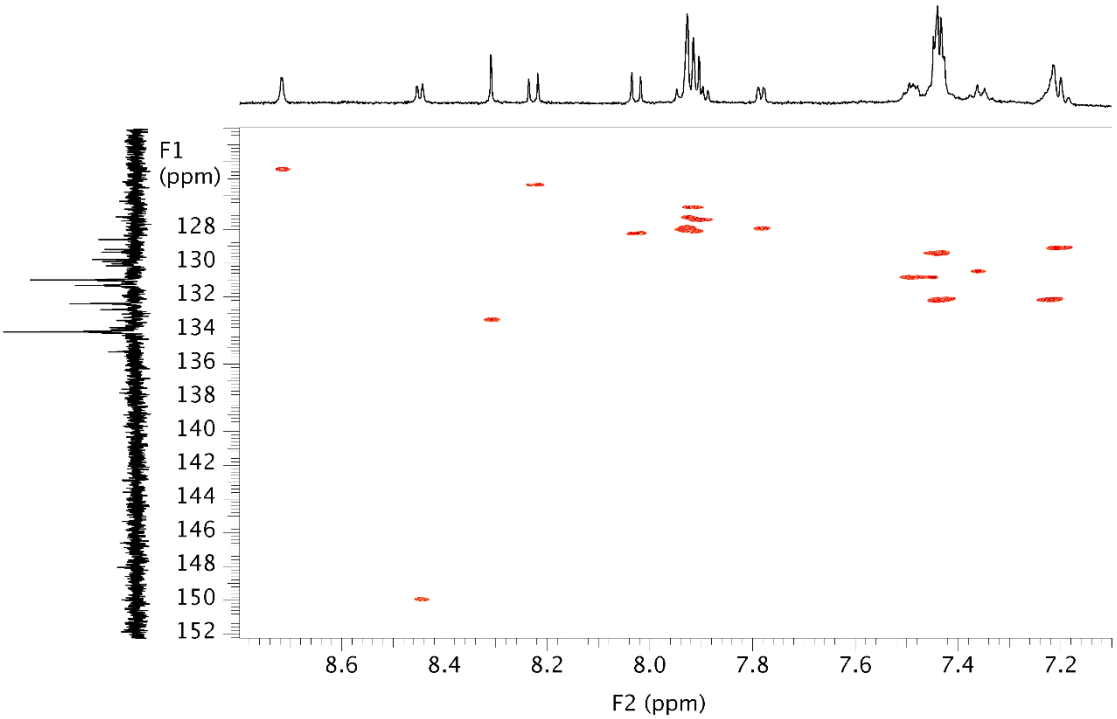

Figure S 49. ^{1}H-^{13}C bsgHSQCAD (500 MHz, CD_2Cl_2) spectrum of complex **Cu2a**.

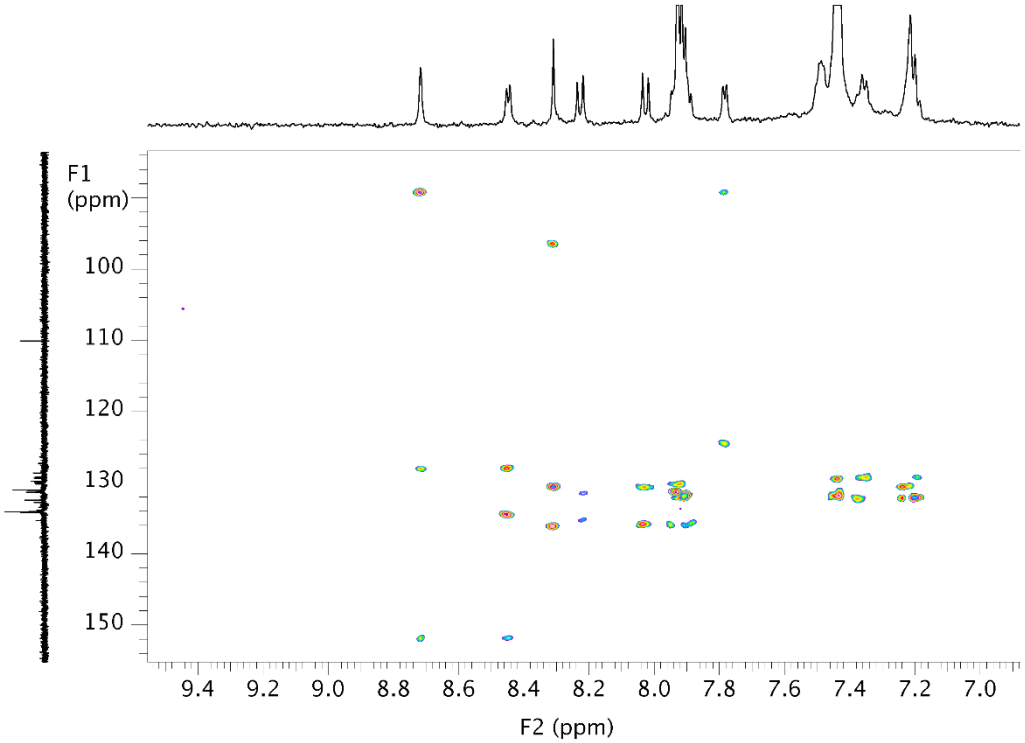

Figure S 50. ^{1}H-^{13}C gc2HMBC (500 MHz, CD_2Cl_2) spectrum of complex **Cu2a**.

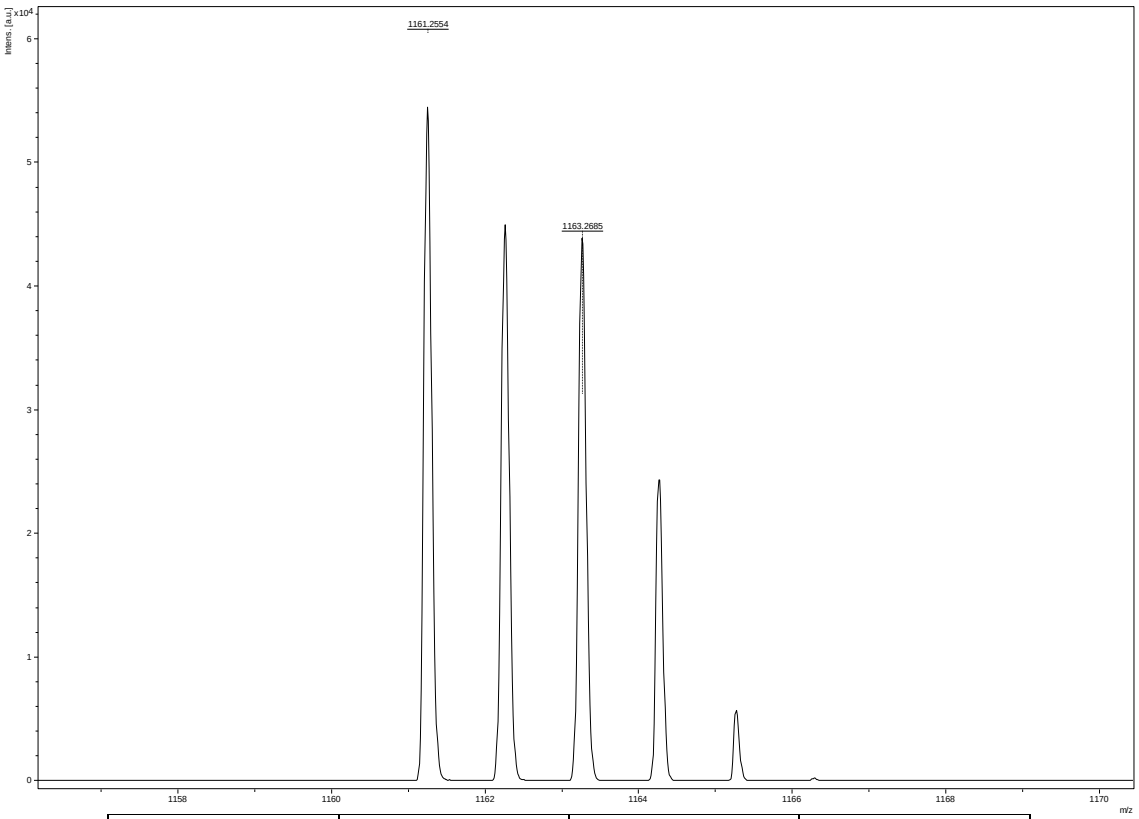

Meas. m/z	m/z	err [ppm	Ion Formula
1161.2554	1161.2583	-2.9	$C_{80}H_{48}CuN_2P_2$

Figure S 51. HRMS (MALDI) of **Cu2a** $[M]^+$.

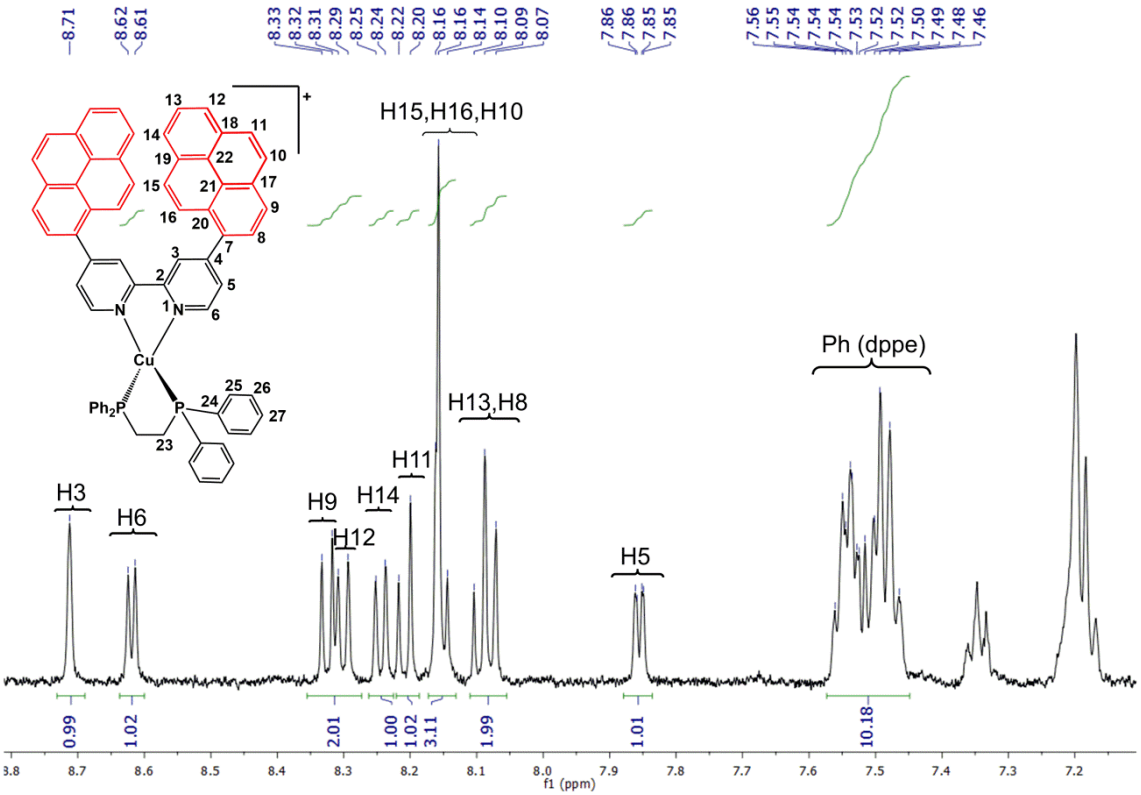

Figure S 52. ^{1}H-NMR (500 MHz, CD_2Cl_2) spectrum of complex **Cu1b**.

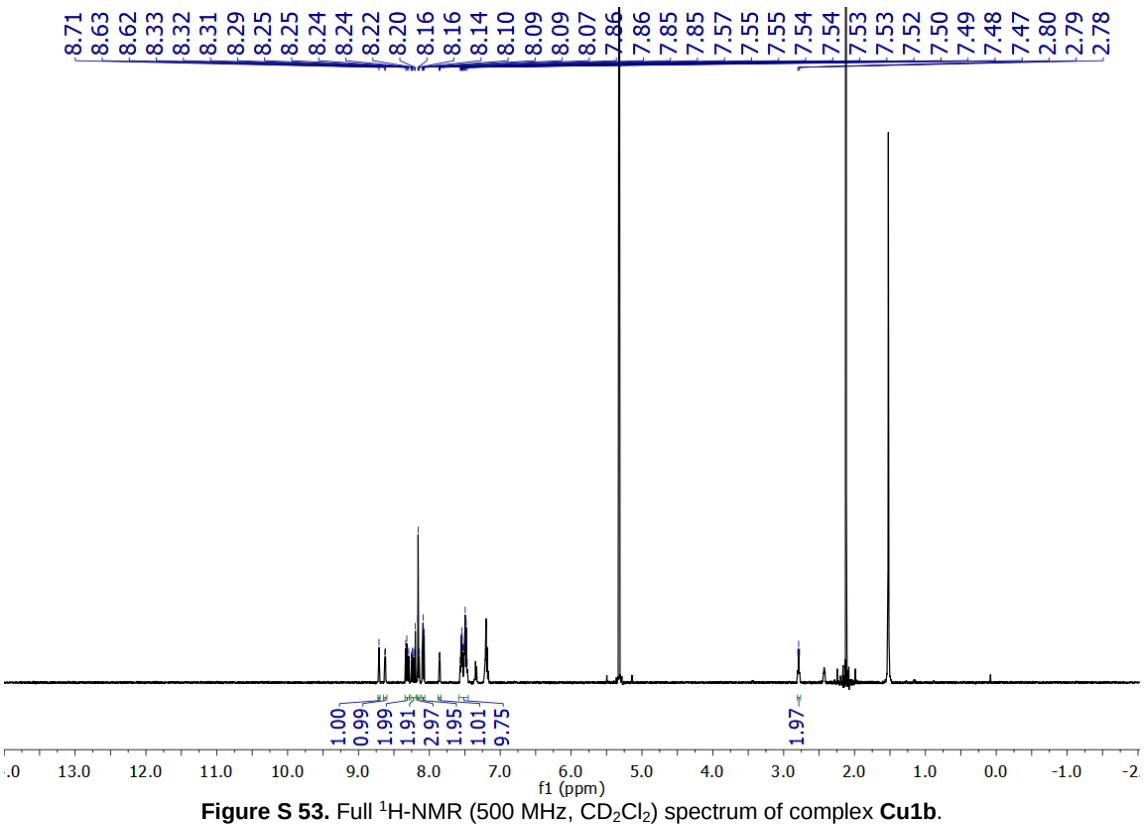

Figure S 53. Full ^{1}H-NMR (500 MHz, CD_2Cl_2) spectrum of complex **Cu1b**.

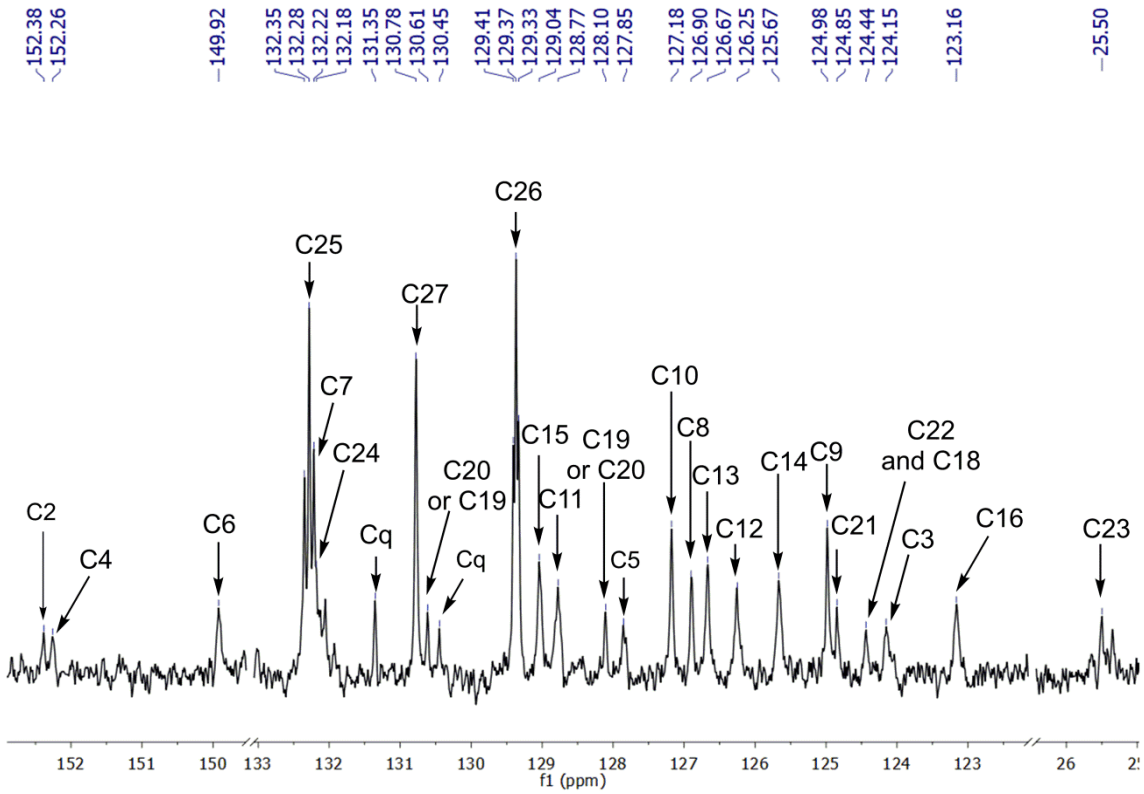

Figure S 54. $^{13}C\{^{1}H\}$-NMR (126 MHz, CD_2Cl_2) spectrum of complex **Cu1b**.

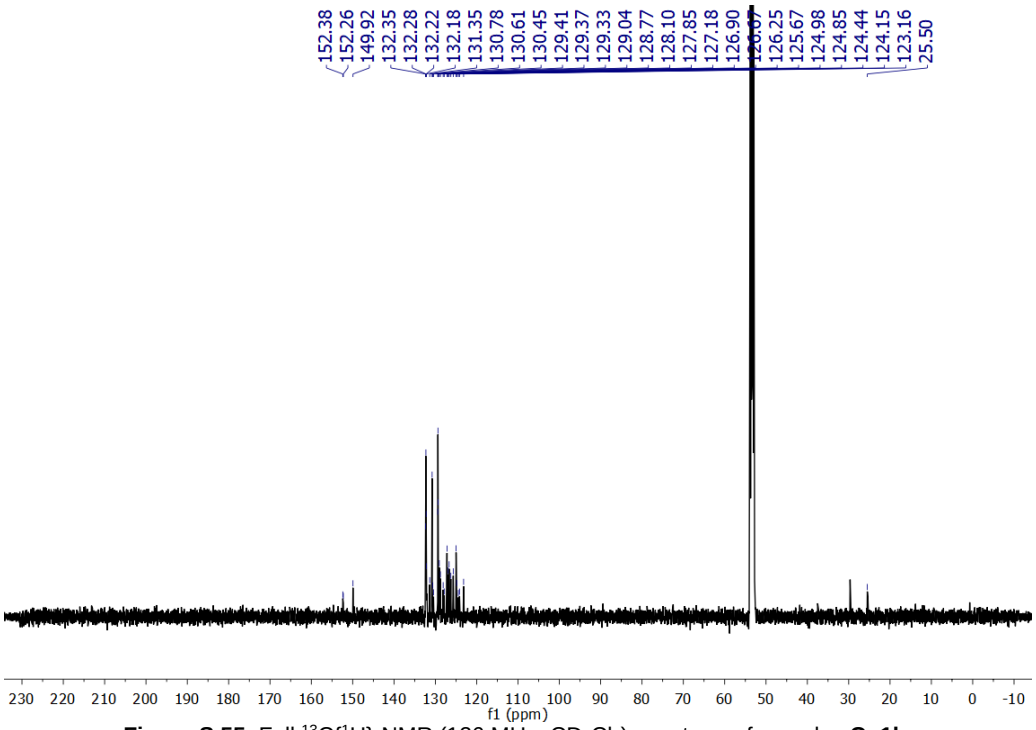

Figure S 55. Full $^{13}C\{^{1}H\}$-NMR (126 MHz, CD_2Cl_2) spectrum of complex **Cu1b**.

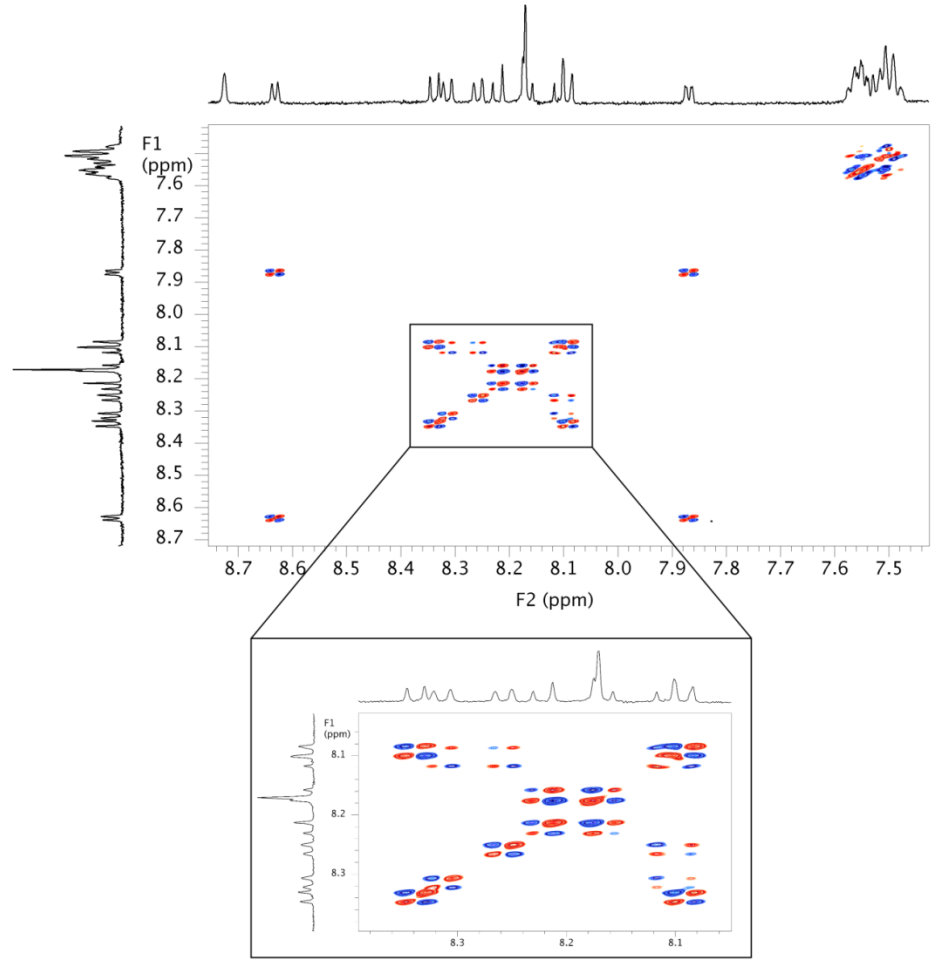

Figure S 56. ^{1}H-^{1}H gDQFCOSY (500 MHz, CD_2Cl_2) spectrum of complex **Cu1b**.

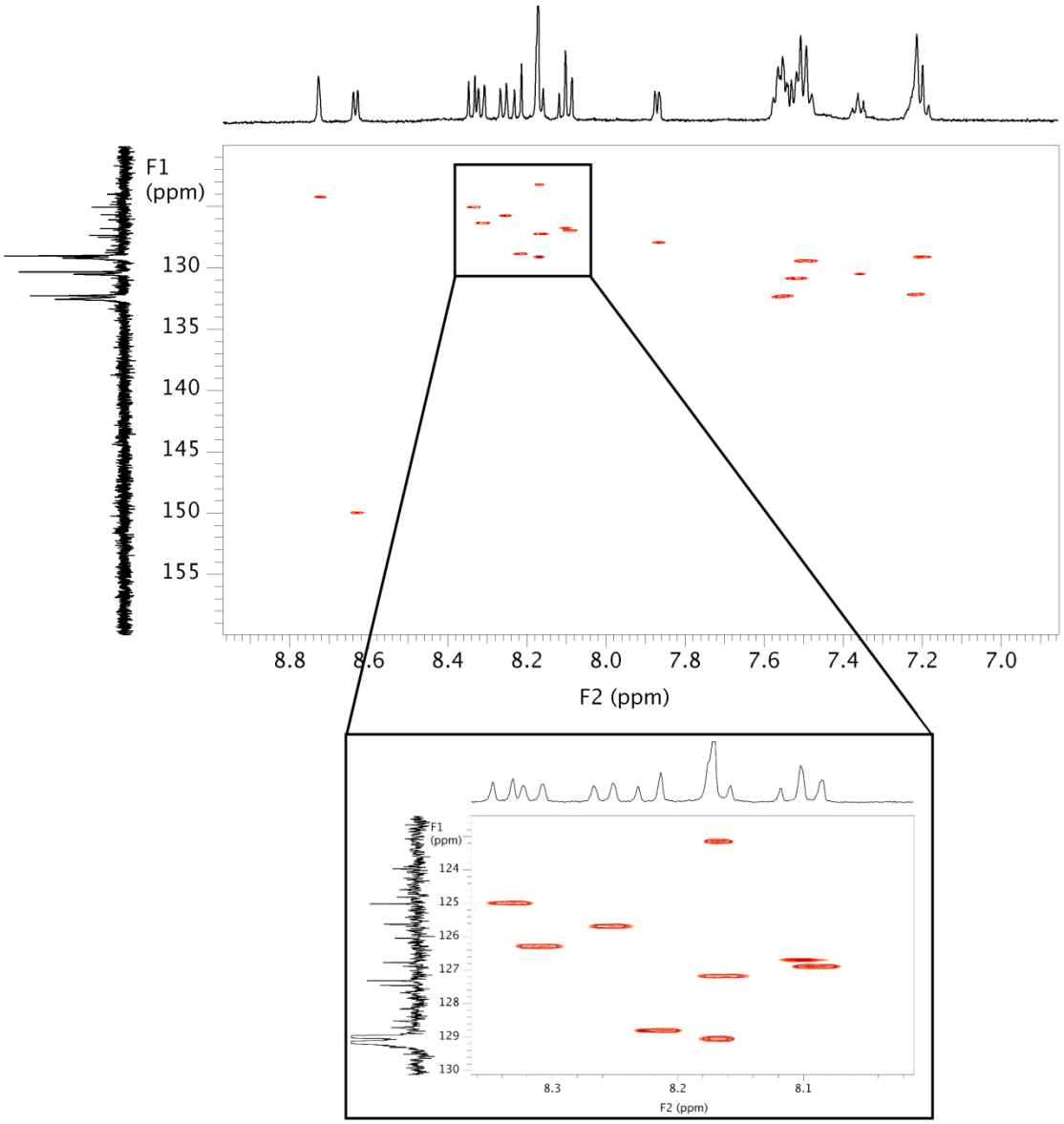

Figure S 57. ^{1}H-^{13}C bsgHSQCAD (500 MHz, CD_2Cl_2) spectrum of complex **Cu1b**.

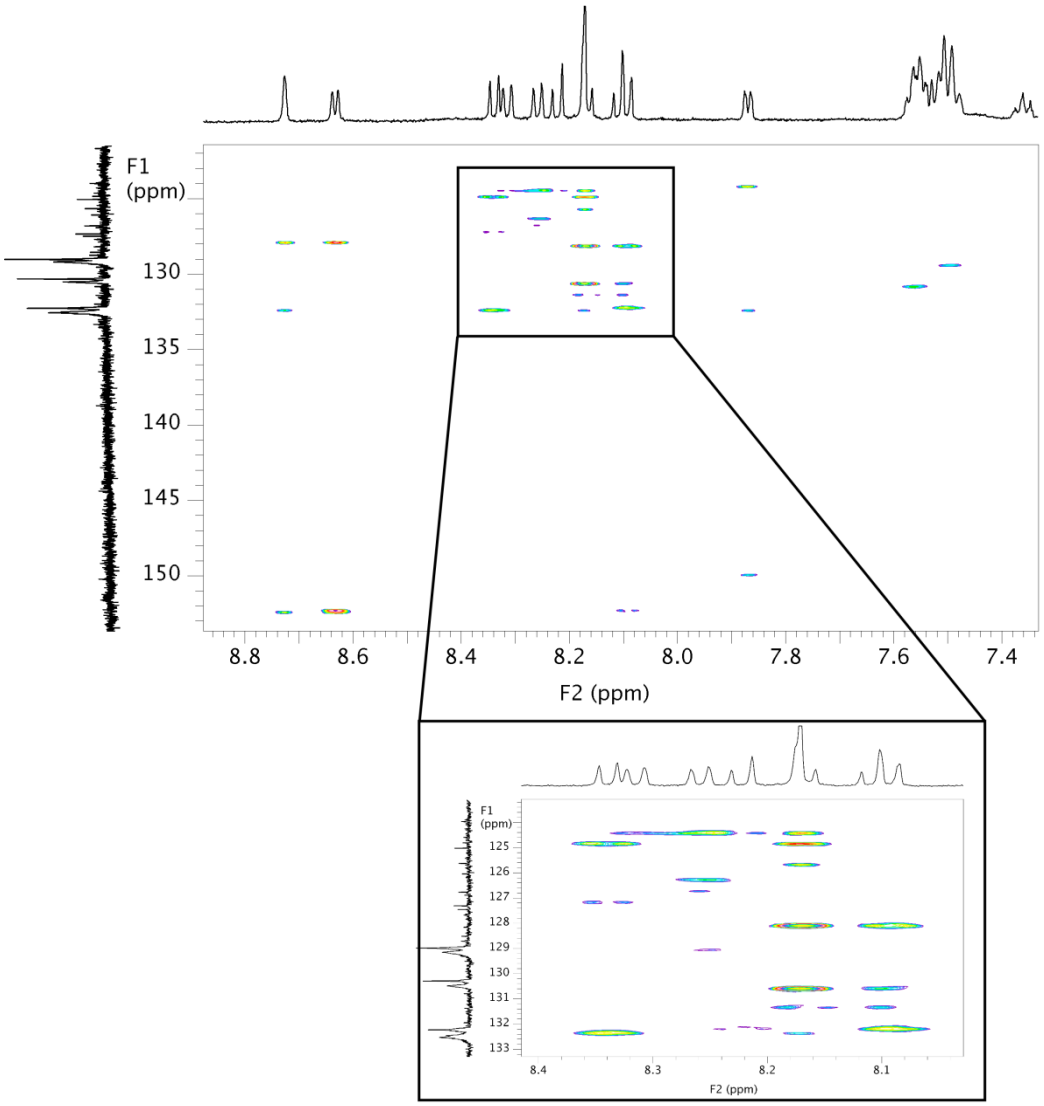

Figure S 58. ^{1}H-^{13}C bsgHMBC (500 MHz, CD_2Cl_2) spectrum of complex **Cu1b**.

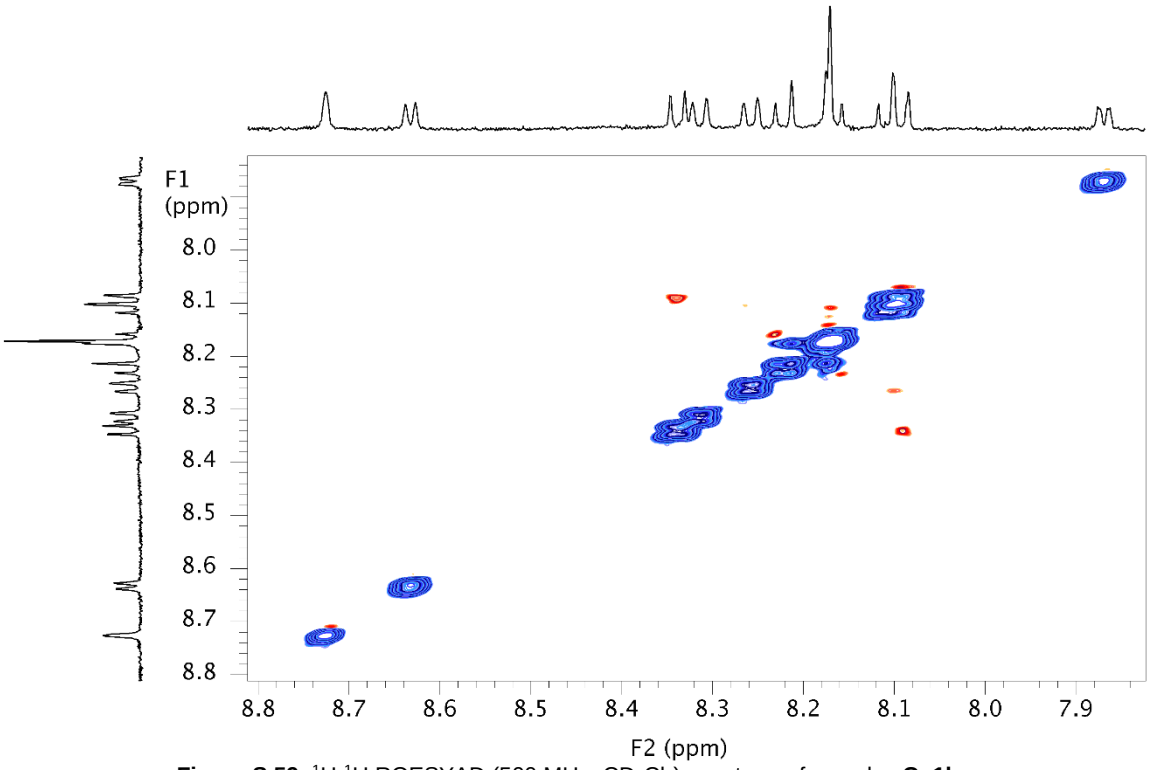

Figure S 59. ^{1}H-^{1}H ROESYAD (500 MHz, CD_2Cl_2) spectrum of complex **Cu1b**.

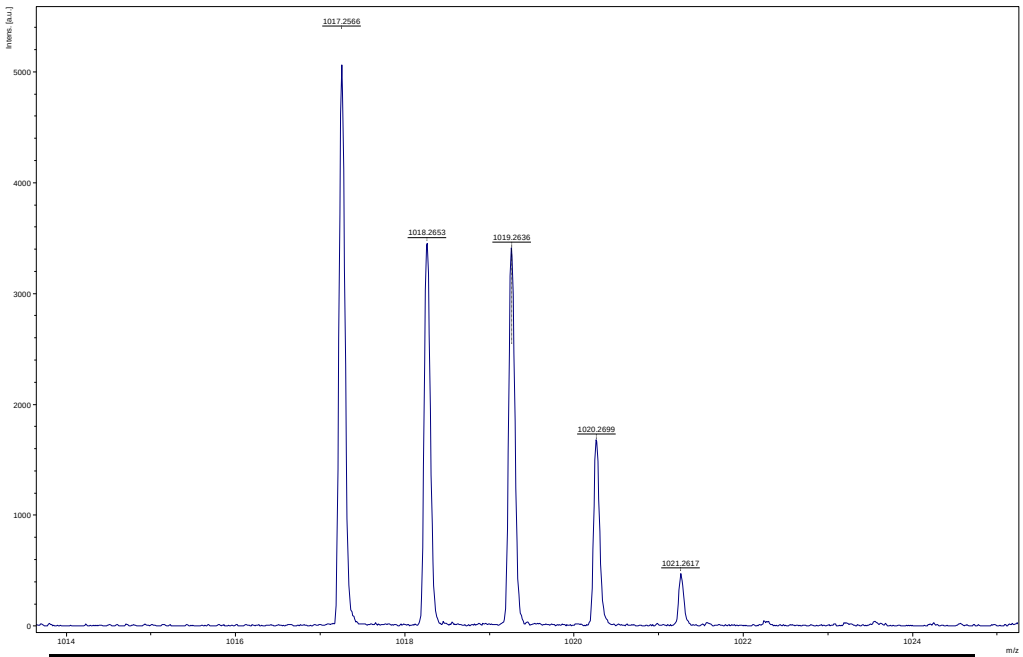

Meas. m/z	m/z	err [ppm]	Ion Formula
1017.2566	1017.2583	-1.7	$C_{68}H_{48}CuN_2P_2$

Figure S 60. HRMS (MALDI) of complex **Cu1b** $[M]^+$.

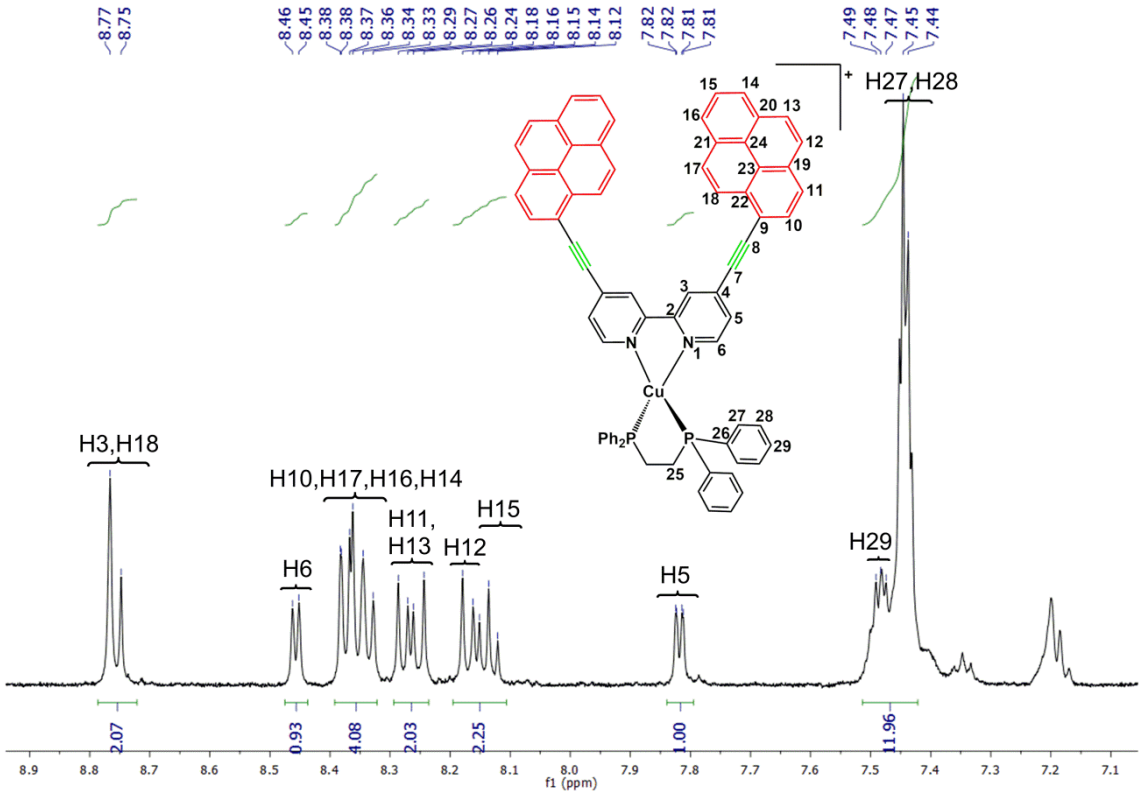

Figure S 61. ^{1}H-NMR (500 MHz, CD_2Cl_2) spectrum of complex **Cu2b**.

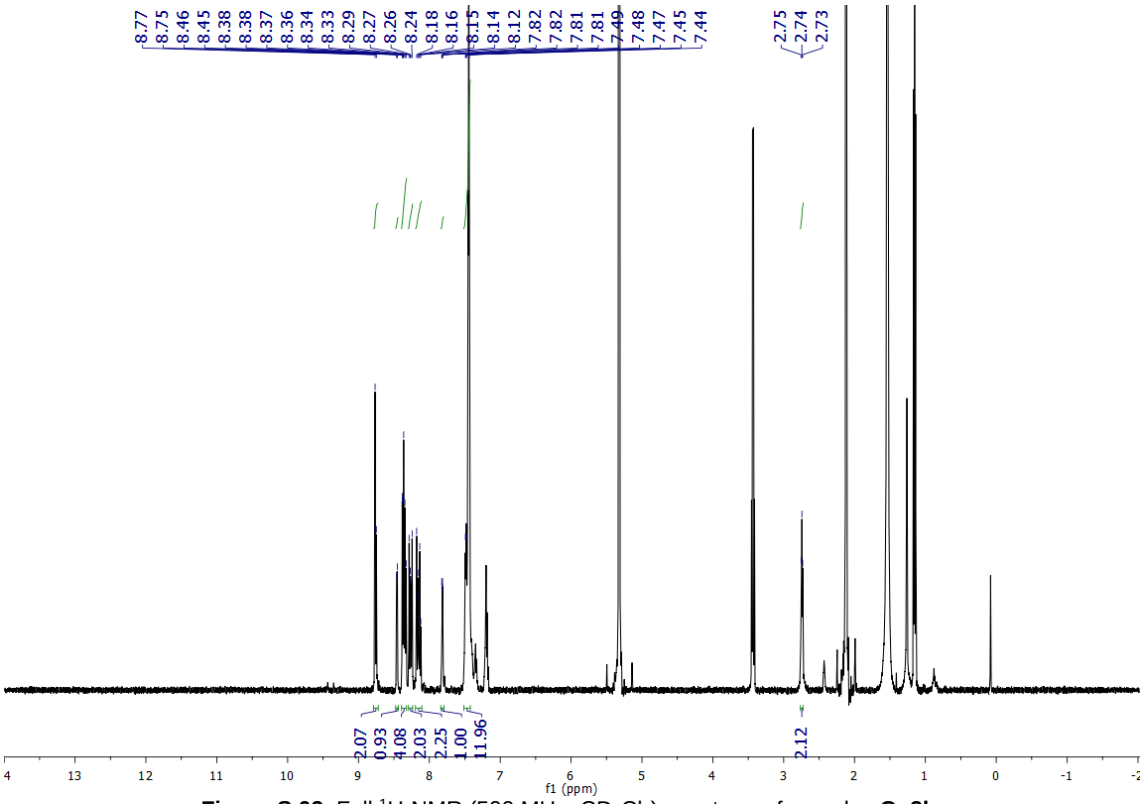

Figure S 62. Full ^{1}H-NMR (500 MHz, CD_2Cl_2) spectrum of complex **Cu2b**.

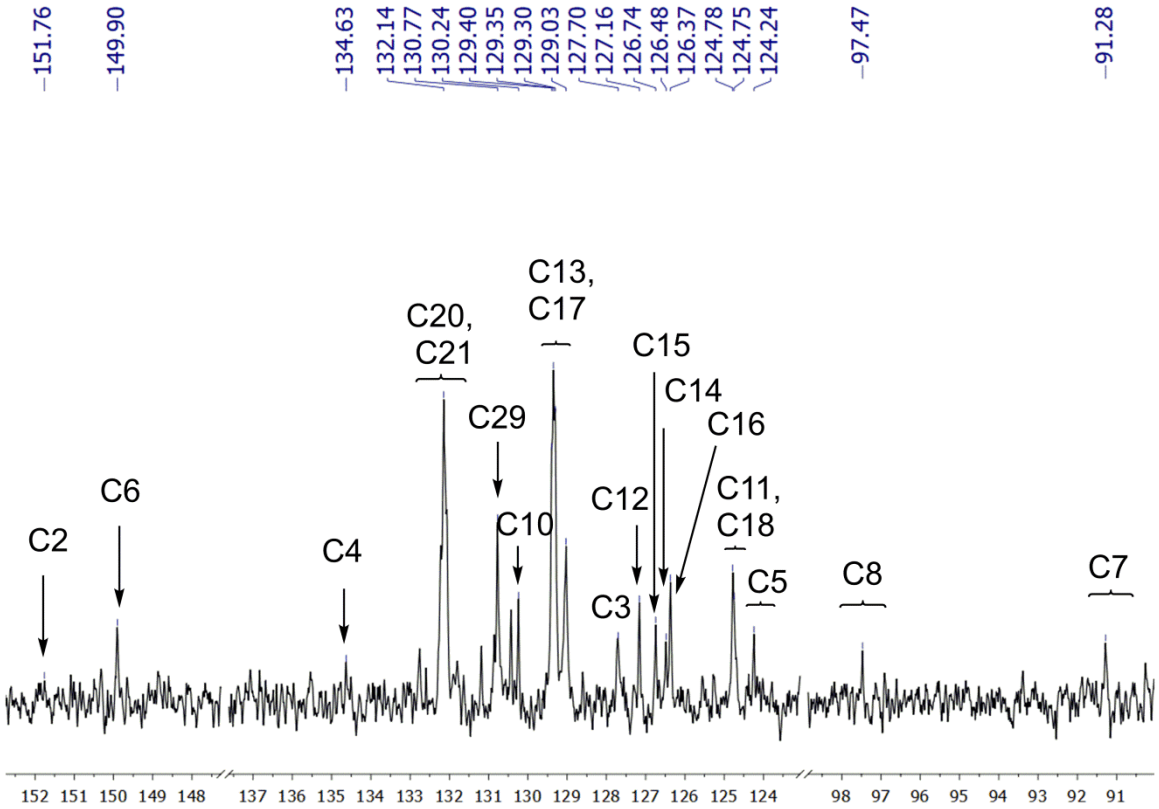

Figure S 63. $^{13}C\{^{1}H\}$-NMR (101 MHz, CD_2Cl_2) spectrum of complex **Cu2b**.

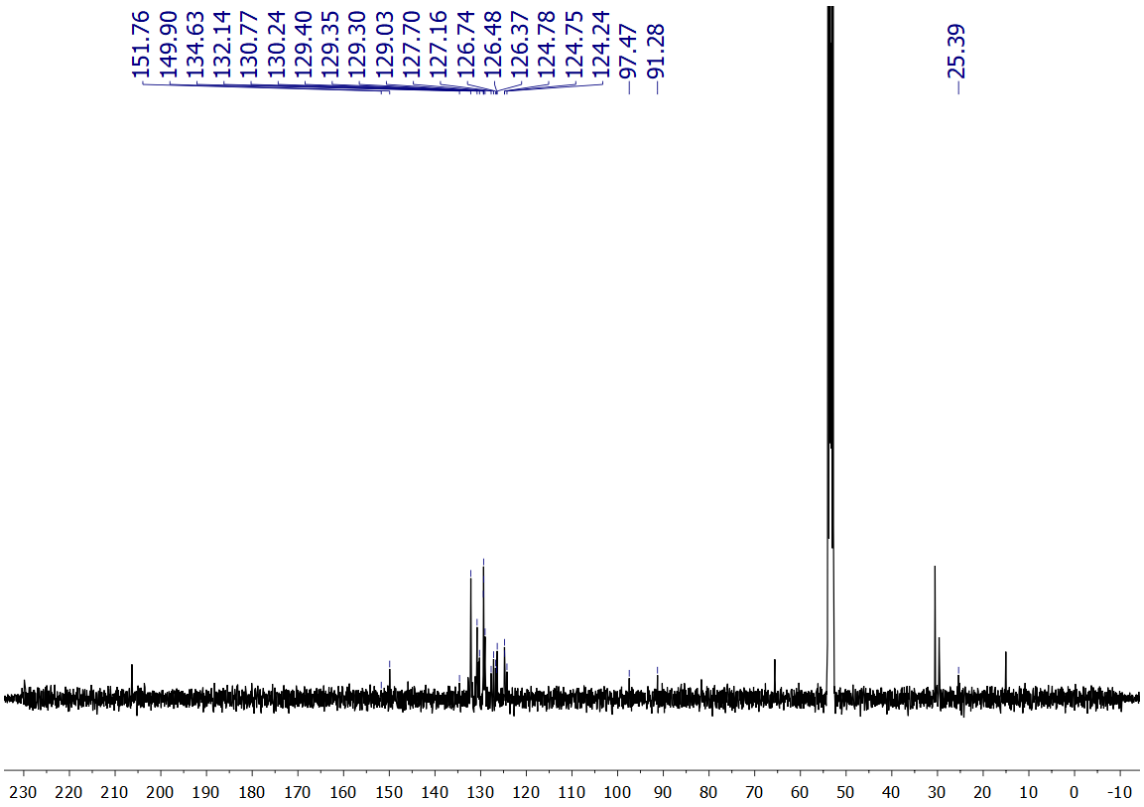

Figure S 64. Full $^{13}C\{^{1}H\}$-NMR (101 MHz, CD_2Cl_2) spectrum of complex **Cu2b**.

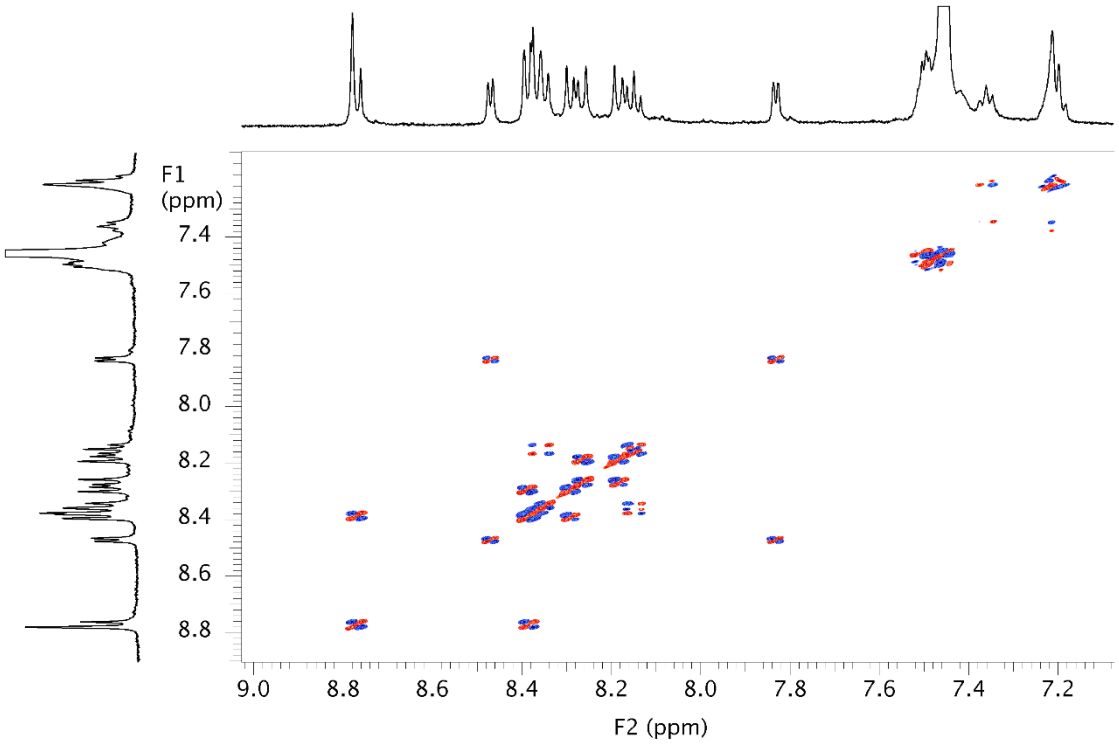

Figure S 65. ^{1}H-^{1}H gDQFCOSY (500 MHz, CD_2Cl_2) spectrum of complex **Cu2b**.

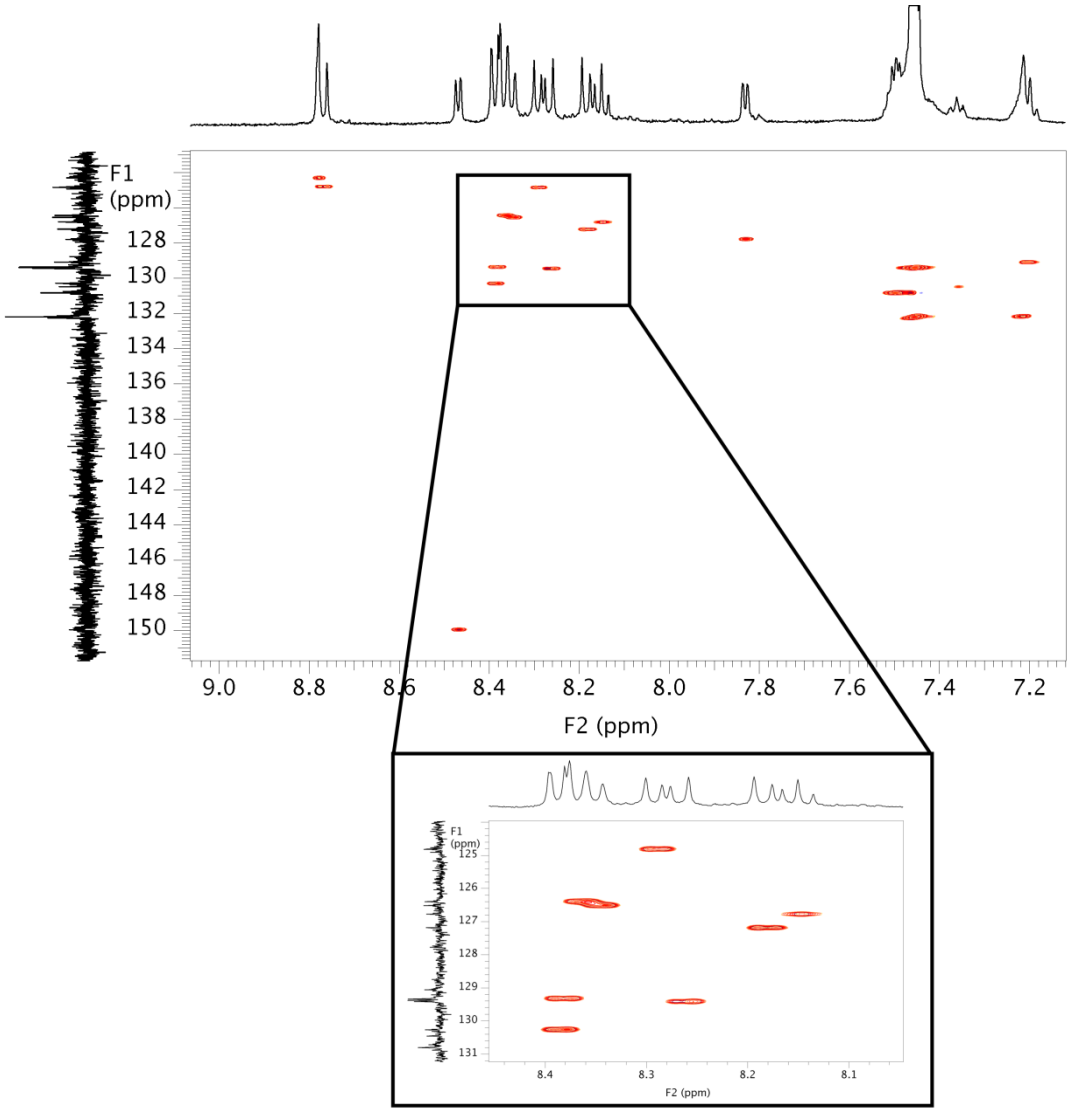

Figure S 66. ^{1}H-^{13}C bsgHSQCAD (500 MHz, CD_2Cl_2) spectrum of complex **Cu2b**.

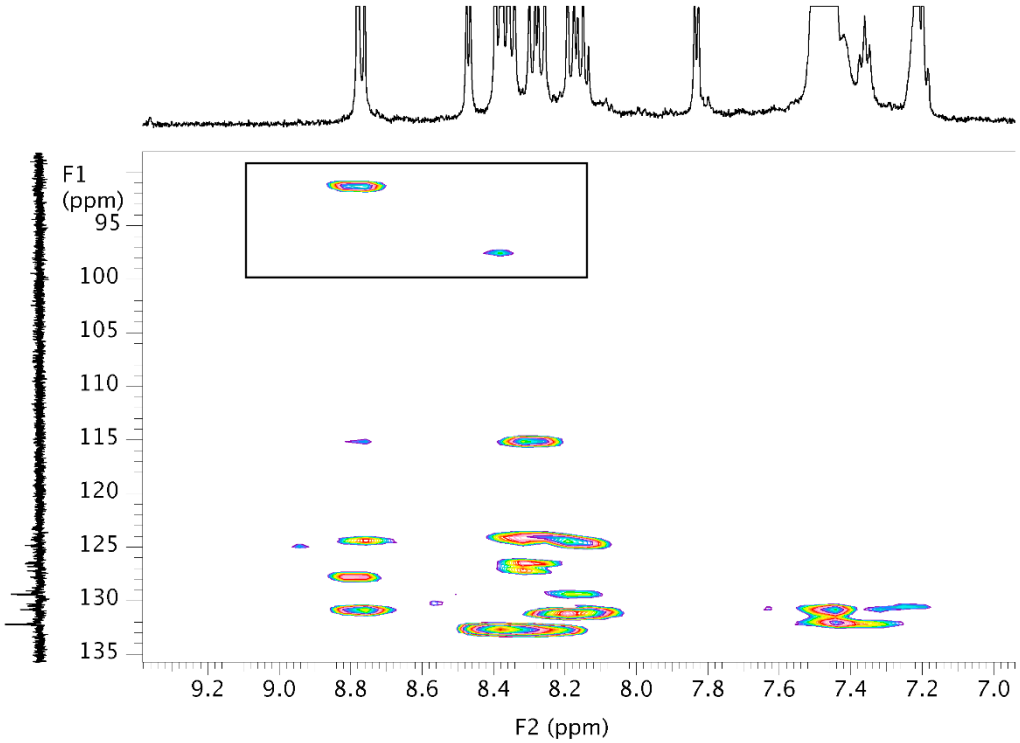

Figure S 67. ^{1}H-^{13}C g2cHMBC (500 MHz, CD_2Cl_2) spectrum of **Cu2b**. In this experiment, carbons C_7 and C_8 have been determined by cross peaks with protons from bipyridine (H_3) and pyrene (H_{11}) moieties.

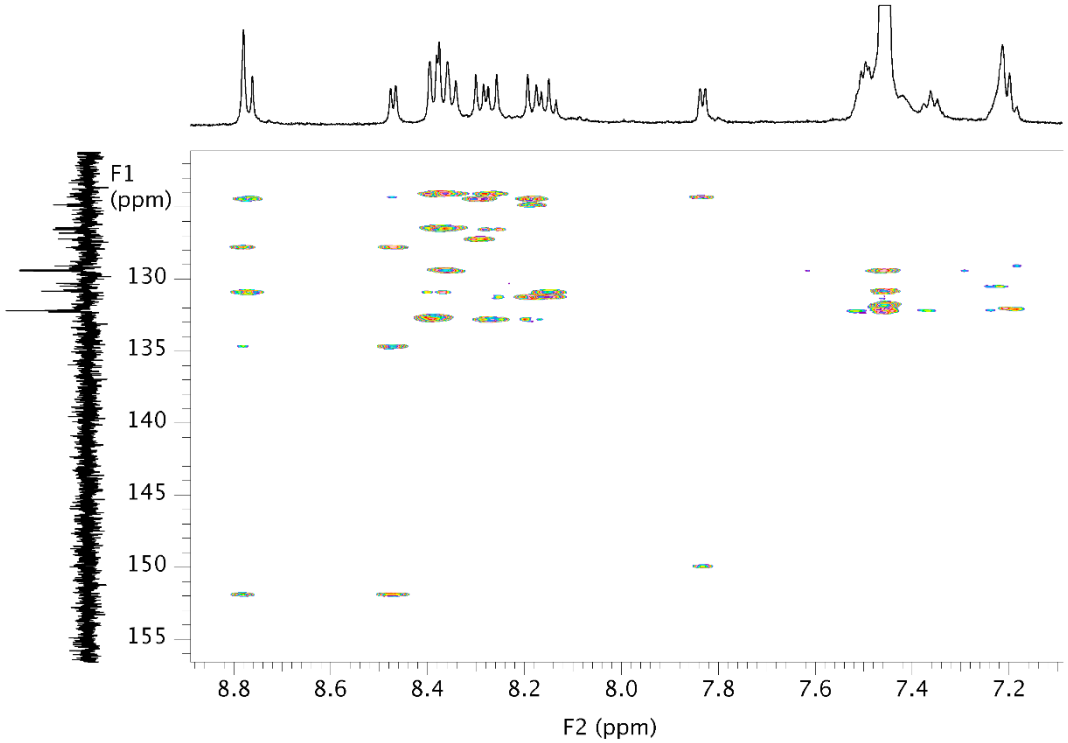

Figure S 68. ^{1}H-^{13}C bsgHMBC (500 MHz, CD_2Cl_2) spectrum of complex **Cu2b**.

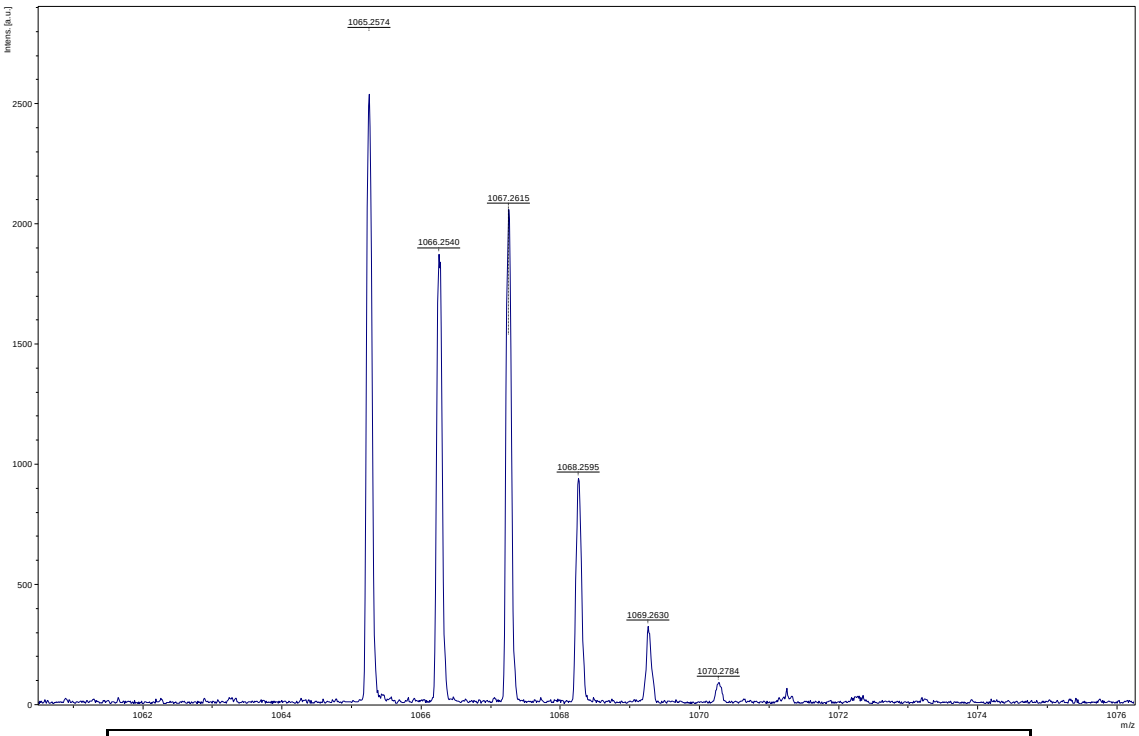

Meas. m/z	m/z	err [ppm]	Ion Formula
1065.2574	1065.2583	-0.9	$C_{72}H_{48}CuN_2P_2$

Figure S 69. HRMS (MALDI) of complex **Cu2b** $[M]^+$.

UV-Vis absorption and emission spectra

Spectra of complexes **Cu1a** and **Cu2a** show the expected intraligand π-π* transition bands in the range 270 nm–370 nm with attenuation coefficients of $3.2 \cdot 10^4$ $M^{-1}cm^{-1}$ – $6.6 \cdot 10^4$ $M^{-1}cm^{-1}$ and ^{1}MLCT bands in the range 375 nm–550 nm with moderate intensity (ε = $4.9 \cdot 10^3$ $M^{-1}cm^{-1}$ – $7.5 \cdot 10^3$ $M^{-1}cm^{-1}$) (Figure S 70).[6–8]

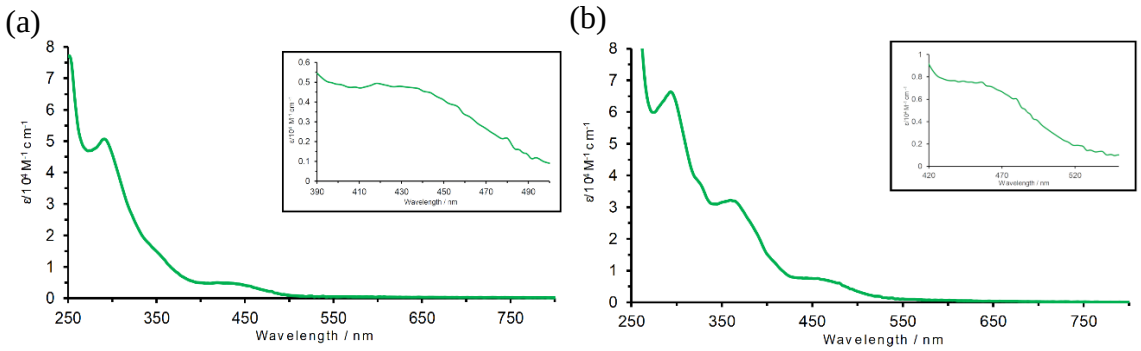

Figure S 70. UV-Vis absorption spectra of complexes (a) **Cu1a** (10^{-5} M) and (b) **Cu2a** (10^{-5} M) in dichloromethane. Inset: magnified spectrum in the region between (a) 390 nm and 500 nm, and (b) 420 and 550 nm.

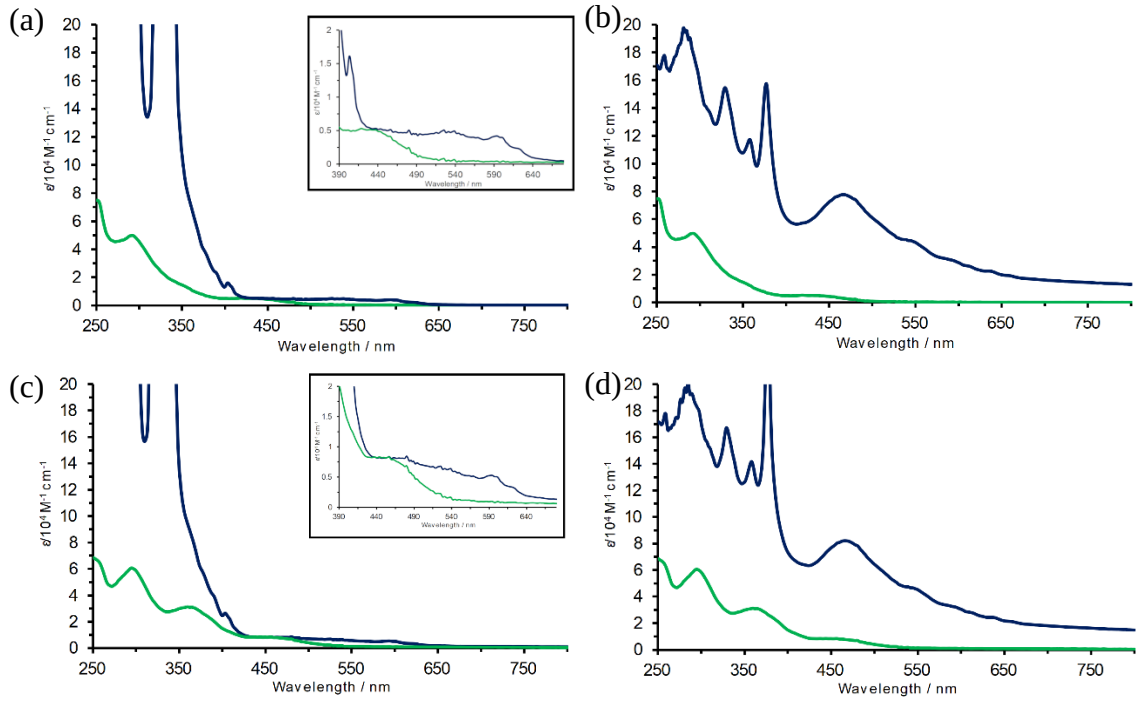

Figure S 71. UV-Vis absorption spectra in dichloromethane of: (a) complex **Cu1a** ($1.7 \cdot 10^{-5}$ M, in green) and its mixture with C_{60} ($8.3 \cdot 10^{-5}$ M, 5 eq, in blue); (b) complex **Cu1a** ($1.7 \cdot 10^{-5}$ M, in green) and its mixture with C_{70} ($8.3 \cdot 10^{-5}$ M, 5 eq, in blue); (c) complex **Cu2a** ($1.7 \cdot 10^{-5}$ M, in green) and its mixture with C_{60} ($8.3 \cdot 10^{-5}$ M, 5 eq, in blue); (d) complex **Cu2a** ($1.7 \cdot 10^{-5}$ M, in green) and its mixture with C_{70} ($8.3 \cdot 10^{-5}$ M, 5 eq, in blue). Insets in spectra (a) and (c) correspond to the magnified region of ^{1}MLCT transition band.

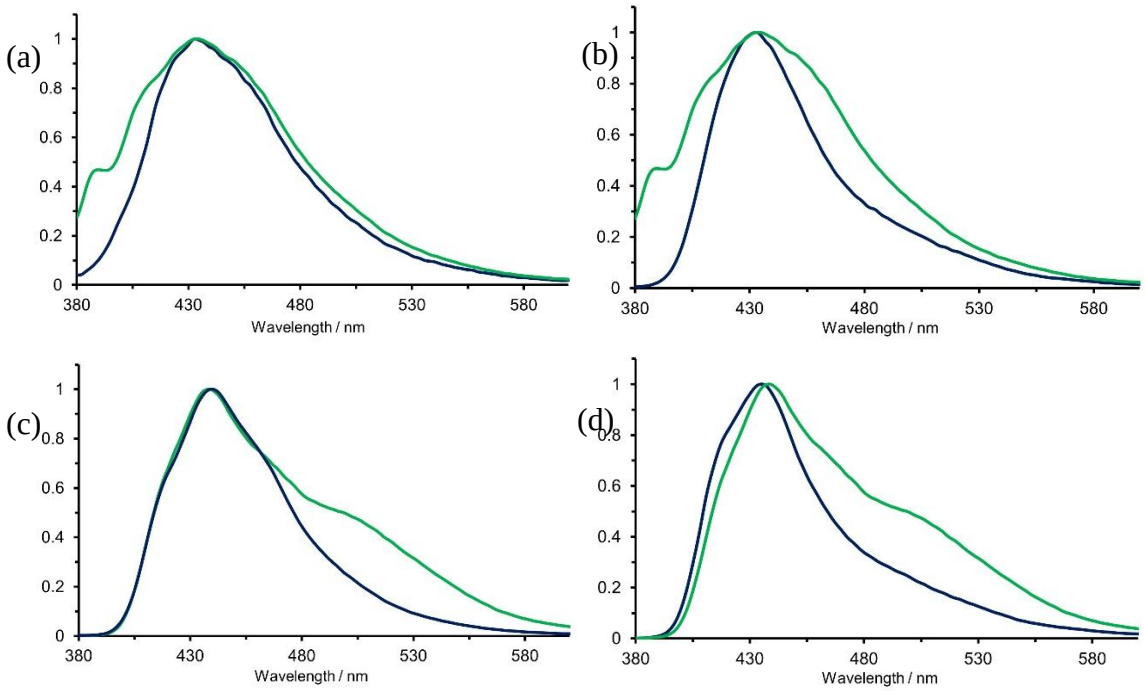

Figure S 72. Emission spectra (λ_{exc} = 350 nm) in dichloromethane of: (a) complex **Cu1a** ($1.7 \cdot 10^{-5}$ M, in green) and its mixture with C_{60} ($8.3 \cdot 10^{-5}$ M, 5 eq, in blue); (b) complex **Cu1a** ($1.7 \cdot 10^{-5}$ M, in green) and its mixture with C_{70} ($8.3 \cdot 10^{-5}$ M, 5 eq, in blue); (c) complex **Cu2a** ($1.7 \cdot 10^{-5}$ M, in green) and its mixture with C_{60} ($8.3 \cdot 10^{-5}$ M, 5 eq, in blue); (d) complex **Cu2a** ($1.7 \cdot 10^{-5}$ M, in green) and its mixture with C_{70} ($8.3 \cdot 10^{-5}$ M, 5 eq, in blue).

Cyclic voltammograms

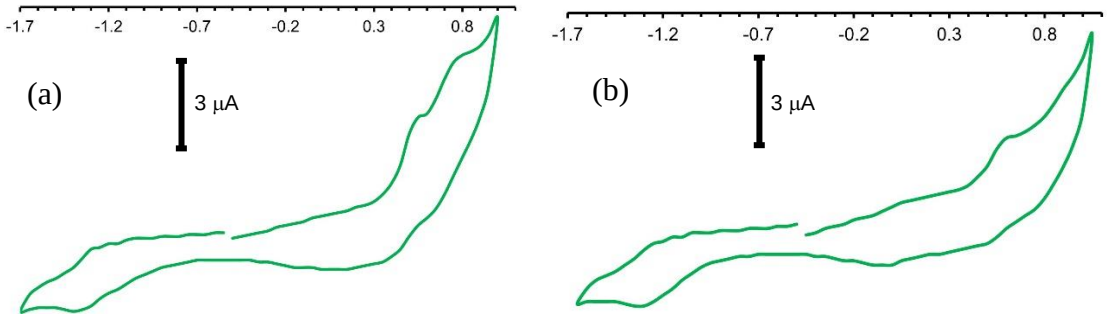

Figure S 73. Cyclic voltammograms of **Cu1a** (a) and **Cu2a** (b) in deaerated dichloromethane at a concentration of 10^{-5} M containing a solution of NBu_4PF_6 (0.1 M). Scan rate of 100 mV · s^{-1}. Potentials are referenced against Fc/Fc^+.

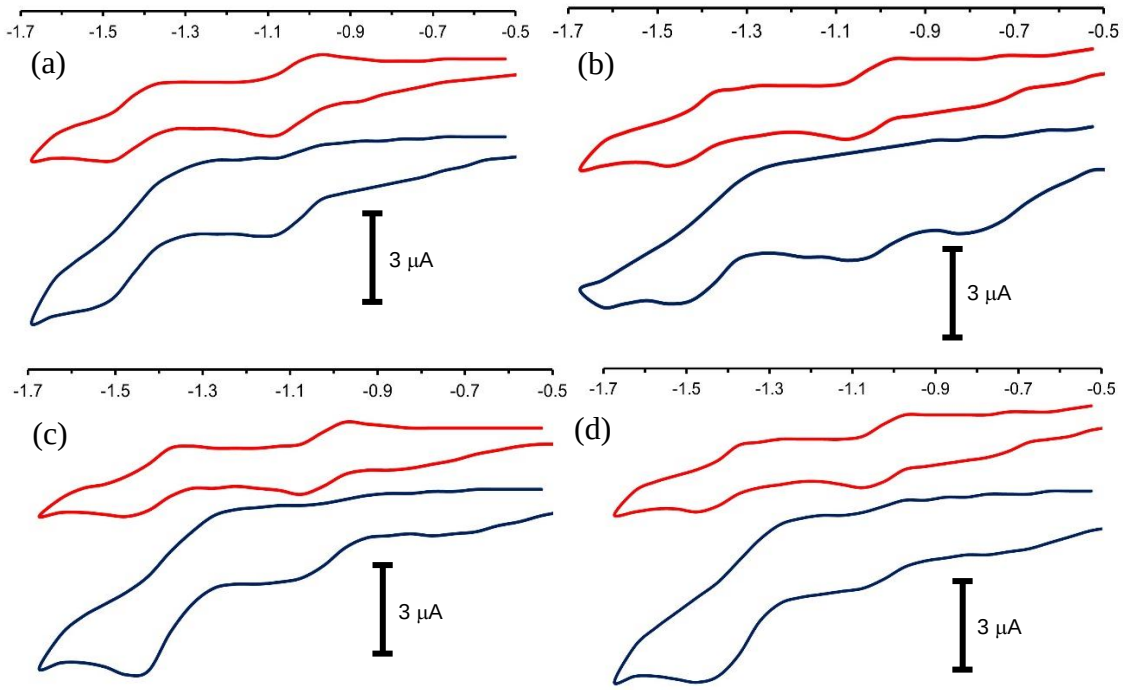

Figure S 74. Cathodic side of cyclic voltammograms in deaerated dichloromethane showing reduction processes of: (a) pristine C_{60} (5 · 10^{-5} M, in red) and its mixture with **Cu1a** (10^{-5} M, in blue); (b) pristine C_{70} (5 · 10^{-5} M, in red) and its mixture with **Cu1a** (10^{-5} M, in blue); (c) pristine C_{60} (5 · 10^{-5} M, in red) and its mixture with **Cu2a** (10^{-5} M, in blue); (d) pristine C_{70} (5 · 10^{-5} M, in red) and its mixture with **Cu2a** (10^{-5} M, in blue). All voltammograms were acquired in the presence of a solution of NBu_4PF_6 (0.1 M) and with a scan rate of 100 mV · s^{-1}. Potentials are referenced against Fc/Fc^+.

General procedure for in situ complexation and ligand cleavage

Different stock solutions of final complexes **Cu1a**, **Cu1b**, **Cu2a** and **Cu2b** (1.0×10^{-3} M), ligand dppe (1,2-Bis(diphenylphosphino)ethane) (5.0×10^{-2} M) and starting copper complex $[Cu(NCMe)_4]BF_4$ (5.0×10^{-2} M) were prepared in CD_2Cl_2 and stored conveniently at 0° C.
Switching procedure consisted of the addition of 1.0 equivalent of dppe stock solution to the final complex solution in an NMR tube capped with a septum. After being gently shaken, ligand was decoordinated as revealed by a color change from yellow/orange to colorless/yellow (depending on substituents **1** or **2**). Further addition of 0.50 equivalents of $[Cu(NCMe)_4]BF_4$ stock solution immediately forms original copper complex after a gently shaking. Color turned back to yellow/orange as well. A ^{1}H-NMR spectrum at 298 K was recorded at each stage whose chemical shift changes confirmed the existence of described compounds. The entire cyclic process could be repeated at least 4 times to demonstrate its reversible nature (see

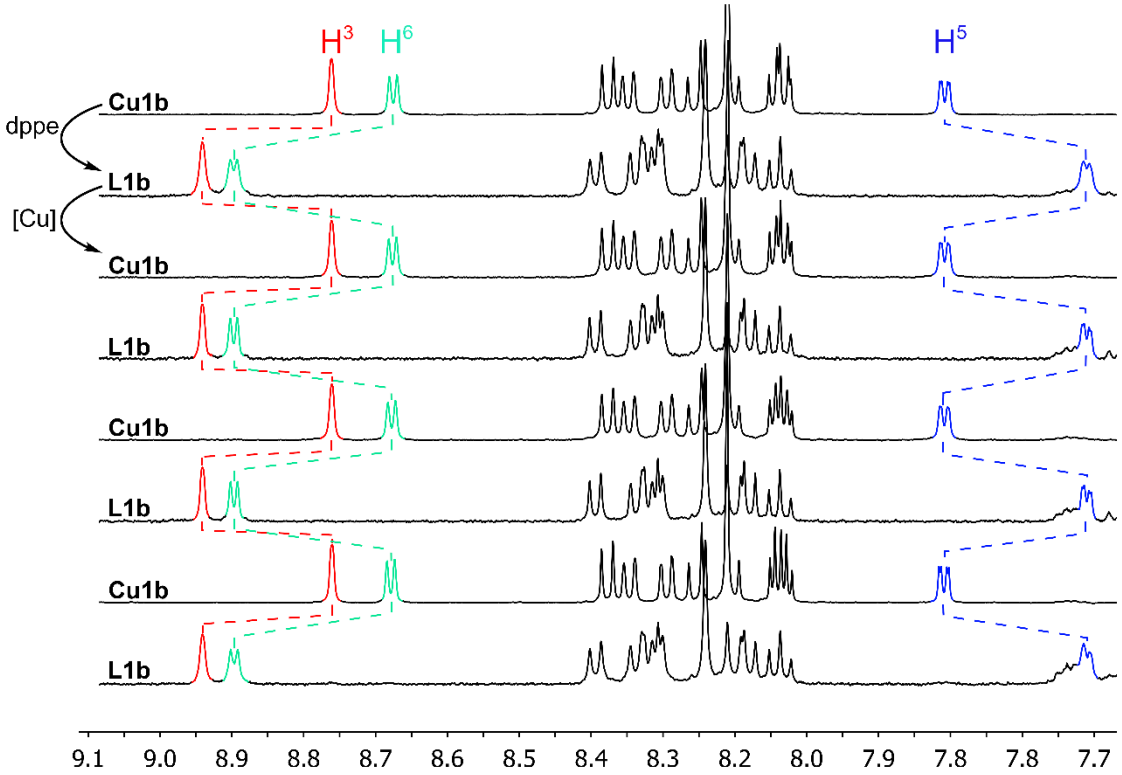

Figure **S 77** - Figure S 76) and is summarized in Scheme S3.

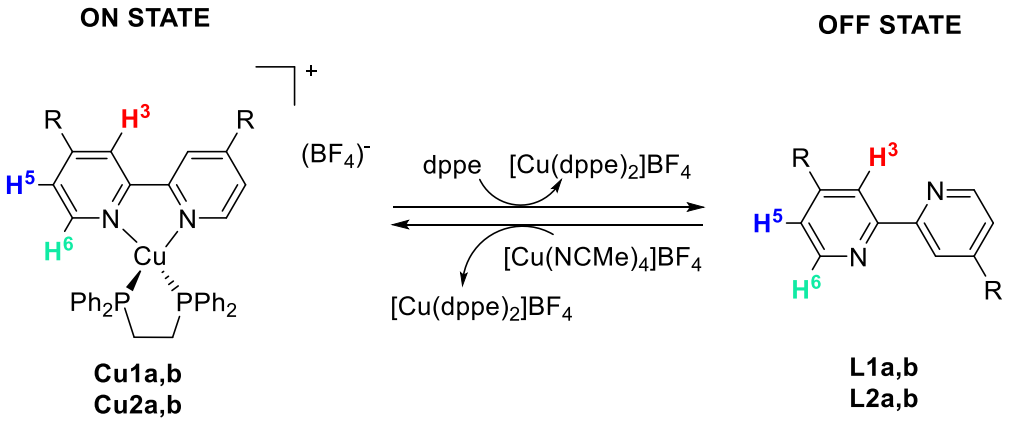

Scheme S3. Chemical switching process carried out for all copper complexes reported in this work. Relevant aromatic protons have been highlighted in different colors for differentiation purposes (see below).

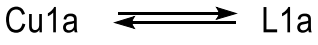

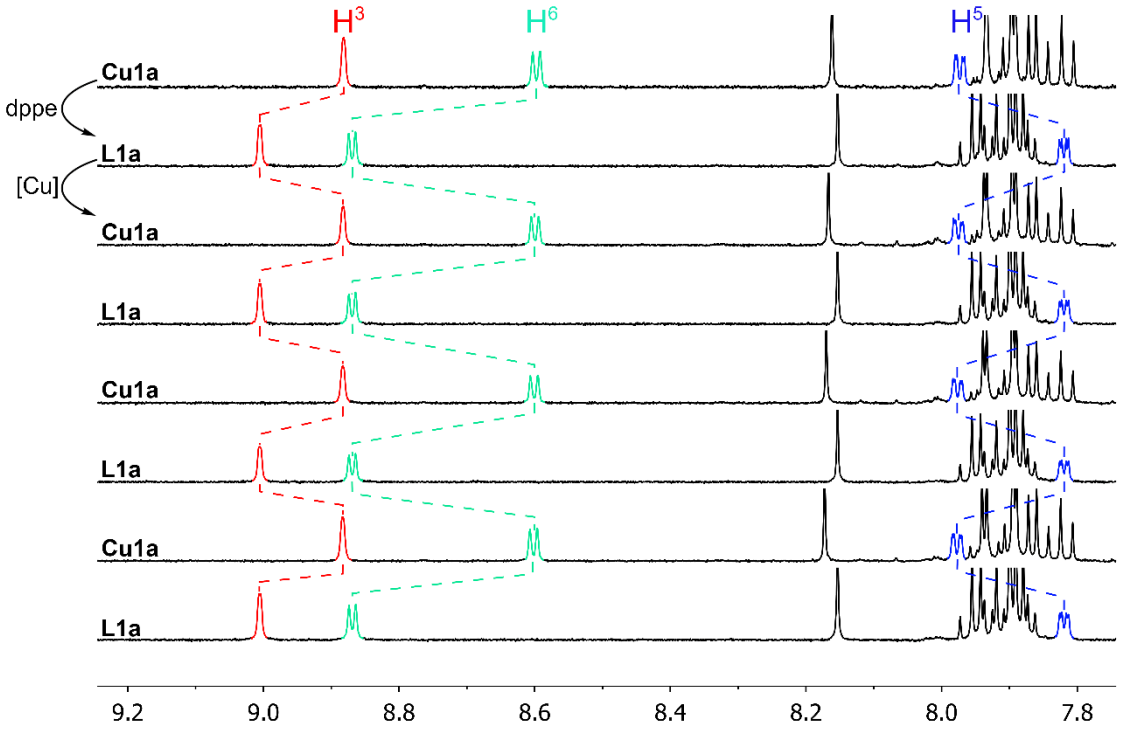

Figure S 75. Stacked ^{1}H-NMR (500 MHz, CD_2Cl_2) spectra of compounds **Cu1a/L1a** coordination/decoordination experiments at 298 K. Chemical shifts in ppm.

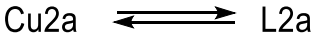

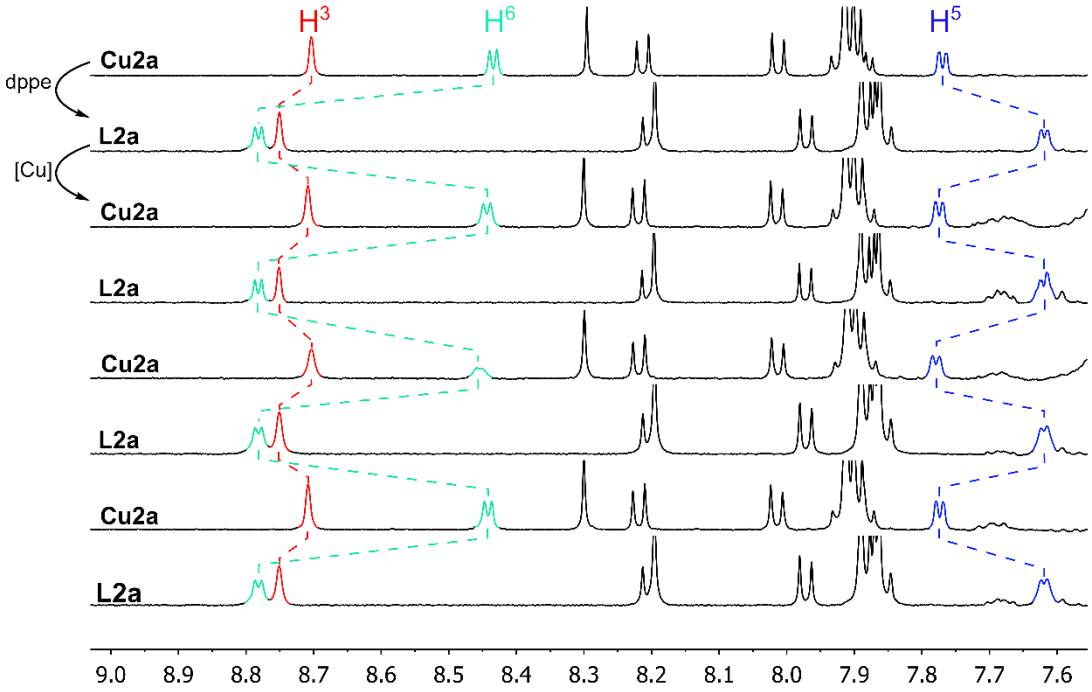

Figure S 76. Stacked ^{1}H-NMR (500 MHz, CD_2Cl_2) spectra of compounds **Cu2a/L2a** coordination/decoordination experiments at 298 K. Chemical shifts in ppm.

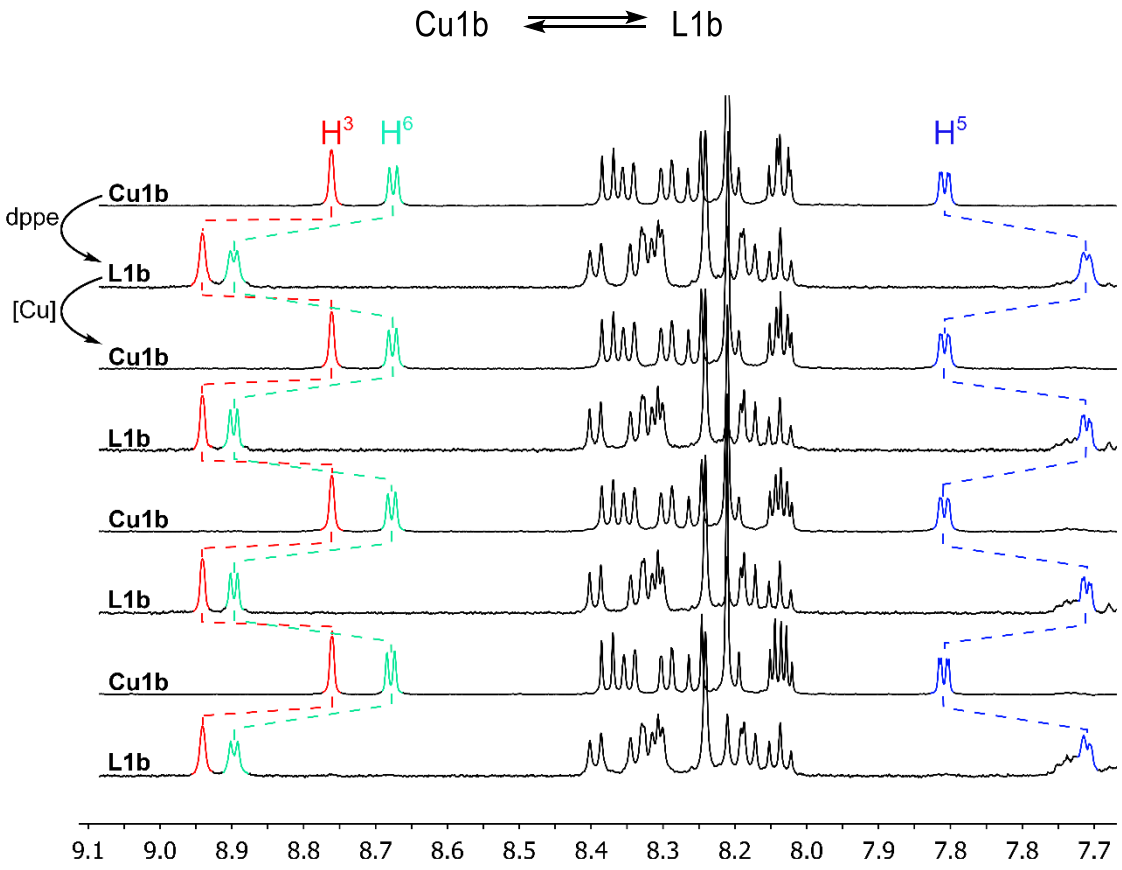

Figure S 77. Stacked ^{1}H-NMR (500 MHz, CD_2Cl_2) spectra of compounds **Cu1b**/**L1b** coordination/decoordination experiments at 298 K. Chemical shifts in ppm.

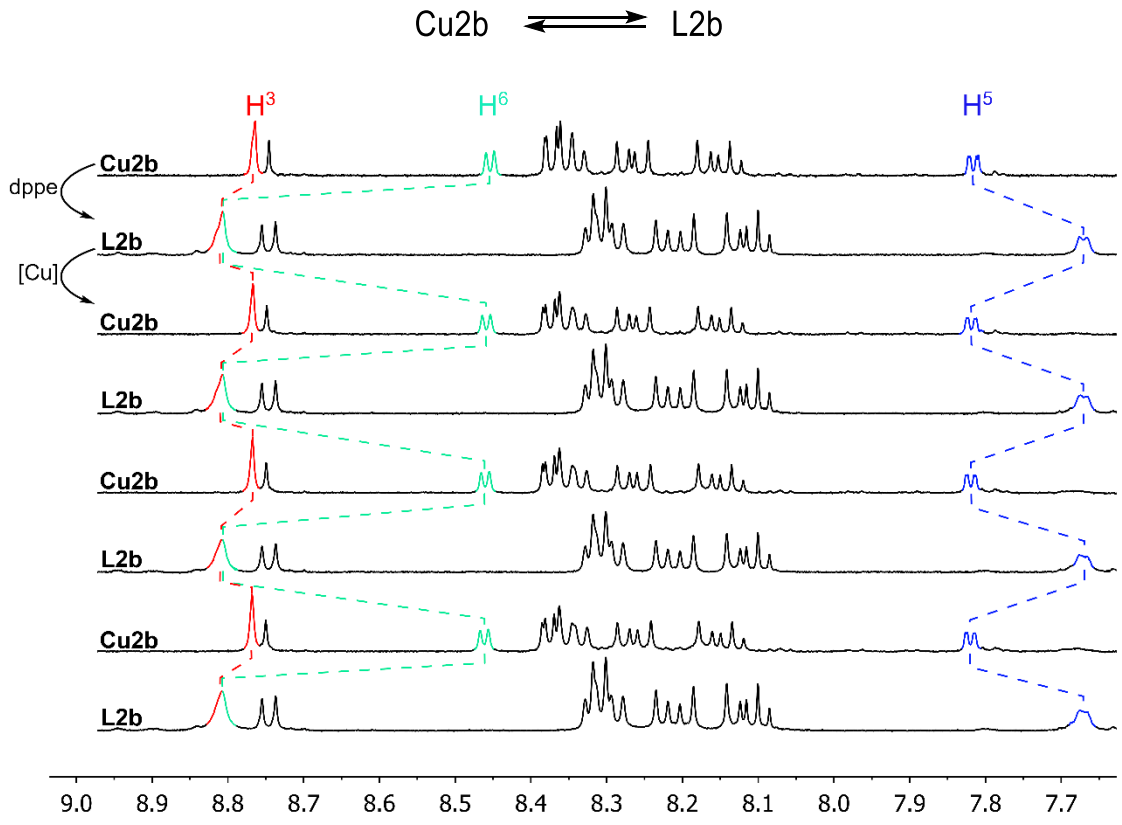

Figure S 78. Stacked ^{1}H-NMR (500 MHz, CD_2Cl_2) spectra of compounds **Cu2b**/**L2b** coordination/decoordination experiments at 298 K. Chemical shifts in ppm.

After several cycles, fullerenes C_{60} and C_{70} were added to the NMR tube (10 eq) and more coordination/decoordination cycles were carried out following the procedure described above (see Figure S 87 - Figure S 85). In this second sequence of experiments, ^{1}H NMR chemical shifts of complexes **Cu1a** and **Cu2a** were changed with respect to the parent spectra whereas those for ligands **L1a**, **L1b**, **L2a** and **L2b** and complexes **Cu1b** and **Cu2b** were invariant. This clearly indicates that corannulene-based complexes have engaged in fullerene recognition as opposed to pyrene-based complexes and free ligands.

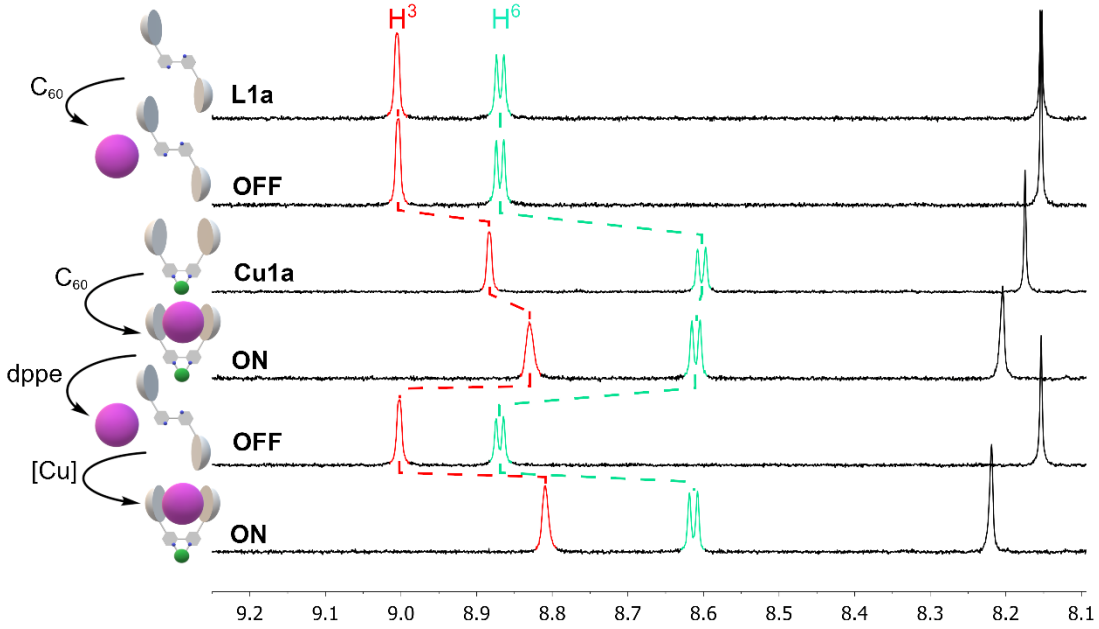

Figure S 79. Stacked ^{1}H-NMR (500 MHz, CD_2Cl_2) spectra of mixtures **Cu1a+C_{60}**/**L1a+C_{60}** coordination/decoordination experiments at 298 K. Chemical shifts in ppm.

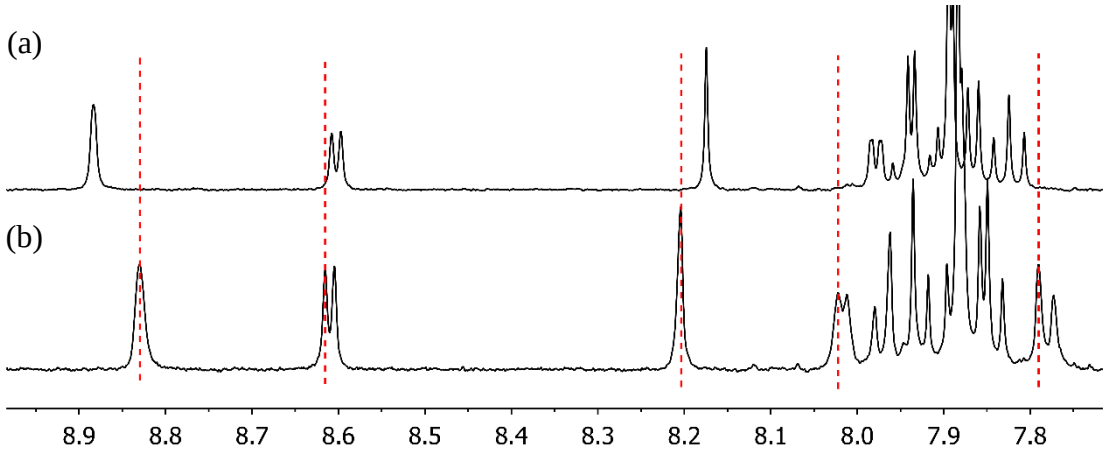

Figure S 80. ^{1}H-NMR (500 MHz, CD_2Cl_2) spectra of (a) **Cu1a** and (b) **Cu1a** with an excess of C_{60} at 298 K. Vertical straight dashed red lines were drawn to show the chemical shift changes of both the bpy and corannulene moieties.

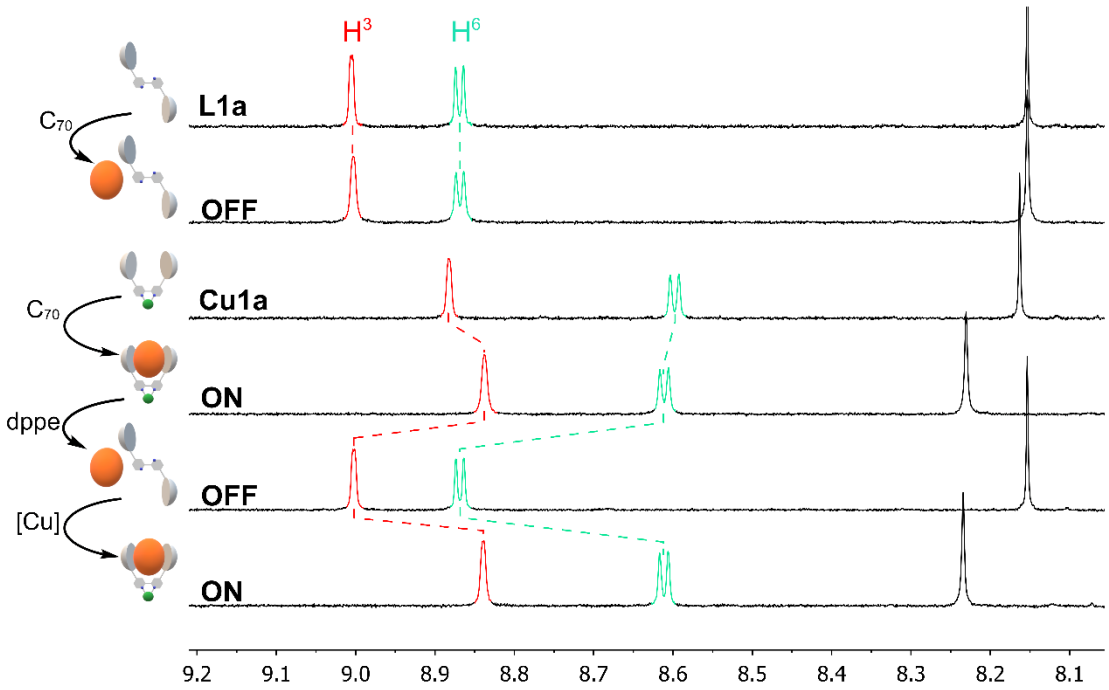

Figure S 81. Stacked ^{1}H-NMR (500 MHz, CD_2Cl_2) spectra of mixtures **Cu1a+C_{70}/L1a+C_{70}** coordination/decoordination experiments at 298 K. Chemical shifts in ppm

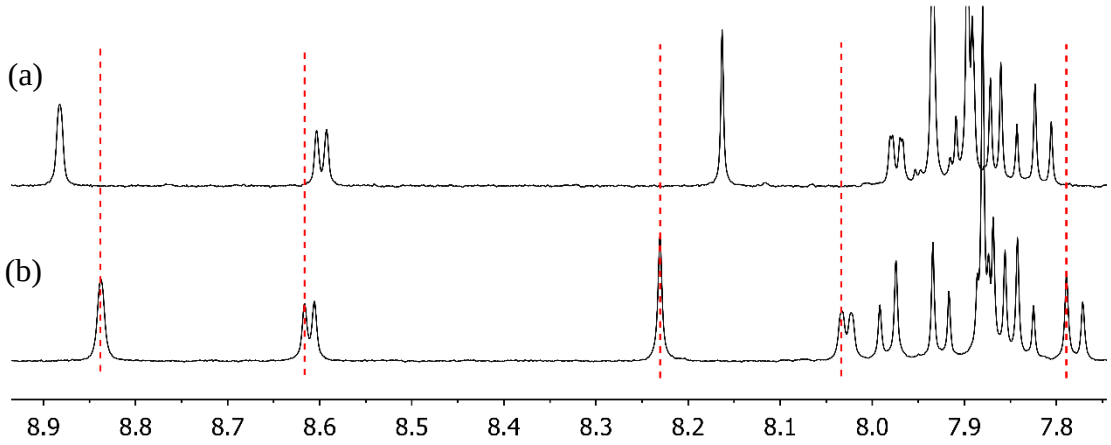

Figure S 82. ^{1}H-NMR (500 MHz, CD_2Cl_2) spectra of (a) **Cu1a** and (b) **Cu1a** with an excess of C_{70} at 298 K. Vertical straight dashed red lines were drawn to show the chemical shift changes of both the bpy and corannulene moieties.

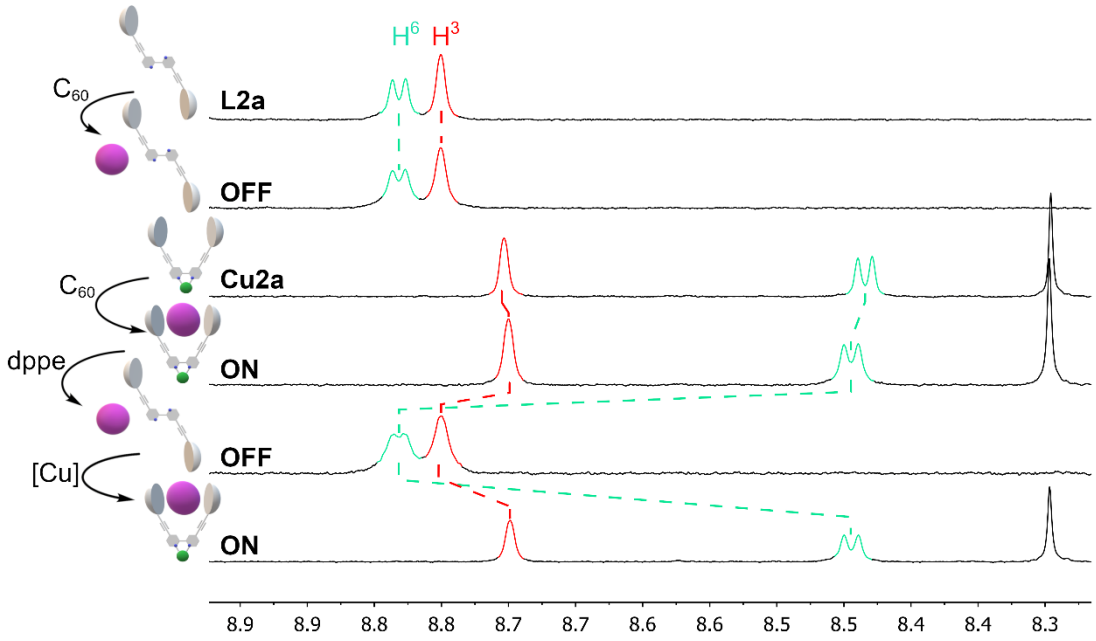

Figure S 83. Stacked ^{1}H-NMR (500 MHz, CD_2Cl_2) spectra of mixtures **Cu2a+C_{60}/L2a+C_{60}** coordination/decoordination experiments at 298 K. Chemical shifts in ppm.

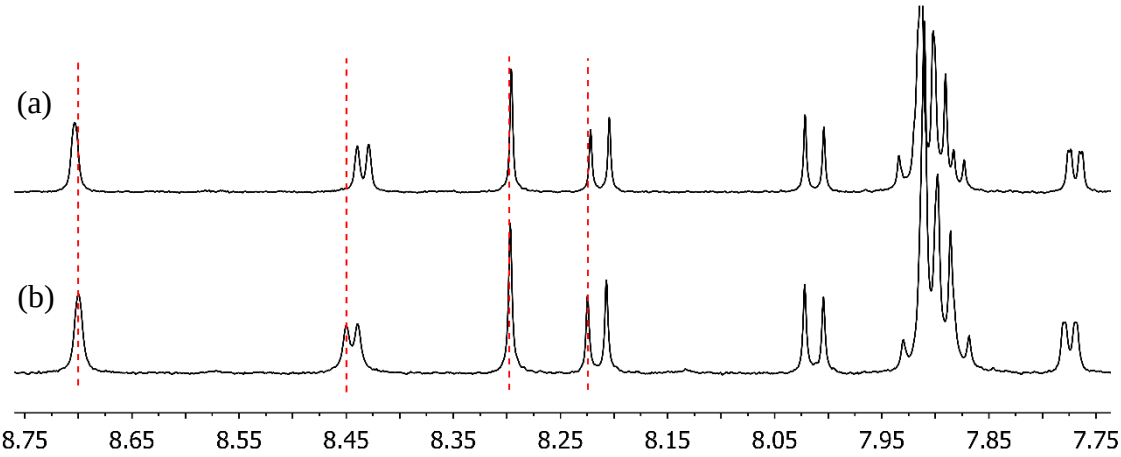

Figure S 84. ^{1}H-NMR (500 MHz, CD_2Cl_2) spectra of (a) **Cu2a** and (b) **Cu2a** with an excess of C_{60} at 298 K. Vertical straight dashed red lines were drawn to show the chemical shift changes of both the bpy and corannulene moieties.

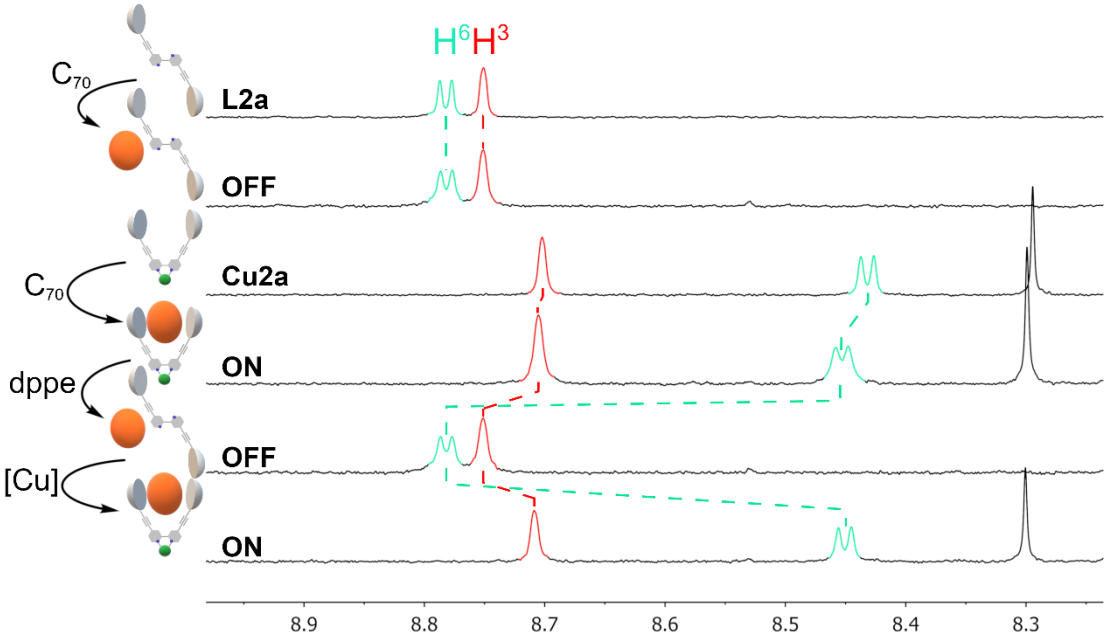

Figure S 85. Stacked ^{1}H-NMR (500 MHz, CD_2Cl_2) spectra of mixtures **Cu2a+C_{70}/L2a+C_{70}** coordination/decoordination experiments at 298 K. Chemical shifts in ppm.

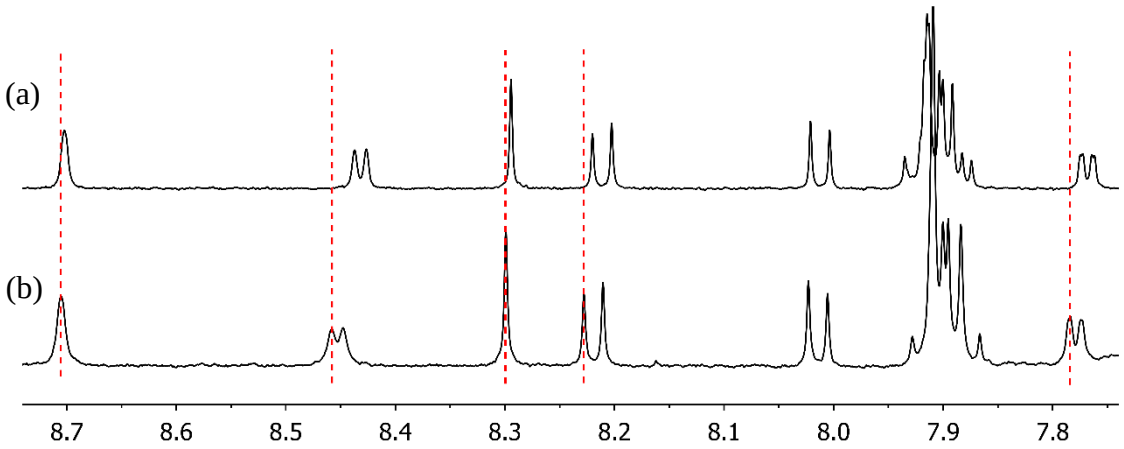

Figure S 86. ^{1}H-NMR (500 MHz, CD_2Cl_2) spectra of (a) **Cu2a** and (b) **Cu2a** with an excess of C_{70} at 298 K. Vertical straight dashed red lines were drawn to show the chemical shift changes of both the bpy and corannulene moieties.

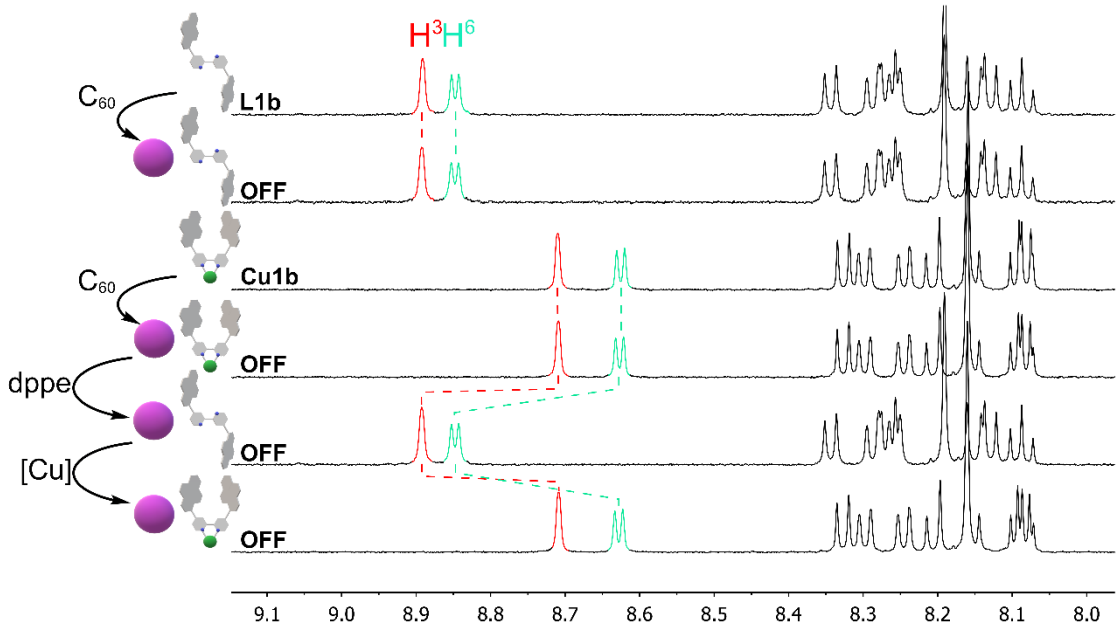

Figure S 87. Stacked ^{1}H-NMR (500 MHz, CD_2Cl_2) spectra of mixtures **Cu1b+C_{60}/L1b+C_{60}** coordination/decoordination experiments at 298 K. Chemical shifts in ppm.

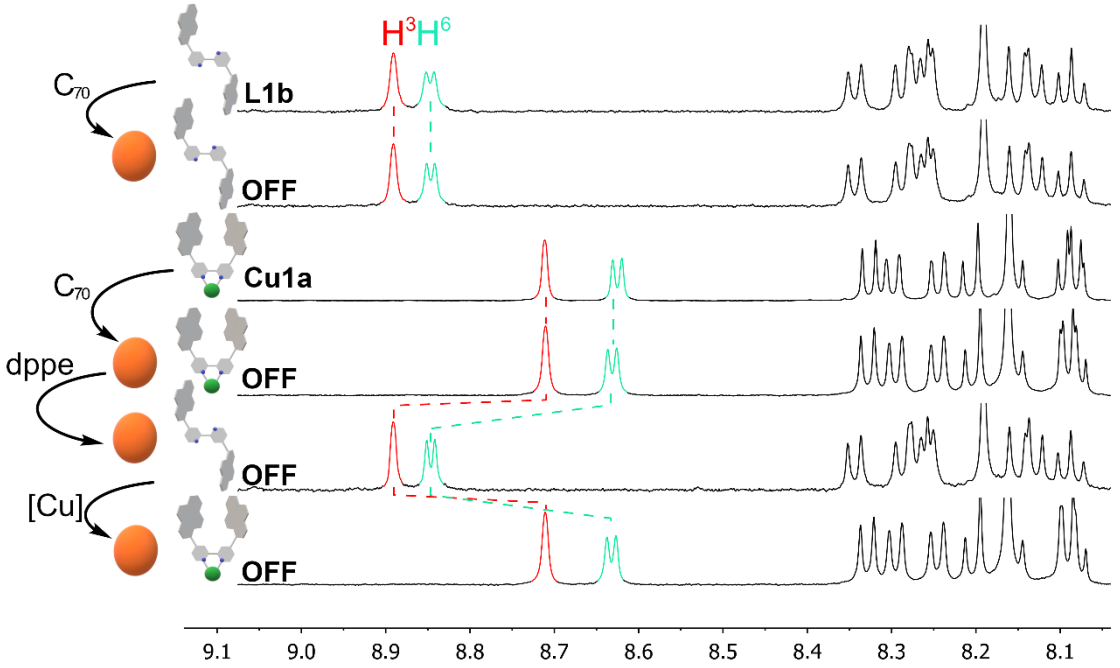

Figure S 88. Stacked ^{1}H-NMR (500 MHz, CD_2Cl_2) spectra of mixtures **Cu1b+C_{70}/L1b+C_{70}** coordination/decoordination experiments at 298 K. Chemical shifts in ppm.

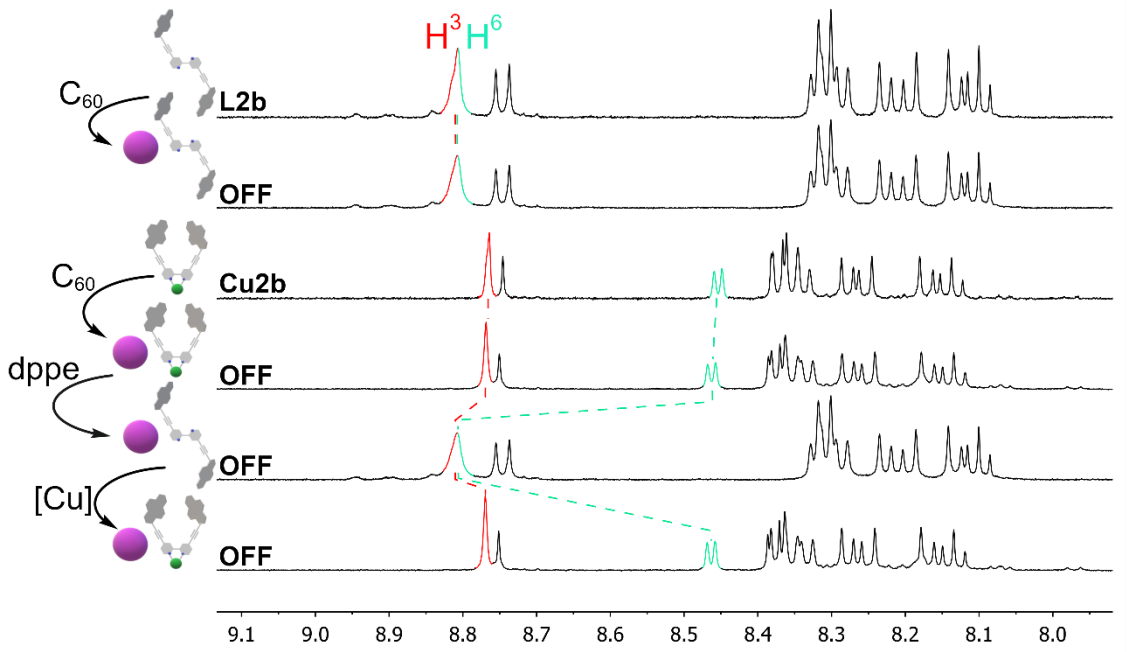

Figure S 89. Stacked ^{1}H-NMR (500 MHz, CD_2Cl_2) spectra of mixtures **Cu2b+C_{60}/L2b+C_{60}** coordination/decoordination experiments at 298 K. Chemical shifts in ppm.

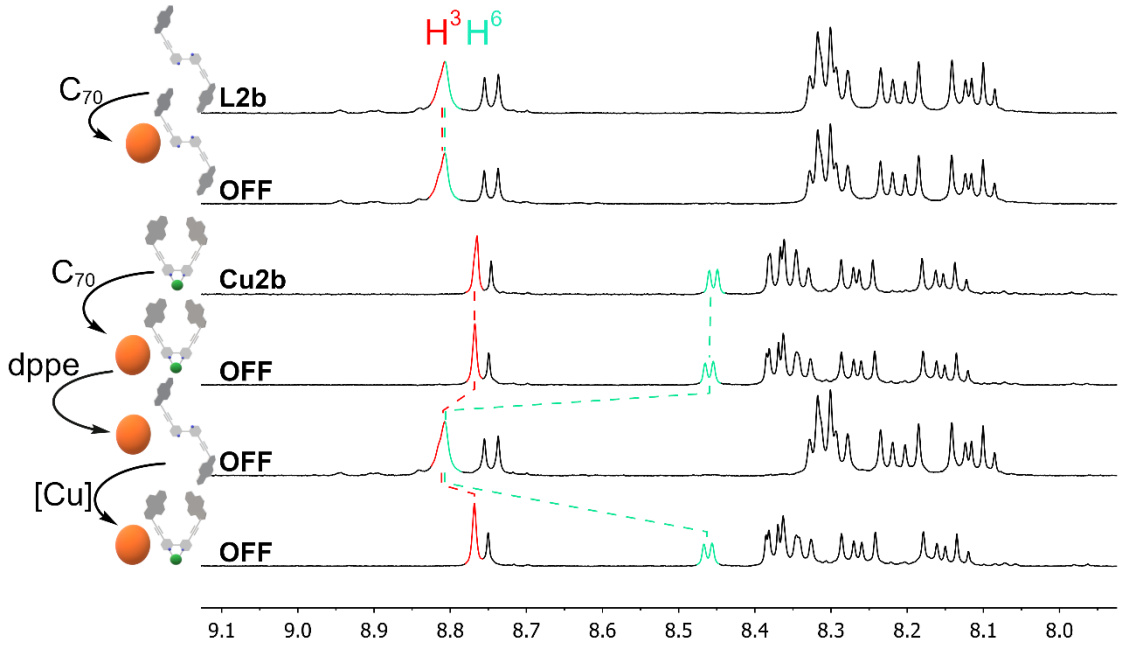

Figure S 90. Stacked ^{1}H-NMR (500 MHz, CD_2Cl_2) spectra of mixtures **Cu2b+C_{70}/L2b+C_{70}** coordination/decoordination experiments at 298 K. Chemical shifts in ppm.

Association constants measurements

In order to estimate the association constants (K_a) of complexes **Cu1a** and **Cu2a** with fullerenes C_{60} and C_{70}, the following procedure was carried out: a solution of each compound (2.0×10^{-5} M) in deuterated dichloromethane was prepared and a known volume was transferred to an NMR tube capped with a septum (0.50 mL). The titration was carried out by injecting through the septum known portions of a stock solution of C_{60} (2.0×10^{-4} M) in deuterated dichloromethane to cover a wide range of equivalents. The same protocol was followed for C_{70}. A ^{1}H-NMR spectrum was recorded at room temperature (298 K) after each addition. Once all data had been obtained, the changes in chemical shifts (Δδ) of selected protons were plotted as a function of the molar fraction of the guest, and the resulting curve was fitted by a nonlinear method using the global analysis approach according to the following equations assuming a 1:1 equilibrium:

$$K_a = \frac{[HG]}{[H][G]} \qquad \text{eq. 1}$$

Changes in chemical shifts upon NMR titration are expressed:

$$\Delta\delta = \Delta\delta_{max}\left(\frac{[HG]}{H_0}\right) \qquad \text{eq. 2}$$

Where:

[HG] is the concentration of the guest of the complex, and is calculated using the following equatic...

$$[HG] = \frac{1}{2}\left([G_0] + [H_0] + \frac{1}{K_a}\right) - \sqrt{\left([G_0] + [H_0] + \frac{1}{K_a}\right)^2 + 4[G_0][H_0]} \qquad \text{eq. 3}$$

Where:

$[G_0]$ is the total concentration of the guest (C_{60} or C_{70}).
$[H_0]$ is the total concentration of the host (**Cu1a** or **Cu2a**).
$\Delta\delta_{max}$ is Δδ at maximum complexation (100% supramolecular complex formation).
K_a is the estimated association constant for 1:1 equilibrium.
In each case, $\Delta\delta_{max}$ and K_a for a 1:1 equilibrium were extracted by using the non-linear fitting tool provided by the open access web portal Supramolecular.org (*http://supramolecular.org*) applying equations 2 and 3. Links to all the fittings of the data are provided below.

Cu1a Vs C_{60}
http://app.supramolecular.org/bindfit/view/49f7f748-f993-4d63-8d7d-0a588f8af0ff
Cu1a Vs C_{70}
http://app.supramolecular.org/bindfit/view/82d040c4-de8c-4567-aa76-7a38bcd01444
Cu2a Vs C_{60}
http://app.supramolecular.org/bindfit/view/f64f17a6-cbe1-4829-adc0-9b7a79731c77
Cu2a Vs C_{70}
http://app.supramolecular.org/bindfit/view/218dfb73-8470-462e-b5f6-f83d28202bd3

Table S 1. Estimated K_a values calculated from selected protons in each compound (in M^{-1}).

	C_{60}	C_{70}
Cu1a	$2.00 \pm 0.01 \times 10^3$	$4.99 \pm 0.01 \times 10^4$
Cu2a	$1.15 \pm 0.01 \times 10^3$	$2.11 \pm 0.01 \times 10^4$

The most affected chemical shifts were those belonging to protons in the bpy unit (especially for hydrogen H^3, as it points toward the fullerene upon inclusion complex formation) as well as the singlet and doublet from the corannulene group (H^8 and H^{16} for complex **Cu1a**; H^{10} and H^{18} for complex **Cu2a**), which correspond to the hydrogens closest to the substituted carbon. They were also selected because they appear in a relatively clean section of the spectrum and their signals can be reliably followed.

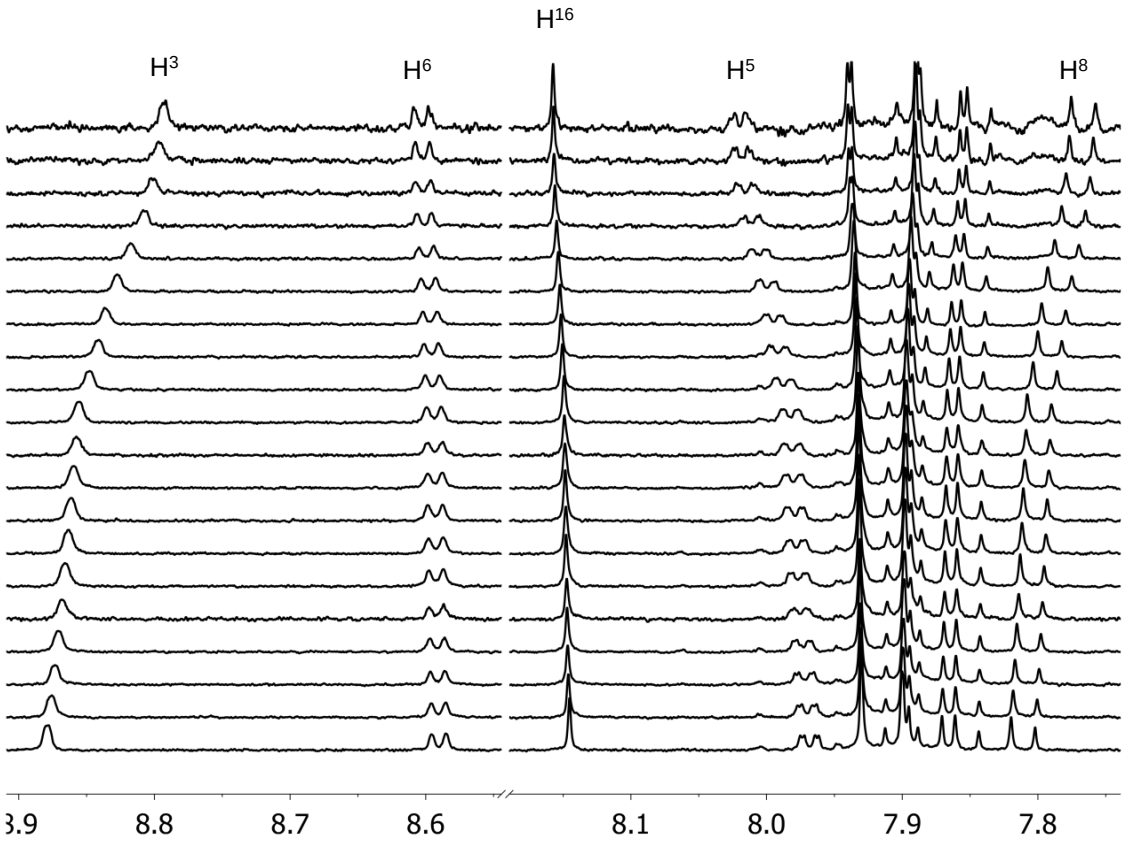

Figure S 91. Stacked ^{1}H-NMR spectra for the titration of complex **Cu1a** with variable concentrations of C_{60} in methylene chloride-d_2 at 298 K. Chemical shifts in ppm. The most significant chemical shifts corresponding to the bpy moiety (H^3, H^5, H^6) and the corannulene substituent (H^8, H^{16}) have been labeled accordingly.

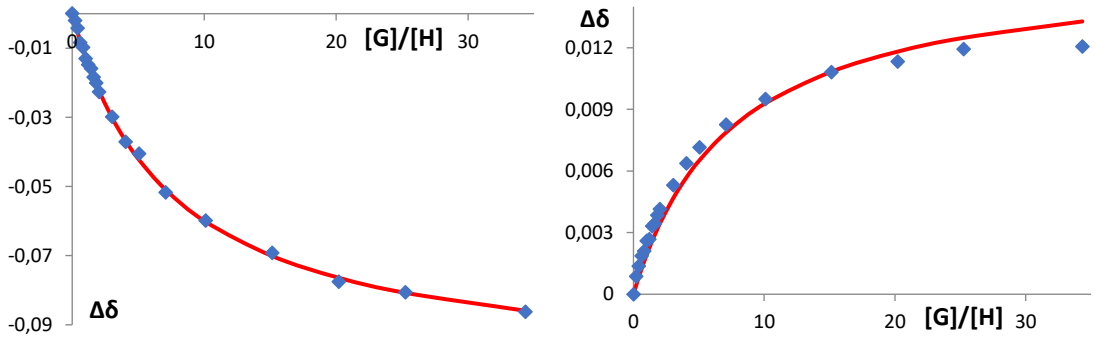

Figure S 92. Nonlinear regressions for selected protons (left plot: H_3, right plot: H_{16},) for the titration of complex **Cu1a** with C_{60}.

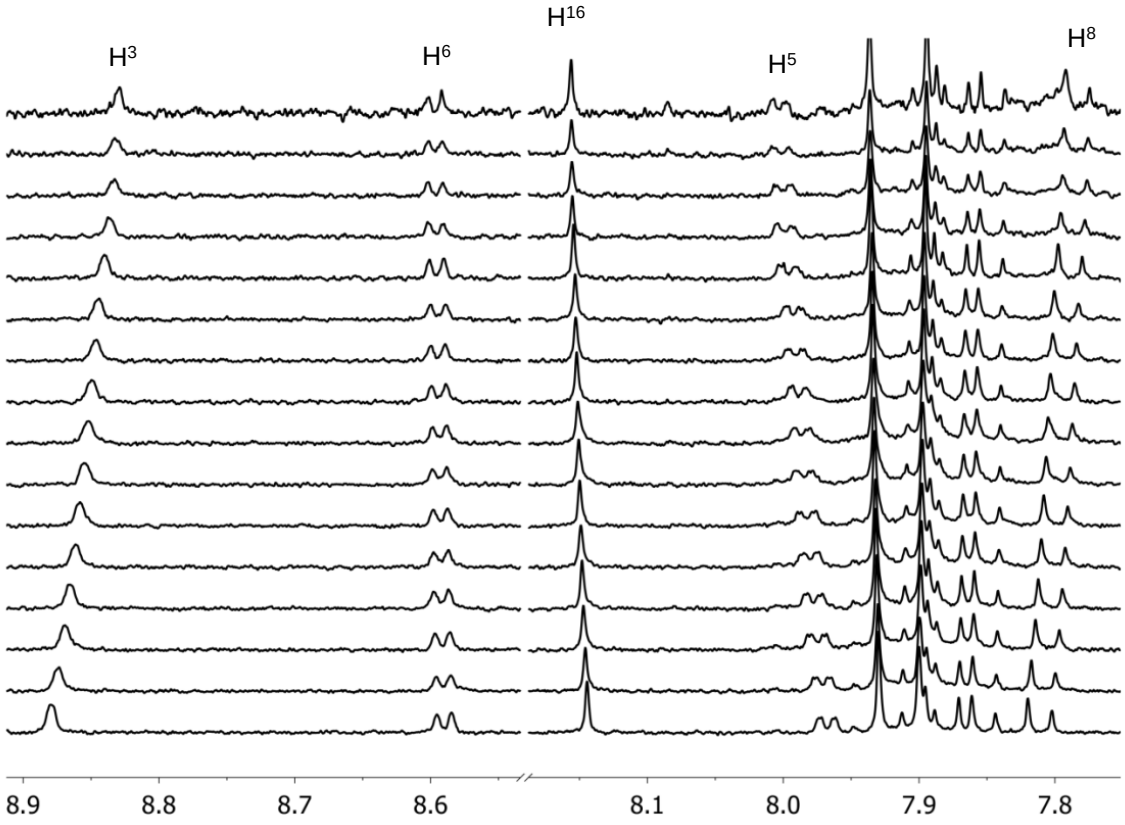

Figure S 93. Stacked ^{1}H-NMR spectra for the titration of complex **Cu1a** with variable concentrations of C_{70} in methylene chloride-d_2 at 298 K. Chemical shifts in ppm. The most significant chemical shifts corresponding to the bpy moiety (H^3, H^5, H^6) and thecorannulene substituent (H^8, H^{16}) have been labeled accordingly.

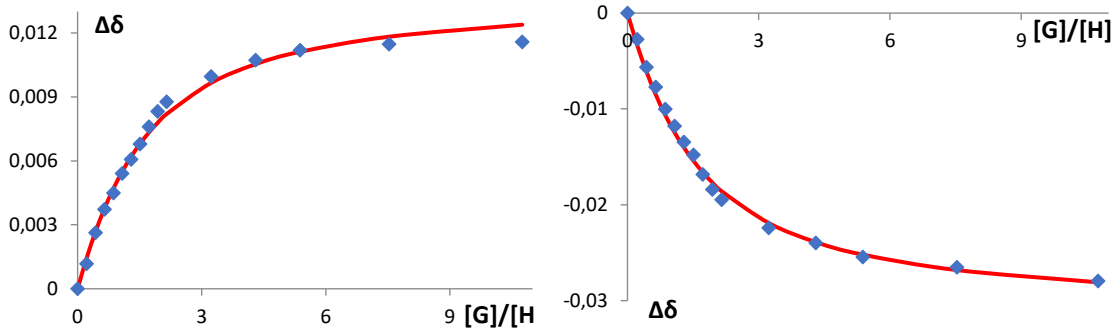

Figure S 94. Nonlinear regressions for selected protons (left plot: H_{16}, right plot: H_{8},) for the titration of complex **Cu1a** with C_{70}.

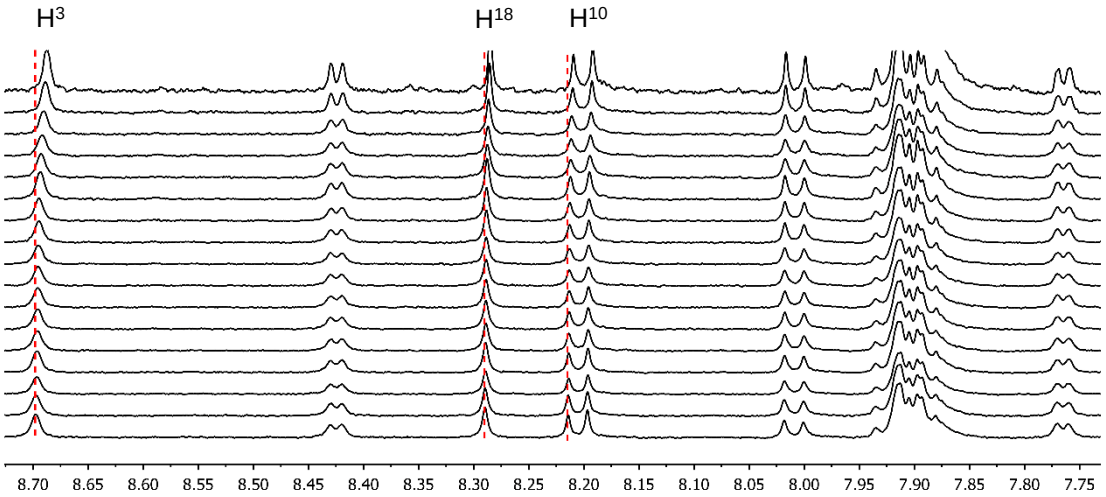

Figure S 95. Stacked ^{1}H-NMR spectra for the titration of complex **Cu2a** with variable concentrations of C_{60} in methylene chloride-d_2 at 298 K. Chemical shifts in ppm. Only the aromatic region in which the bpy and corannulene signals appear is shown. The most significant chemical shifts corresponding to the bpy moiety (H^3) and the corannulene substituent (H^{18}, H^{10}) have been labeled accordingly, and a vertical straight dashed red line has been placed to guide the reader and highlight the changes in chemical shift.

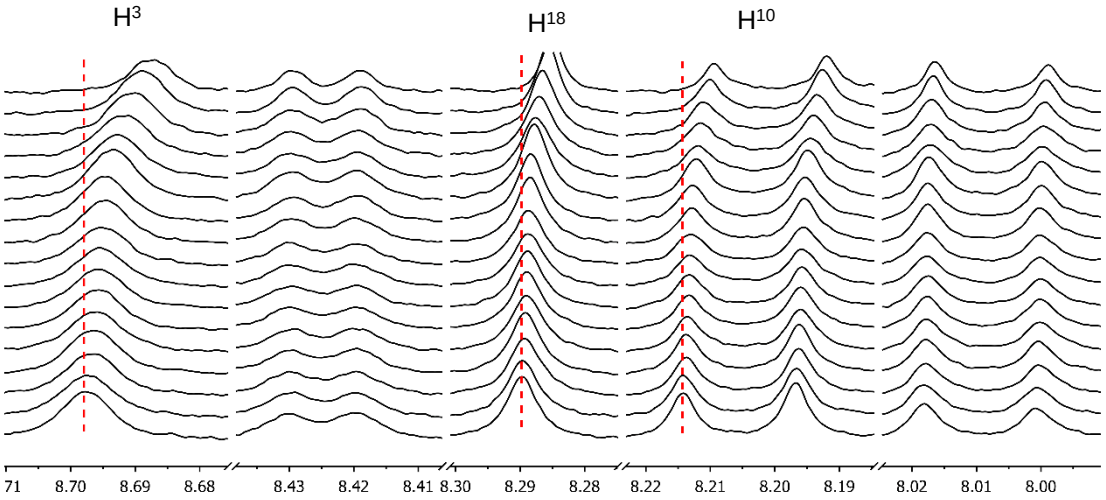

Figure S 96. Close-up of stacked ^{1}H-NMR spectra for the titration of complex **Cu2a** with variable concentrations of C_{60} in methylene chloride-d_2 at 298 K.

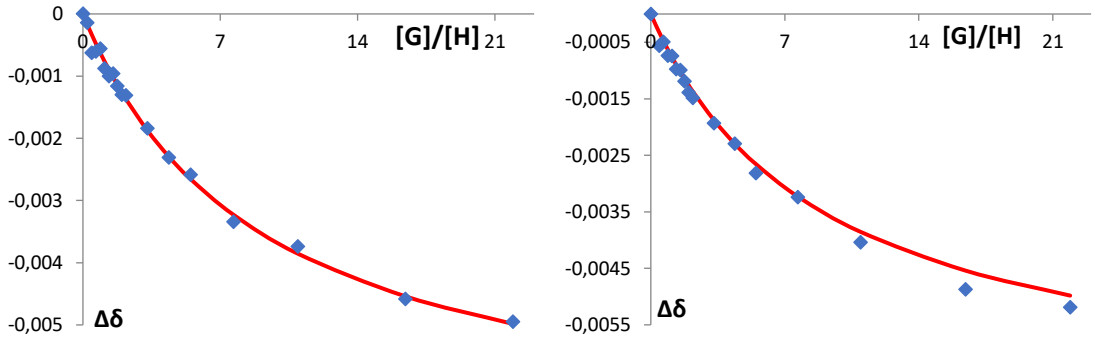

Figure S 97. Nonlinear regressions for selected protons (left plot: H_{18}, right plot: H_{10},) for the titration of complex **Cu2a** with C_{60}.

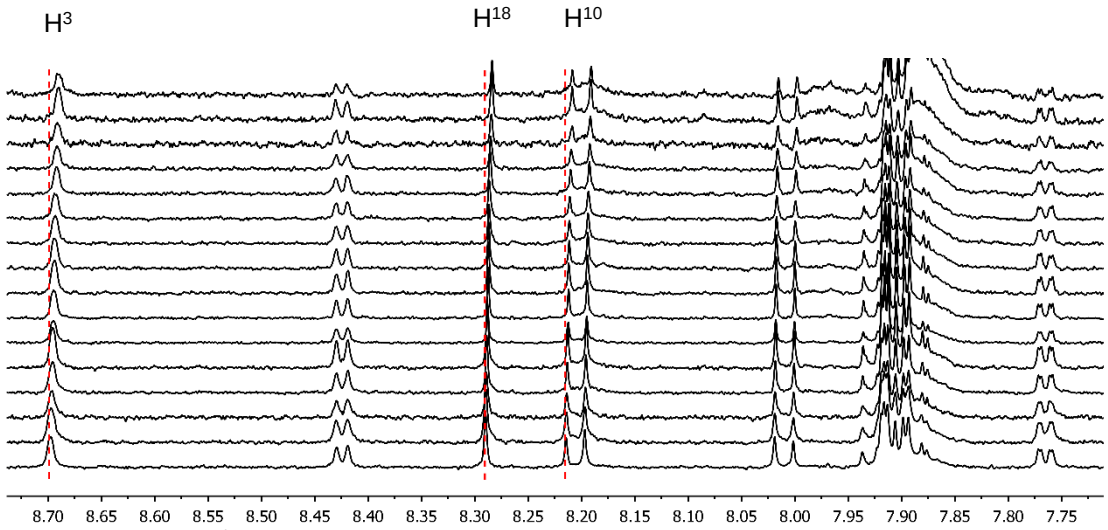

Figure S 98. Stacked ^{1}H-NMR spectra for the titration of complex **Cu2a** with variable concentrations of C_{70} in methylene chloride-d_2 at 298K. Chemical shifts in ppm. Only the aromatic region in which bpy and corannulene signals appear is shown. The most significant chemical shifts corresponding to the bpy moiety (H^3) and the corannulene substituent (H^{18}, H^{10}) have been labeled accordingly, and a vertical straight dashed red line has been placed to guide the reader and highlight the changes in chemical shift.

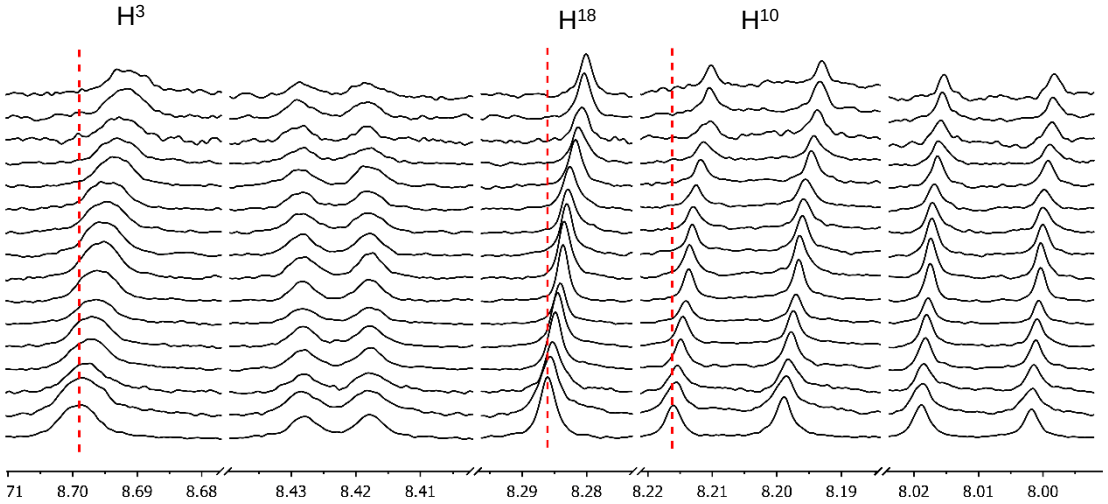

Figure S 99. Close-up of stacked ^{1}H-NMR spectra for the titration of complex **Cu2a** with variable concentrations of C_{70} in methylene chloride-d_2 at 298 K.

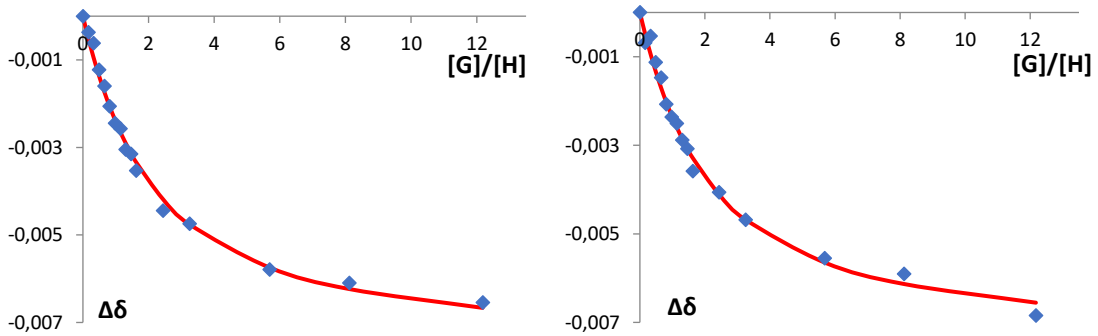

Figure S 100. Nonlinear regressions for selected protons (left plot: H_{18}, right plot: H_{10},) for the titration of complex **Cu2a** with C_{70}.

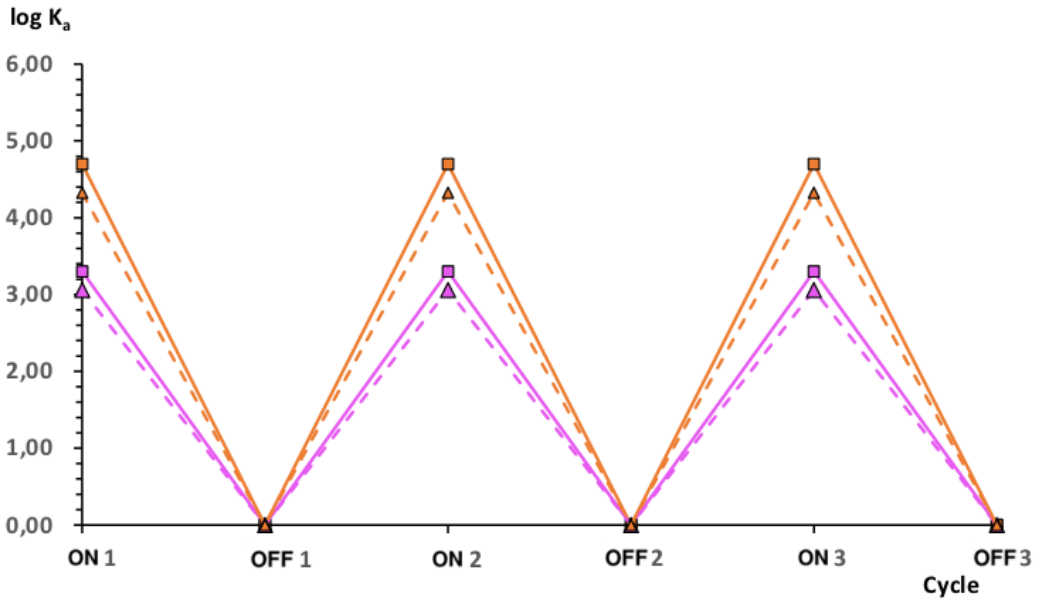

Figure S 101. Association constant variation throughout three complete ON/OFF cycles. Squares with solid lines correspond to complex **Cu1a**, whereas triangles with dashed lines correspond to complex **Cu2a**. Pink and orange traces represent fullerenes C_{60} and C_{70}, respectively.

Computational calculations details

In order to optimize the geometry of supramolecular assemblies **C_{60}@Cu1a** and **C_{60}@Cu2a**, structures of surrogate protonated bpy, namely **C_{60}@HL1a** and **C_{60}@HL2a**, were used replacing the metal fragment by a hydrogen to reduce the computational cost. Calculations were carried out by DFT methods with Grimme's B97D3 functional containing the Becke-Johnson damping empirical dispersion correction.[9–11] Pople and collaborators' split valence basis set 6-31G(d,p) was chosen.[12–15] Hydrogen atom was then replaced by Cu(dppe) fragment and further optimized with Perdew, Burke and Ernzerhof's PBE0 functional[16,17] along with Los Alamos Electron Core Potential and the associated double zeta basis set[18–20] keeping the supramolecular assembly moiety frozen. All minima were confirmed by vibrational analysis to have zero imaginary frequencies in all cases. More accurate energies were calculated on the optimized geometries by using a more extended 6-31+G(d,p) basis set that includes diffuse functions.[12–15]
For the estimation of the rotational barrier of compound **L1a**, a relaxed PES scan was performed by rotating NCCN dihedral angle 10 degrees at each step for a total of 20 points.

All the above calculations were carried out by describing the impact of the solvent via the implicit Polarizable Continuum Model (PCM)[21] and choosing dichloromethane (ε = 8.93) as the solvent.

Interaction energies were calculated in the gas phase over already optimized structures by using a more extended 6-31+G(d,p) basis set that includes diffuse functions and taking into account basis set superposition error (BSSE) with the Boys–Bernardi functional counterpoise scheme[22–25] using Equation 4:

$$E_{int}(AB) = E_{AB}^{\alpha\beta}(AB) - E_{AB}^{\alpha\beta}(A) - E_{AB}^{\alpha\beta}(B) \qquad \text{eq. 4}$$

Subscripts denote the geometry used (AB, inclusion complex in all cases) and the superscripts refer to the basis set ($\alpha\beta$, the one belonging to supramolecular assembly in all cases). A and B correspond to host and guest entities that interact to furnish the AB adduct.

Previously described computational methods were performed in Gaussian 16 package.[26]

Non-covalent interactions were obtained by the location of critical points where the reduced density gradient decreases at low electronic density values according to Yang and collaborators' scheme with the help of the NCIPlot package.[27,28] Calculations were performed with promolecular densities, and gradient isosurfaces were plotted with an isovalue of 0.3 a.u. and colored on a blue-green-red scale according to values of the sign of λ_2 (second eigenvalue of the electron-density Hessian). Red indicates repulsion, green means weak attraction, and blue represents strong attraction. Graphics were visualized in Chimera[29] with the help of Tangram NCIPlot GUI built by Insilichem Group.[30]

C_{60}@Cu1a (G = -6191,911611 a.u.)

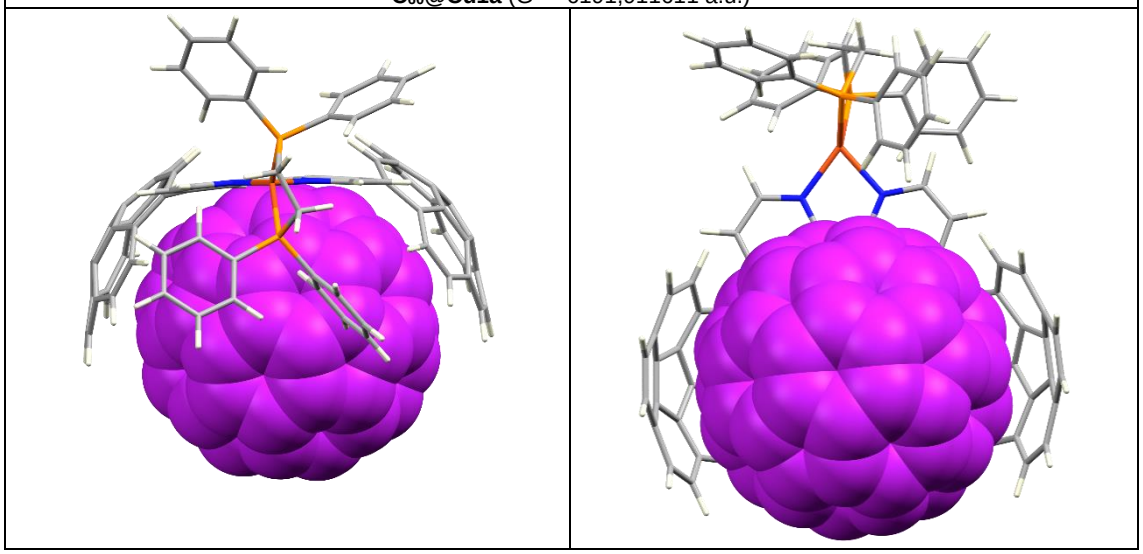

C	-4.107649	-2.862664	-0.806481	C	1.578587	-5.206004	-3.037520	C	1.085803	0.327414	-1.253020
C	-2.993366	-0.937003	-1.393075	C	-0.016067	-3.457449	-3.359921	C	2.475762	3.248088	0.297314
C	-1.887377	-1.653623	-1.862440	C	2.934229	-6.662015	1.055515	C	2.709461	3.311885	1.735851
C	-1.893000	-3.059825	-1.780053	C	3.065351	-6.358718	-1.706175	C	4.146726	3.445208	1.953129
C	-3.043793	-3.665489	-1.238706	C	1.227351	-4.067003	-3.762000	C	4.799655	3.462287	0.647281
H	-5.006237	-3.317715	-0.388975	C	2.923262	-5.669235	-2.946145	C	3.765597	3.338857	-0.374551
H	-1.004919	-1.144738	-2.236655	H	-0.393286	-2.605826	-3.925848	C	4.755738	2.790789	3.033920
H	-3.112612	-4.748023	-1.161642	H	2.920080	-6.757579	2.141217	C	3.950922	1.977540	3.940982
N	-4.093841	-1.523110	-0.867358	C	4.164863	-6.689890	0.398803	C	4.740744	0.810358	4.318832
C	-3.015303	0.540686	-1.361867	C	4.280142	-6.424786	-1.021700	C	6.032981	0.902134	3.646264
C	-2.022444	1.392048	-1.835668	C	2.278761	-3.523181	-4.598775	C	6.042823	2.126244	2.852163
C	-4.240590	2.423160	-0.544070	C	3.985000	-5.011129	-3.569198	C	4.118438	-0.437987	4.475594
C	-2.099238	2.784830	-1.623048	H	5.070790	-6.803683	0.994296	C	2.681261	-0.568252	4.258670
H	-1.145008	0.972017	-2.311585	C	5.424539	-5.940114	-1.767554	C	2.437098	-1.855718	3.616162
C	-3.249487	3.291745	-0.966804	C	3.595461	-3.974508	-4.504440	C	3.723977	-2.520916	3.435020
H	-5.150537	2.743775	-0.047281	H	2.063411	-2.665346	-5.235588	C	4.763086	-1.644267	3.966310
H	-3.371482	4.358273	-0.806506	C	5.284458	-5.264661	-2.980811	C	1.442329	-1.971414	2.632669
N	-4.094578	1.093403	-0.740689	H	6.415828	-6.001631	-1.318487	C	0.650792	-0.803769	2.254578
C	-0.991580	3.666399	-2.025409	H	4.366290	-3.452021	-5.070948	C	0.417120	-0.867310	0.814740
C	-0.533469	4.722289	-1.115982	H	6.171060	-4.825048	-3.437640	C	1.063931	-2.072944	0.304019
C	-0.292714	3.378675	-3.215051	H	-1.278823	-4.634135	0.563620	C	1.696877	-2.754559	1.427523
C	0.486806	5.522298	-1.629977	C	5.797338	-2.463922	-0.708334	C	0.885982	0.435291	2.872632
C	-0.734948	4.847822	0.316412	C	5.164716	-1.783474	-1.834272	C	1.920891	0.554655	3.895391
C	0.887091	4.097373	-3.618889	C	5.811382	-0.483852	-1.995767	C	2.568274	1.852483	3.733108
H	-0.625942	2.535027	-3.818813	C	6.844904	-0.363516	-0.971982	C	1.932922	2.537130	2.610414
C	1.177165	5.219962	-2.843655	C	6.835164	-1.587361	-0.176183	C	0.892471	1.660876	2.078653
C	1.380366	6.261968	-0.797896	C	2.971772	1.712720	-2.064883	Cu	-5.532851	-0.256039	-0.063697
H	-1.518893	4.273046	0.805255	C	4.009097	2.588551	-1.533036	P	-6.065389	-0.148190	2.214548
C	0.138901	5.572072	1.127309	C	5.297240	1.927156	-1.718117	P	-7.771392	0.093814	-0.603726
C	1.951833	3.668010	-4.504979	C	5.054304	0.639720	-2.363204	C	-7.782139	0.567092	2.169759
C	2.486371	5.775828	-2.765492	C	3.615318	0.507773	-2.578015	C	-8.603714	-0.070686	1.045973
C	1.311691	6.232739	0.594806	C	6.038206	2.827299	0.471936	C	-8.120405	1.802875	-1.157329
C	2.614051	6.416476	-1.498887	C	6.670448	2.143280	1.596489	C	-9.059676	2.647234	-0.554395
H	-0.008572	5.534825	2.206416	C	7.314088	0.937022	1.086504	C	-9.258689	3.939017	-1.038776
H	1.779283	2.827633	-5.176727	C	7.079123	0.874527	-0.353019	C	-8.528940	4.398380	-2.131840
C	3.234982	4.206735	-4.419255	C	6.291695	2.043074	-0.733837	C	-7.589897	3.565370	-2.738282
C	3.575386	5.227228	-3.445898	C	6.652526	-0.258046	3.156122	C	-7.379777	2.280755	-2.248128
C	2.540385	6.593735	1.274844	C	6.005659	-1.555965	3.319442	H	-9.644374	2.309511	0.295875
C	3.839809	6.544957	-0.845120	C	6.259136	-2.340718	2.114941	H	-9.989062	4.584908	-0.560307
H	4.025383	3.768027	-5.028277	C	7.062672	-1.527430	1.207786	H	-8.687598	5.404695	-2.508005
C	4.869701	5.557019	-2.884240	C	7.305326	-0.240174	1.851034	H	-7.013717	3.919597	-3.587997
C	3.745771	6.740667	0.588384	C	3.966736	-3.274302	2.276020	H	-6.632952	1.640833	-2.712477
H	2.551283	6.642464	2.363424	C	2.934019	-3.391640	1.252282	C	-8.788351	-0.966540	-1.691642
C	4.995203	6.185500	-1.644381	C	3.586832	-3.373454	-0.052256	C	-10.063581	-0.589833	-2.129827
H	5.772446	5.209022	-3.385991	C	5.023662	-3.243757	0.164525	C	-10.809831	-1.451332	-2.927989
H	4.656880	6.899646	1.164840	C	5.259884	-3.183434	1.602921	C	-10.291283	-2.692976	-3.294421
H	5.992310	6.305732	-1.220808	C	1.694446	-2.055752	-0.948466	C	-9.021040	-3.071665	-2.867133
C	-0.436323	-5.122763	0.077975	C	1.703271	-0.833239	-1.745487	C	-8.269479	-2.208570	-2.073104
C	-0.203846	-4.910782	-1.338707	C	2.993873	-0.741985	-2.422934	H	-10.469494	0.380411	-1.855899
C	0.466294	-5.821173	0.880943	C	3.782967	-1.908493	-2.040093	H	-11.797621	-1.152875	-3.266881
C	0.883333	-5.613303	-1.859296	C	2.977896	-2.723846	-1.134363	H	-10.876048	-3.361762	-3.919206
C	-0.715411	-3.847679	-2.204506	C	0.428307	0.310600	0.052975	H	-8.610731	-4.034010	-3.158823
C	1.699342	-6.365821	0.355161	C	0.668619	1.599129	0.693815	H	-7.270179	-2.492874	-1.751971
H	0.287206	-5.848263	1.955783	C	1.476763	2.409106	-0.213458	C	-6.290880	-1.718877	3.128624
C	1.806860	-6.326014	-1.035335	C	1.730660	1.625553	-1.417121	C	-6.646527	-2.854640	2.388809

C	-6.871324	-4.072321	3.025249	C	-5.127673	0.948693	3.329073	H	-5.398579	3.080321	5.969165
C	-6.721241	-4.172361	4.406596	C	-3.748539	1.060863	3.108890	H	-6.783185	1.616411	4.553400
C	-6.351521	-3.051701	5.147884	C	-2.968138	1.880563	3.919232	H	-9.621666	0.332361	1.024938
C	-6.140286	-1.829243	4.515386	C	-3.561227	2.608363	4.948830	H	-8.706325	-1.149172	1.215401
H	-6.746260	-2.782513	1.307737	C	-4.933884	2.511846	5.168960	H	-7.669433	1.645029	2.002911
H	-7.153354	-4.943666	2.441465	C	-5.715540	1.684785	4.366010	H	-8.289411	0.428937	3.130218
H	-6.885889	-5.123530	4.904198	H	-3.290097	0.506844	2.293250				
H	-6.227267	-3.128190	6.224205	H	-1.899244	1.955444	3.740350				
H	-5.852219	-0.961737	5.102158	H	-2.955147	3.253843	5.577771				

C_{60}@Cu2a (G = -6344,010745 a.u.)

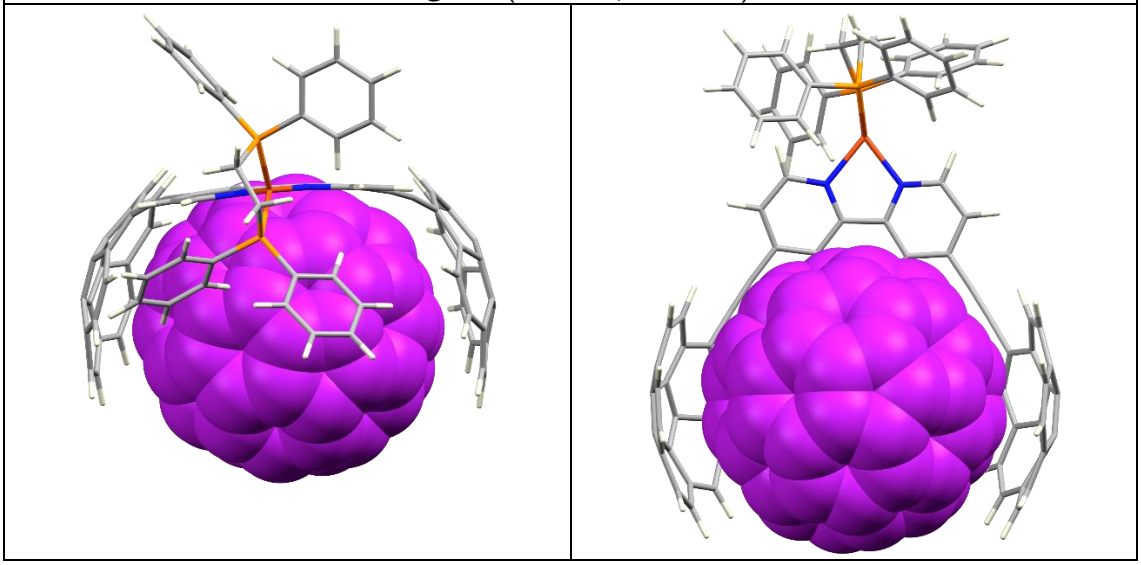

C	-4.920953	-2.470990	-0.316695	H	7.709611	5.018680	-1.742332	C	7.129975	0.551760	0.068760
C	-3.702227	-0.623013	-1.231915	H	5.735311	6.344835	2.630355	C	6.591653	1.904005	-0.041382
C	-2.695588	-1.479645	-1.656210	H	7.531560	5.722318	0.584568	C	6.005014	-1.371448	3.038519
C	-2.777690	-2.866926	-1.369624	C	0.474485	-5.911432	0.418323	C	5.155991	-2.523969	2.752343
C	-3.924182	-3.355513	-0.683495	C	0.962857	-5.917825	-0.944025	C	5.472665	-2.991653	1.406475
H	-5.827331	-2.767991	0.199305	C	1.288669	-6.279547	1.488121	C	6.518757	-2.131845	0.861642
H	-1.824727	-1.094209	-2.173047	C	2.206069	-6.514655	-1.130947	C	6.846953	-1.129267	1.870502
H	-4.021164	-4.410862	-0.450830	C	0.504609	-5.103169	-2.074752	C	3.071295	-3.489897	1.048358
N	-4.783639	-1.143577	-0.592623	C	2.669333	-6.677322	1.296630	C	2.202038	-3.137933	-0.068536
C	-3.716410	0.857303	-1.335854	H	0.906497	-6.150807	2.500763	C	3.044312	-2.892930	-1.233561
C	-2.626897	1.584971	-1.818642	C	3.040645	-6.885218	-0.032456	C	4.431887	-3.095569	-0.838801
C	-4.906757	2.766641	-0.826223	C	3.051436	-6.221034	-2.245352	C	4.449704	-3.463330	0.571802
C	-2.678446	2.997594	-1.751592	C	1.345891	-4.828540	-3.178730	C	1.521255	-1.063928	-1.919666
H	-1.732150	1.101780	-2.197097	C	3.771678	-6.608038	2.235270	C	1.832451	0.303726	-2.325243
C	-3.858622	3.591663	-1.249377	C	4.397575	-6.815898	-0.468817	C	3.213915	0.329524	-2.802731
H	-5.826009	3.201521	-0.436632	C	2.695309	-5.316664	-3.249914	C	3.755410	-1.021848	-2.691743
H	-3.943060	4.673140	-1.181416	C	4.404298	-6.412115	-1.837737	C	2.710751	-1.880169	-2.143896
N	-4.841280	1.416874	-0.844901	H	0.990301	-4.114354	-3.919867	C	0.481889	1.143790	-0.418321
C	0.707280	5.119127	-2.383756	H	3.558676	-6.496197	3.298338	C	0.810881	2.147953	0.590390
C	1.095024	5.932219	-1.226162	C	5.097103	-6.534901	1.808086	C	1.861587	3.002442	0.046650
C	1.620368	4.835138	-3.423630	C	5.449272	-6.527768	0.401975	C	2.178455	2.530799	-1.295014
C	2.358016	6.509600	-1.321558	C	3.806198	-4.759781	-4.001020	C	1.324462	1.385058	-1.587436
C	0.502804	5.952219	0.094321	C	5.463953	-5.702356	-2.406218	C	2.883782	3.477165	0.880051
C	2.983104	5.297514	-3.393064	H	5.876039	-6.367098	2.551899	C	2.899106	3.116755	2.293417
H	1.309694	4.124269	-4.188153	C	6.636810	-5.991841	-0.234357	C	4.290385	2.918237	2.691704
C	3.279502	6.198901	-2.367756	C	5.125686	-4.943569	-3.595627	C	5.131903	3.157973	1.522961
C	3.111834	6.874952	-0.165327	H	3.600712	-4.087405	-4.833454	C	4.260616	3.504178	0.404498
H	-0.506749	5.565615	0.227631	C	6.644462	-5.599342	-1.573179	C	4.621345	1.897678	3.596053
C	1.237324	6.320171	1.221172	H	7.517696	-5.785220	0.373567	C	3.575093	1.036445	4.139291
C	4.140287	4.722121	-4.055018	H	5.913081	-4.407578	-4.125304	C	4.115640	-0.314772	4.247862
C	4.600102	6.370257	-1.858666	H	7.529765	-5.098936	-1.965148	C	5.495498	-0.288718	3.772142
C	2.636346	6.687360	1.133684	C	5.437608	-2.272673	-1.365532	C	5.808168	1.078560	3.369086
C	4.496464	6.783258	-0.496998	C	5.093751	-1.214646	-2.309476	C	3.298887	-1.422715	3.973166
H	0.774626	6.210993	2.202133	C	5.943837	-0.063146	-2.021352	C	1.908079	-1.222634	3.576215
H	3.990181	4.050677	-4.900145	C	6.814581	-0.412281	-0.902040	C	1.577295	-2.225798	2.568897
C	5.430107	4.887334	-3.552228	C	6.502533	-1.779900	-0.497883	C	2.765330	-3.044014	2.342223
C	5.689884	5.643114	-2.342051	C	3.502929	2.555128	-1.751645	C	3.828724	-2.549314	3.210993
C	3.664223	6.611344	2.153051	C	4.564046	3.051895	-0.885845	C	0.738182	-1.889668	1.493492
C	5.475783	6.489071	0.452767	C	5.752832	2.237258	-1.115573	C	0.196564	-0.537767	1.384376
H	6.245931	4.337244	-4.021281	C	5.424446	1.236763	-2.126979	C	0.180118	-0.171500	-0.029845
C	6.803430	5.531956	-1.420943	C	4.031738	1.435117	-2.521520	C	0.713734	-1.296307	-0.793745
C	5.017585	6.514894	1.827878	C	6.274906	2.374471	1.305321	C	1.058394	-2.356036	0.148076
H	3.370745	6.514824	3.198394	C	6.617293	1.311587	2.245787	C	0.516675	0.427196	2.352920
C	6.700975	5.934185	-0.088828	C	7.146908	0.185956	1.482060	C	1.388525	0.077538	3.470209

C	2.238044	1.229121	3.757707	H	-6.191885	-4.994403	4.501909	H	-9.265167	4.741261	-0.758188
C	1.891945	2.291735	2.818310	H	-4.360078	-3.413202	3.934968	H	-10.956345	4.796551	-2.577412
C	0.827429	1.796316	1.949386	H	-4.876869	-1.256539	2.851763	H	-11.548740	2.706018	-3.775759
H	-0.514029	-5.503618	0.625547	C	-7.106575	1.252022	3.393158	H	-10.478885	0.570195	-3.157075
C	-1.548836	3.779054	-2.102732	C	-7.623488	1.011226	4.672184	C	-8.754889	-1.333523	-2.359183
C	-0.523956	4.417583	-2.316881	C	-7.497291	1.973689	5.668678	C	-7.719358	-1.611799	-3.260170
C	-1.714227	-3.723316	-1.712819	C	-6.854686	3.181730	5.398110	C	-7.902822	-2.541572	-4.280019
C	-0.705448	-4.385991	-1.941463	C	-6.333894	3.425755	4.130052	C	-9.118284	-3.211485	-4.400632
Cu	-6.319720	0.168605	-0.096369	C	-6.455665	2.461804	3.131481	C	-10.150964	-2.948990	-3.502299
P	-8.429751	-0.099996	-1.057510	H	-8.116622	0.067867	4.891688	C	-9.973587	-2.013376	-2.486513
P	-7.284604	0.044708	2.031954	H	-7.898929	1.780721	6.659150	H	-6.765611	-1.100589	-3.153489
C	-9.462825	-0.659644	0.384119	H	-6.755838	3.929885	6.179169	H	-7.094057	-2.748509	-4.974556
C	-9.099245	0.111704	1.655283	H	-5.826131	4.362325	3.919120	H	-9.260286	-3.941769	-5.191848
C	-7.012217	-1.579164	2.832670	H	-6.037522	2.642867	2.144626	H	-11.098109	-3.472654	-3.592485
C	-8.036723	-2.476203	3.154273	C	-9.260564	1.438711	-1.601033	H	-10.789074	-1.815626	-1.796811
C	-7.739281	-3.701226	3.749865	C	-8.918820	2.627565	-0.941721	H	-9.693920	-0.231842	2.508652
C	-6.420031	-4.040426	4.035868	C	-9.534244	3.828724	-1.282127	H	-9.331183	1.176055	1.530958
C	-5.392037	-3.153688	3.717674	C	-10.482489	3.858874	-2.302410	H	-9.264324	-1.730729	0.507279
C	-5.684750	-1.936971	3.111355	C	-10.815171	2.684940	-2.975015	H	-10.529413	-0.540768	0.167568
H	-9.074229	-2.232301	2.947502	C	-10.211837	1.479104	-2.625990				
H	-8.544284	-4.388460	3.993118	H	-8.163878	2.610524	-0.157995				

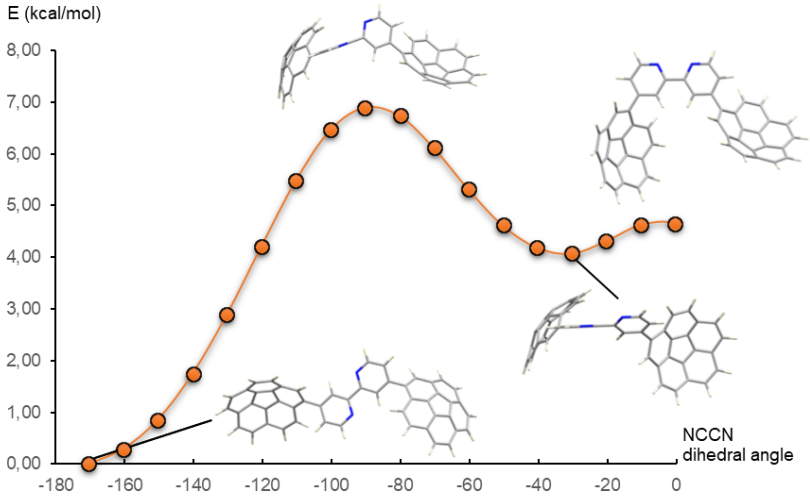

Figure S 102. Plot of electronic energy (in kcal/mol) vs NCCN dihedral angle for compound **L1a** showing that a bent arrangement is more stable than the canonical syn conformation.[31,32]

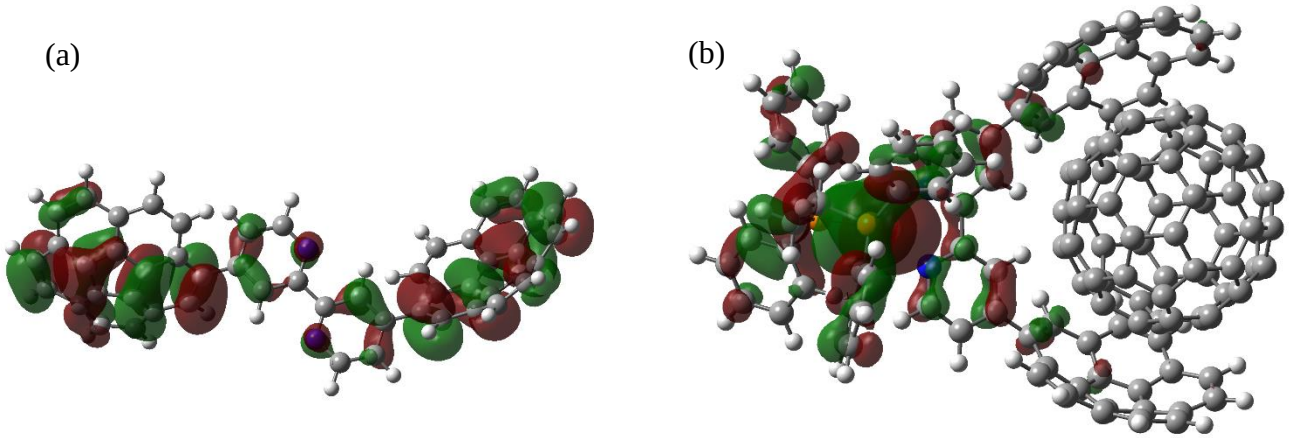

Figure S 103. HOMO surface of compound **L1a** (a) and assembly **C_{60}@Cu1a** (b) represented with isovalues of 0.015 e/Å^3.

Electronic interaction energies for assemblies **C_{60}@Cu1a** and **C_{60}@Cu2a**, are - 42.7 kcal/mol and - 43.3 kcal/mol, respectively. They fall within the expected range for a molecular pincer bearing two substituted corannulene groups,[33,34] albeit slightly higher. The almost negligible difference of 0.6 kcal/mol suggests a good performance of the cavity regardless the small difference in size (1.4 Å). NCI plots corroborate this feature due to the fact that attractive interaction surfaces are similar as shown in Figures S103-S106.

Additionally, the average H^3(bpy)–C(C_{60}) were 2.7 Å and 2.9 Å for supramolecular adducts **C_{60}@Cu1a** and **C_{60}@Cu2a,** respectively suggesting that the way that the host and guest interact is almost the same in both systems, and, therefore, the fullerene is close to the bpy moiety regardless of the presence or absence of the ethylene moiety.

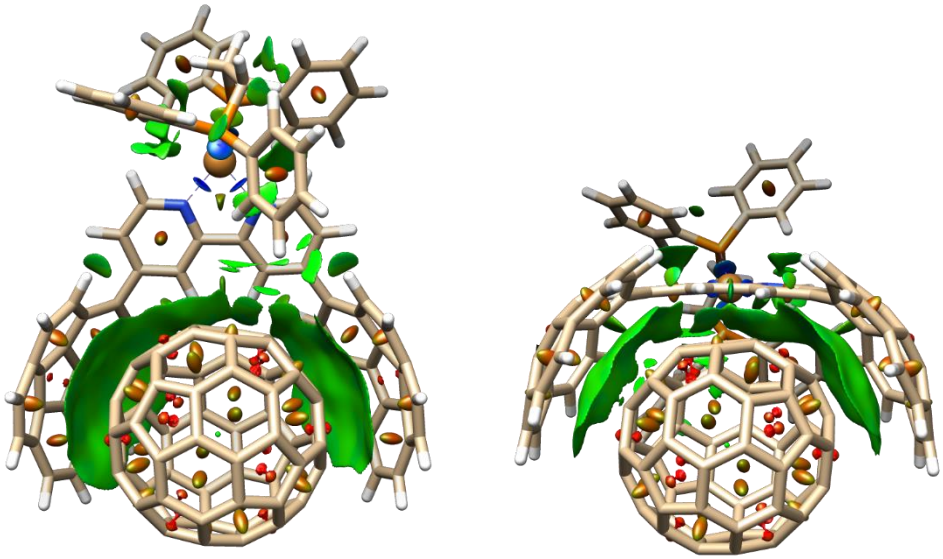

Figure S 104. Non-covalent interactions represented as gradient isosurfaces for supramolecular assembly **C_{60}@Cu1a**.

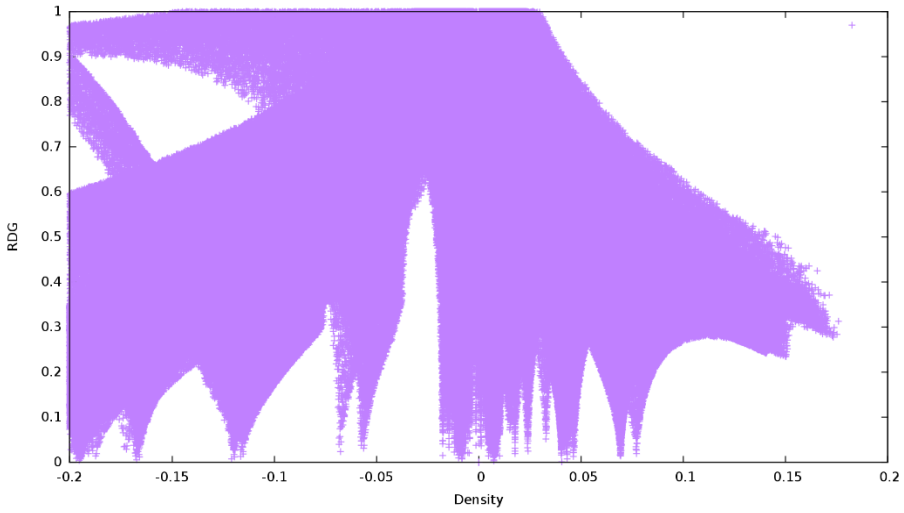

Figure S 105. Plot of the reduced density gradient versus the electron density for supramolecular assembly **C_{60}@Cu1a**.

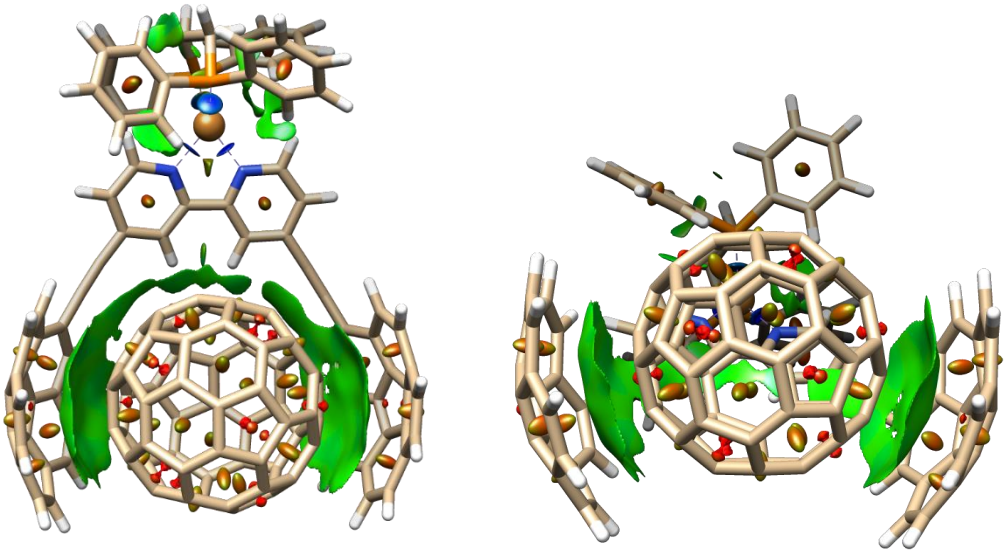

Figure S 106. Non-covalent interactions represented as gradient isosurfaces for supramolecular assembly **C_{60}@Cu2a**.

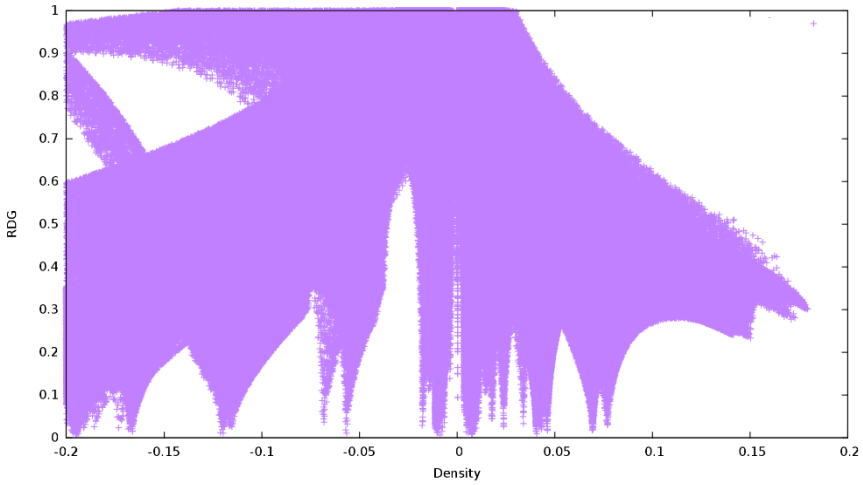

Figure S 107. Plot of the reduced density gradient versus the electron density for supramolecular assembly **C_{60}@Cu2a**.

References

1 D. B. G. Williams and M. Lawton, *J. Org. Chem.*, 2010, **75**, 8351–8354.

2 W. L. F. Armarego and C. L. L. Chai, *Purification of Laboratory Chemicals*, Butterworth-Heinemann, 2012.

3 M. Beinhoff, W. Weigel, M. Jurczok, W. Rettig, C. Modrakowski, I. Brüdgam, H. Hartl and A. D. Schlüter, *Eur. J. Org. Chem.*, 2001, **2001**, 3819–3829.

4 S. Da Ros, A. Linden, K. K. Baldridge and J. S. Siegel, *Org. Chem. Front.*, 2015, **2**, 626–633.

5 C. S. Jones, E. Elliott and J. S. Siegel, *Synlett*, 2004, **2004**, 187–191.

6 M. Ruthkosky, C. A. Kelly, F. N. Castellano and G. J. Meyer, *Coord. Chem. Rev.*, 1998, **171**, 309–322.

7 J. Lopes, D. Alves, T. S. Morais, P. J. Costa, M. F. M. Piedade, F. Marques, M. J. Villa de Brito and M. Helena Garcia, *J. Inorg. Biochem.*, 2017, **169**, 68–78.

8 H. Takeda, Y. Monma, H. Sugiyama, H. Uekusa and O. Ishitani, *Front. Chem.*, 2019, **7**, 1–12.

9 S. Grimme, *J. Comput. Chem.*, 2006, **27**, 1787–1799.

10 S. Grimme, J. Antony, S. Ehrlich and H. Krieg, *J. Chem. Phys.*, 2010, **132**, 154104.

11 S. Grimme, S. Ehrlich and L. Goerigk, *J. Comput. Chem.*, 2011, **32**, 1456–1465.

12 R. Ditchfield, W. J. Hehre and J. A. Pople, *J. Chem. Phys.*, 1971, **54**, 724–728.

13 W. J. Hehre, K. Ditchfield and J. A. Pople, *J. Chem. Phys.*, 1972, **56**, 2257–2261.

14 M. M. Francl, W. J. Pietro, W. J. Hehre, J. S. Binkley, M. S. Gordon, D. J. DeFrees and J. A. Pople, *J. Chem. Phys.*, 1982, **77**, 3654–3665.

15 M. J. Frisch, J. A. Pople and J. S. Binkley, *J. Chem. Phys.*, 1984, **80**, 3265–3269.

16 M. Ernzerhof and G. E. Scuseria, *J. Chem. Phys.*, 1999, **110**, 5029–5036.

17 C. Adamo and V. Barone, *J. Chem. Phys.*, 1999, **110**, 6158–6170.

18 W. R. Wadt and P. J. Hay, *J. Chem. Phys.*, 1985, **82**, 284–298.

19 P. J. Hay and W. R. Wadt, *J. Chem. Phys.*, 1985, **82**, 299–310.
20 P. J. Hay and W. R. Wadt, *J. Chem. Phys.*, 1985, **82**, 270–283.
21 J. Tomasi, B. Mennucci and R. Cammi, *Chem. Rev.*, 2005, **105**, 2999–3093.
22 S. F. Boys and F. Bernardi, *Mol. Phys.*, 1970, **19**, 553–566.
23 F. B. van Duijneveldt, J. G. C. M. va. D. van de Rijdt and J. H. van Lenthe, *Chem. Rev.*, 1994, **94**, 1873–1885.
24 J. P. Bowen, J. B. Sorensen and K. N. Kirschner, *J. Chem. Educ.*, 2007, **84**, 1225–1229.
25 F. Jensen, *J. Chem. Theory Comput.*, 2010, **6**, 100–106.
26 *Gaussian 16, Revision C.01, M. J. Frisch, G. W. Trucks, H. B. Schlegel, G. E. Scuseria, M. A. Robb, J. R. Cheeseman, G. Scalmani, V. Barone, G. A. Petersson, H. Nakatsuji, X. Li, M. Caricato, A. V. Marenich, J. Bloino, B. G. Janesko, R. Gomperts, B. Mennucci, H. P. Hratchian, J. V. Ortiz, A. F. Izmaylov, J. L. Sonnenberg, D. Williams-Young, F. Ding, F. Lipparini, F. Egidi, J. Goings, B. Peng, A. Petrone, T. Henderson, D. Ranasinghe, V. G. Zakrzewski, J. Gao, N. Rega, G. Zheng, W. Liang, M. Hada, M. Ehara, K. Toyota, R. Fukuda, J. Hasegawa, M. Ishida, T. Nakajima, Y. Honda, O. Kitao, H. Nakai, T. Vreven, K. Throssell, J. A. Montgomery, Jr., J. E. Peralta, F. Ogliaro, M. J. Bearpark, J. J. Heyd, E. N. Brothers, K. N. Kudin, V. N. Staroverov, T. A. Keith, R. Kobayashi, J. Normand, K. Raghavachari, A. P. Rendell, J. C. Burant, S. S. Iyengar, J. Tomasi, M. Cossi, J. M. Millam, M. Klene, C. Adamo, R. Cammi, J. W. Ochterski, R. L. Martin, K. Morokuma, O. Farkas, J. B. Foresman, and D. J. Fox, Gaussian, Inc., Wallingford CT, 2016.*
27 E. R. Johnson, S. Keinan, P. Mori-Sánchez, J. Contreras-García, A. J. Cohen and W. Yang, *J. Am. Chem. Soc.*, 2010, **132**, 6498–6506.
28 J. Contreras-García, E. R. Johnson, S. Keinan, R. Chaudret, J. P. Piquemal, D. N. Beratan and W. Yang, *J. Chem. Theory Comput.*, 2011, **7**, 625–632.
29 E. F. Pettersen, T. D. Goddard, C. C. Huang, G. S. Couch, D. M. Greenblatt, E. C. Meng and T. E. Ferrin, *J. Comput. Chem.*, 2004, **25**, 1605–1612.
30 *Rodríguez-Guerra Pedregal, Jaime, autor.; Maréchal, Jean-Didier, supervisor acadèmic.; Cairó Badillo, Jordi Joan, supervisor acadèmic. Development and application of a computational platform for complex molecular design. 1 recurs en línia (167 pàgines). ISBN 9788449082382. <https://ddd.uab.cat/record/201498> [Consulta: 29 juliol 2020].*
31 S. T. Howard, *J. Am. Chem. Soc.*, 1996, **118**, 10269–10274.
32 S. Zahn, W. Reckien, B. Kirchner, H. Staats, J. Matthey and A. Lützen, *Chem. - Eur. J.*, 2009, **15**, 2572–2580.
33 C. Mück-Lichtenfeld, S. Grimme, L. Kobryn and A. Sygula, *Phys. Chem. Chem. Phys.*, 2010, **12**, 7091–7097.
34 D. Josa, J. Rodríguez-Otero, E. M. Cabaleiro-Lago, L. A. Santos and T. C. Ramalho, *J. Phys. Chem. A*, 2014, **118**, 9521–9528.